

5-1996

## Residence time of groundwater issuing from the South Rim Aquifer in the eastern Grand Canyon

Jim Fitzgerald  
*University of Nevada, Las Vegas*

Follow this and additional works at: <https://digitalscholarship.unlv.edu/thesesdissertations>



Part of the [Geochemistry Commons](#), and the [Hydrology Commons](#)

---

### Repository Citation

Fitzgerald, Jim, "Residence time of groundwater issuing from the South Rim Aquifer in the eastern Grand Canyon" (1996). *UNLV Theses, Dissertations, Professional Papers, and Capstones*. 1426.  
<http://dx.doi.org/10.34917/3347466>

This Thesis is protected by copyright and/or related rights. It has been brought to you by Digital Scholarship@UNLV with permission from the rights-holder(s). You are free to use this Thesis in any way that is permitted by the copyright and related rights legislation that applies to your use. For other uses you need to obtain permission from the rights-holder(s) directly, unless additional rights are indicated by a Creative Commons license in the record and/or on the work itself.

This Thesis has been accepted for inclusion in UNLV Theses, Dissertations, Professional Papers, and Capstones by an authorized administrator of Digital Scholarship@UNLV. For more information, please contact [digitalscholarship@unlv.edu](mailto:digitalscholarship@unlv.edu).

**RESIDENCE TIME OF GROUNDWATER ISSUING FROM THE  
SOUTH RIM AQUIFER IN THE EASTERN GRAND CANYON**

**by  
Jim Fitzgerald**

**A thesis submitted in partial satisfaction of the  
requirement for the degree of**

**Master of Science  
in  
Geoscience**

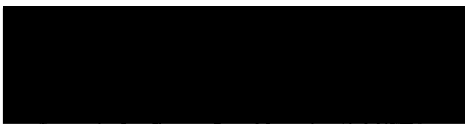
**Department of Geoscience  
University of Nevada, Las Vegas  
May 1996**

The thesis of Jim Fitzgerald for the degree of Master of Science in Geosciences is approved.



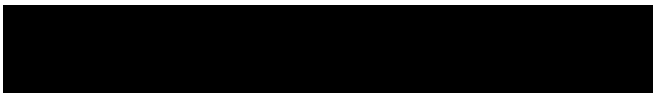
---

Chairperson, David K. Kreamer, Ph.D.



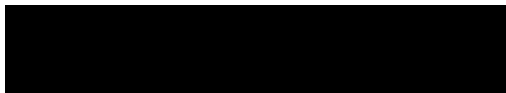
---

Examining Committee Member, Jean S. Cline, Ph.D.



---

Examining Committee Member, Kevin H. Johannesson, Ph.D.



---

Graduate Faculty Representative, Vernon F. Hodge, Ph.D.

---

Dean of the Graduate College, Ronald Smith, Ph.D.

University of Nevada, Las Vegas  
May 1996

## ABSTRACT

In the eastern Grand Canyon, secondary porosity created by north trending faults, folds, and breccia pipes, facilitates groundwater flow through the South Rim carbonate aquifer. Springs associated with the South Rim Aquifer have low  $^3\text{H}$  concentrations,  $[\text{Ca}^{2+}]/[\text{Mg}^{2+}]$  ratios close to unity, and variable uranium concentrations. For a geochemical comparison, springs are subcategorized on the basis of geology and discharge. Type I springs are associated with high-angle normal faults and have high discharge rates. These springs discharge  $\text{Ca}^{2+}\text{-Mg}^{2+}$ ,  $\text{HCO}_3^-$  waters, have  $^3\text{H}$  concentrations  $< 2$  TR, and  $^{234}\text{U}/^{238}\text{U}$  activity ratios  $> 3$  AR, which suggest long groundwater residence times. Type II and IV springs are located on canyon mesas and have low discharge rates. These springs are predominantly  $\text{Ca}^{2+}\text{-Mg}^{2+}$ ,  $\text{SO}_4^{2-}$  waters, have tritium ratios between 1 and 6 TR, and  $^{234}\text{U}/^{238}\text{U}$  activity ratios between 1 and 2 AR. Higher  $^3\text{H}$  and  $^{238}\text{U}$  concentrations and low  $^{234}\text{U}/^{238}\text{U}$  activity ratios in the latter waters may be due to shorter groundwater residence time. Based on  $^3\text{H}$  concentration, the occurrence of dedolomitization, and the resultant uranium isotope fractionation in groundwater, the minimum residence time of water discharging from the South Rim Aquifer is indicated to be  $> 40$  years.

## TABLE OF CONTENTS

ABSTRACT.....	iii
LIST OF FIGURES.....	vi
LIST OF TABLES.....	vi
LIST OF ABBREVIATIONS.....	vii
ACKNOWLEDGMENTS.....	viii
CHAPTER 1.....	1 to 5
INTRODUCTION.....	1
Purpose of Study.....	1
Location of Study.....	2
Justification of Study.....	2
Previous Investigations.....	3
CHAPTER 2.....	6 to 25
SITE CHARACTERIZATION.....	6
Introduction.....	6
Geology.....	7
Structural Geology.....	16
Hydrology.....	17
Hydrogeology.....	17
Hydrogeochemistry.....	24
CHAPTER 3.....	26 to 34
GEOCHEMICAL THEORY.....	26
Introduction.....	26
Tritium .....	26
Uranium-series Disequilibrium .....	30
CHAPTER 4.....	35 to 39
MATERIALS AND METHODS.....	35
Theoretical Design.....	35
Materials.....	35
Methods.....	36
Sample Analysis.....	38

CHAPTER 5	40 to 52
RESULTS.....	40
Introduction.....	40
Seasonal Data.....	42
Sample Limitations.....	43
Spring Outcrop Geology.....	44
Spring Discharge.....	45
Field Physiochemistry.....	46
Major Ion Concentrations.....	46
Tritium.....	46
Uranium.....	48
CHAPTER 6	53 to 83
DISCUSSION.....	53
Introduction.....	53
Spring Types.....	54
Groundwater Residence time.....	62
Geologic Control.....	80
CHAPTER 7	84 to 85
CONCLUSIONS.....	84
Further Research.....	85
APPENDICES	
APPENDIX I      Spring data sheets.....	86 to 96
APPENDIX II     Geochemical data.....	97 to 99
APPENDIX III    Spring discharge data.....	100
BIBLIOGRAPHY.....	101 to 103

## LIST OF FIGURES

Figure 1: Regional base map.....	5
Figure 2: Stratigraphic column.....	8
Figure 3: Site cross-section.....	23
Figure 4: Historic 3H data.....	28
Figure 5: Spring location map.....	42
Figure 6: Piper diagram.....	47
Figure 7: Tritium concentrations in eastern Grand Canyon springs.....	66
Figure 8: Calcium concentration versus magnesium concentration.....	69
Figure 9: Sulfate concentration versus magnesium concentration.....	71
Figure 10: Saturation indices for calcite and gypsum as functions of sulfate....	72
Figure 11: $^{234}\text{U}/^{238}\text{U}$ activity ratio and S line plot.....	75
Figure 12: $^{234}\text{U}$ -excess versus total $^{238}\text{U}$ .....	76
Figure 13: $^{234}\text{U}/^{238}\text{U}$ activity ratio versus S.....	77
Figure 14: $^{234}\text{U}/^{238}\text{U}$ activity ratio versus 3H concentration.....	78
Figure 15: Flow net for South Rim springs.....	82
Figure 16: South Rim springs cross-section of chemical parameters.....	83

## LIST OF TABLES

Table 1: Historic chemical data from Havasu and Blue Springs.....	21
Table 2: A) Tritium and B) uranium seasonal data.....	41 & 43
Table 3: Field physiochemical data.....	49
Table 4: Major ion data.....	50
Table 5: A) tritium analysis data B) uranium analysis data.....	51 & 53
Table 6: Type I spring data.....	54
Table 7: Type II spring data.....	57
Table 8: Type III spring data.....	59
Table 9: Type IV spring data.....	60
Table 10: Type V spring data.....	61
Table 11: Pre-1951 historic 3H data.....	64
Table 12: Post-1951 historic 3H data.....	65
Table 13: PHREEQE output for Type I and II springs.....	73

## LIST OF ABBREVIATIONS

### Concentration

milligrams per liter	mg/l
micrograms per liter	µg/l
parts per million	ppm
parts per billion	ppb
pico curies per liter	pCi/l
tritium ratio	TR
uranium-234/uranium-238 activity ratio	AR

### Discharge

cubic meters per second	cms
cubic feet per second	cfs
gallons per minute	gpm
liters per minute	lpm

### Geochemical Symbols

partial pressure of carbon dioxide	PCO <sub>2</sub>
partial pressure of oxygen	PO <sub>2</sub>

### Spring Name Abbreviations

Page Spring	PGS
Cottonwood Spring	CTWS
Cottonwood West Spring	CTWWS
Grapevine Hell Spring	GVHS
Grapevine East Spring	GVES
Grapevine Spring	GVS
Boulder Spring	BLDS
Lonetree Spring	LTS
Sam Magee Spring	SMS
Cremation Spring	CMS
Burro Spring	BRS
Pipe Spring	PIPS
Two Trees Spring	TTS
Kolb Spring	KBS
Horn Spring	HRNS
Salt Spring	SLTS
Cedar Spring	CDS
Monument Spring	MNS
Hawaii Spring	HWS
Hermit Spring	HSS
Santa Maria Spring	STMS
Squire Inn Well	SIW
Canyon Mine Well	CMW
Valle Well	VLW



## ACKNOWLEDGMENTS

Foremost, I thank my family for their support and love. I owe this research opportunity and adventure to Dr. David Kreamer to whom I would like to thank for technical, financial, and emotional support. In addition, I thank my committee Dr. Kevin Johannesson, Dr. Jean Cline, and Dr. Vernon Hodge for their willingness to assist me in my thesis research.

Several persons have assisted me in the field and laboratory. First I would like to thank the sherpas for their input and help carrying the burden including Sara Cox, Zane Marshall, Steve Giest, Joey Fitzgerald, Jason Johnson, Sam Earman, and David Kreamer. I thank Dennis Farmer, Vernon Hodge, and Kathy Lao for their technical assistance.

I thank the various facilities and government agencies for technical and logistical support. I particularly thank Steve Monroe and Don Bills from the United States Geological Survey in Flagstaff, Arizona, Kim Crumbo, Jon Rihs and personnel from the Grand Canyon Science Center. I thank the Colorado River boatman Dave Desrosiers for beer, whiskey, and a safe ride through Crystal Rapids.

Without financial support from the Natural History Association, Dr. David K. Kreamer, Bernada E. French, Graduate Student Association, Natural Science Scholarship Association, and the Department of Geosciences, University of Nevada Las Vegas, this research project would not have been possible.

## **CHAPTER 1 INTRODUCTION**

### **PURPOSE OF STUDY**

A study of springs in the eastern Grand Canyon was undertaken to determine the subsurface residence time of meteoric-water in the South Rim. Tritium, major ion, and uranium isotope concentrations in groundwaters were used to date relative ages, characterize the geochemical evolution, and fingerprint groundwaters discharging from the South Rim Aquifer. Since the latter aquifer is deep (i.e., > 2000 feet) and composed of non-porous fractured carbonate rock, traditional hydrogeologic methods have limited applicability. Environmental isotopes (i.e., tritium and uranium) are an alternative aquifer characterization method which are non-invasive, in-situ, and low cost.

The residence time of subsurface water was estimated by measuring the concentration of tritium in groundwater. High-yield thermonuclear testing in the 50's and 60's over saturated the atmosphere with anthropogenic tritium. As a result, the tritium bomb-pulse "peak" provides a reference point in time that is used by hydrogeologists to estimate the relative age of young waters (i.e., < 50 years). Gross-chemistry and uranium isotopes concentrations in South Rim spring waters were used

to interpret the geochemical evolution and the subsurface residence time of groundwater.

Over the duration of the investigation (1994-1996), spring waters were sampled from both sides of the Colorado River (Figure 1). Although this thesis introduces and discusses all of the Grand Canyon springs sampled in the reconnaissance, the focus is on South Rim springs (Figure 1). The first four chapters in this thesis introduce background material necessary to support the conclusions made in the final two chapters. A complete list of data collected is provided in Appendices I and II.

### **LOCATION OF STUDY**

The project site is located in northern Arizona on the South Rim of the eastern Grand Canyon and encompasses an area of about 350 km<sup>2</sup> (Figure 1). Tusayan and the Grand Canyon Village are located south of the South Rim springs. This study investigates the discharge zone of the South Rim Aquifer, at the northern edge of the South Rim or Coconino Plateau, and water samples were collected from spring outlets located between Hermit and Page Springs.

### **JUSTIFICATION OF STUDY**

Public and commercial development on the South Rim is increasing due to the amount of tourism to the Grand Canyon. The projected increases in development will require increased use of natural resources, including water. Currently, the majority of water used in Grand Canyon Village is piped from the North Rim, in addition to four production wells which pump groundwater from the South Rim Aquifer. Using

geologic and geochemical evidence, this investigation indicates that groundwater flow through the South Rim Aquifer has a residence time greater than 40 years. If this minimum residence time is correct, then groundwater withdrawal from the South Rim Aquifer may cause decreases in aquifer and basin yield. This thesis will hopefully aid in the accurate prediction of the effects of projected increases in groundwater withdrawal by estimating the relative age of groundwater.

In an arid environment, plant and animal communities evolve in order to survive in otherwise inhospitable conditions. Springs and seeps that discharge groundwater onto the Tonto Plateau in the eastern Grand Canyon are a vital source of water for plants, wild animals, and humans. Projected increases in anthropogenic need for groundwater might induce long-term decreases in spring discharge. Therefore, a better understanding of the South Rim Aquifer hydrogeology is needed to prevent the “mining” of groundwater.

Besides a fragile desert ecosystem, the Grand Canyon is also a sacred place for several Native American tribes (Hopi, Pueblo, Havasu, and Navajo). Interconnections between Native American religions and the Grand Canyon create a moral responsibility to prevent the destruction of the Grand Canyon's spring systems. In other words, the Grand Canyon is morally and intrinsically valuable, and anthropogenic impacts should be minimized if possible.

## **PREVIOUS INVESTIGATION**

The lithology, stratigraphy, and structural geology of the Grand Canyon is described by Beus and Morales (1990), Huntoon (1974, 1982), Wenrich (1986) and

numerous others. Moreover, articles and several geologic maps have been published discussing and interpreting the geology of the Grand Canyon (e.g. Huntoon 1970, 1974, 1980; Wenrich, 1985, 1986).

The hydrology of the Grand Canyon was first investigated by Metzger (1961), who assessed the potential water supply within Grand Canyon National Park. In addition, Huntoon (1982), described the surface and groundwater flow on and through the North and South Rims of the Grand Canyon. More recently, the USGS, National Park Service, and researchers at the University of Nevada, Las Vegas have investigated and described the hydrogeology of the South Rim Aquifer. Previous investigations of the Grand Canyon National Park's spring water chemistry have been conducted by Metzger (1961), Huntoon (1974, 1981) Foust and Hoppe (1985), Goings (1985), and Zukosky (1995). These past studies have focused on establishing seasonal trends and baseline values for major and trace dissolved constituents in spring waters.

Water chemistry trends, established by previous research, support further hydrogeochemical investigations. Measurements for tritium in the Grand Canyon springs have not been reported in the literature. Foust and Hoppe (1985), Goings (1985), and Zukosky (1995) provide baseline data which was used in conjunction with radioactive environmental isotopes (tritium and uranium) to determine the residence time of subsurface waters in the South Rim of the eastern Grand Canyon.

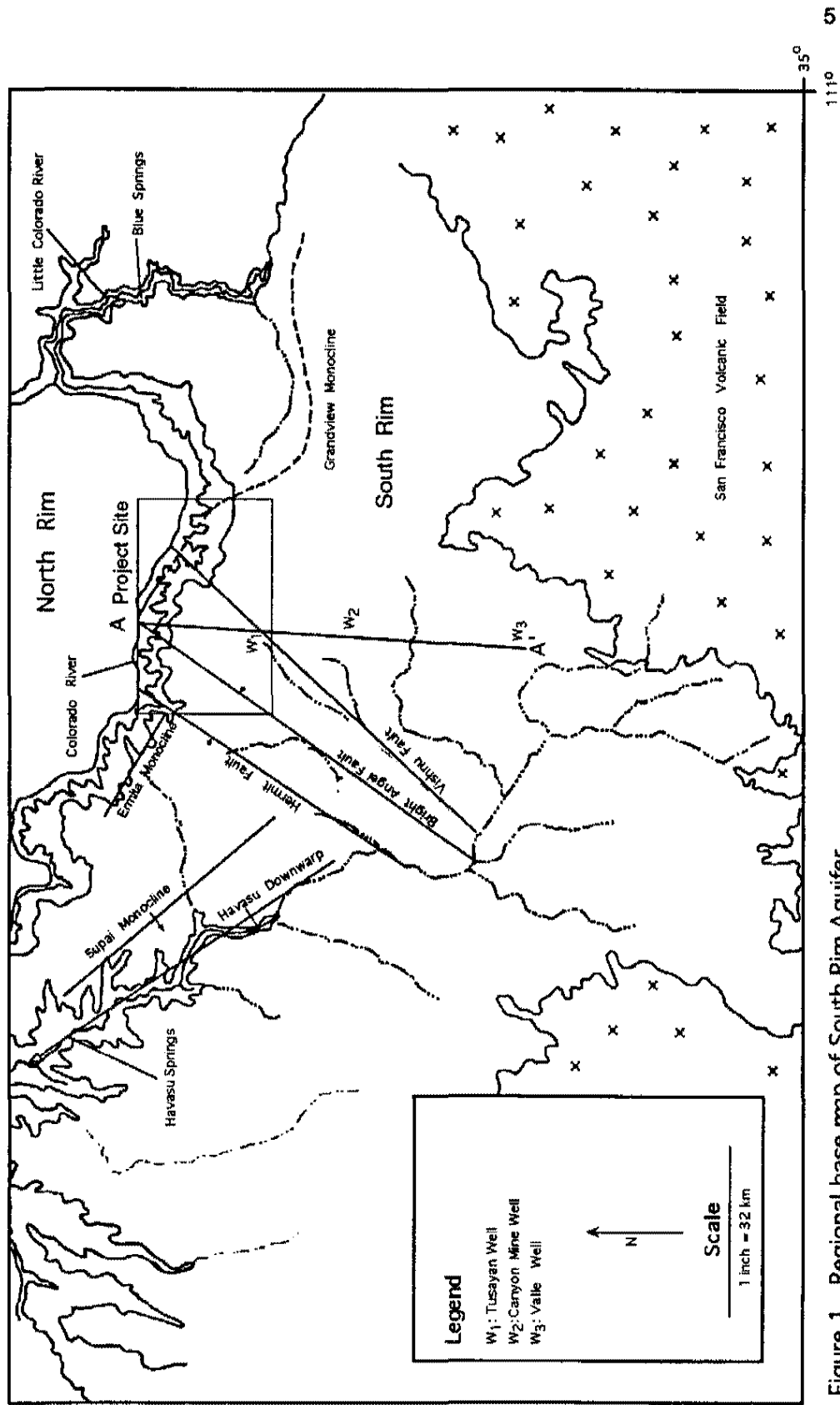


Figure 1. Regional base map of South Rim Aquifer.

## **CHAPTER 2 SITE CHARACTERIZATION**

### **INTRODUCTION**

Geologic and hydrologic information is provided in this chapter to characterize the project site and support conclusions made in this thesis. Topics relevant to the investigation include site climate and vegetation, geology, hydrology, and hydrogeochemistry. In northern Arizona, flat lying plateaus juxtapose the Colorado River gorge to the north, south, and east. To the north and south of the Colorado River are the Kaibab and Coconino (i.e., North and South Rims) Plateaus respectively. Grand Canyon springs discharge from Paleozoic sedimentary rocks which are deeply incised by the Colorado River.

### **Climate and Vegetation**

Typical of a semi-arid climate, the South Rim has an average winter air temperature of 0.5 °C (33 °F) and light snowpacks form. Summers are mild on the South Rim, with an average air temperature of 14 °C (67 °F). Spring and Fall, being transitional seasons are a variation of the latter. The inner gorge of the Colorado River has an average winter air temperature of 15 °C, while during the summer, air temperatures exceed 25 °C. Snow and rain in the winter are coupled by convection

storms in the summer (Brown and Moran, 1979). Within the Colorado River gorge and on the South Rim, the average annual precipitation over the past eleven years was 40 cm/yr (NPS, 1996).

The South Rim is vegetated by conifer, hardwood, shrub, juniper and cacti as a function of physiographic features (Figure 1). Where the Coconino Plateau decreases topographically to the south, high desert plant communities flourish. Approximately 50 miles south of the project site the land surface rises due to the San Francisco Volcanic Field (Figure 1).

## **GEOLOGY**

Within the Colorado River gorge, igneous, metamorphic, and sedimentary rocks are exposed by the down-cutting of the Colorado River. Recent erosion (i.e., 6 Ma) displays large pieces of a complex geologic puzzle that records the history of the earth over the past 2 Ga. Of particular interest to this study are the Paleozoic sedimentary rocks where the majority of input to the groundwater system is stored. The site mineralogy, lithology, stratigraphy, and structure are discussed in this section to support interpretations made regarding the South Rim carbonate aquifer and the geochemical evolution of groundwater .

### **Lithology**

#### **Precambrian Rock**

The Precambrian basement in the Colorado River gorge, is composed of igneous, metamorphic, and metasedimentary rocks. Within the project site, the oldest rocks are the Zoroaster granite and the Vishnu Schist which have absolute ages of 1.7



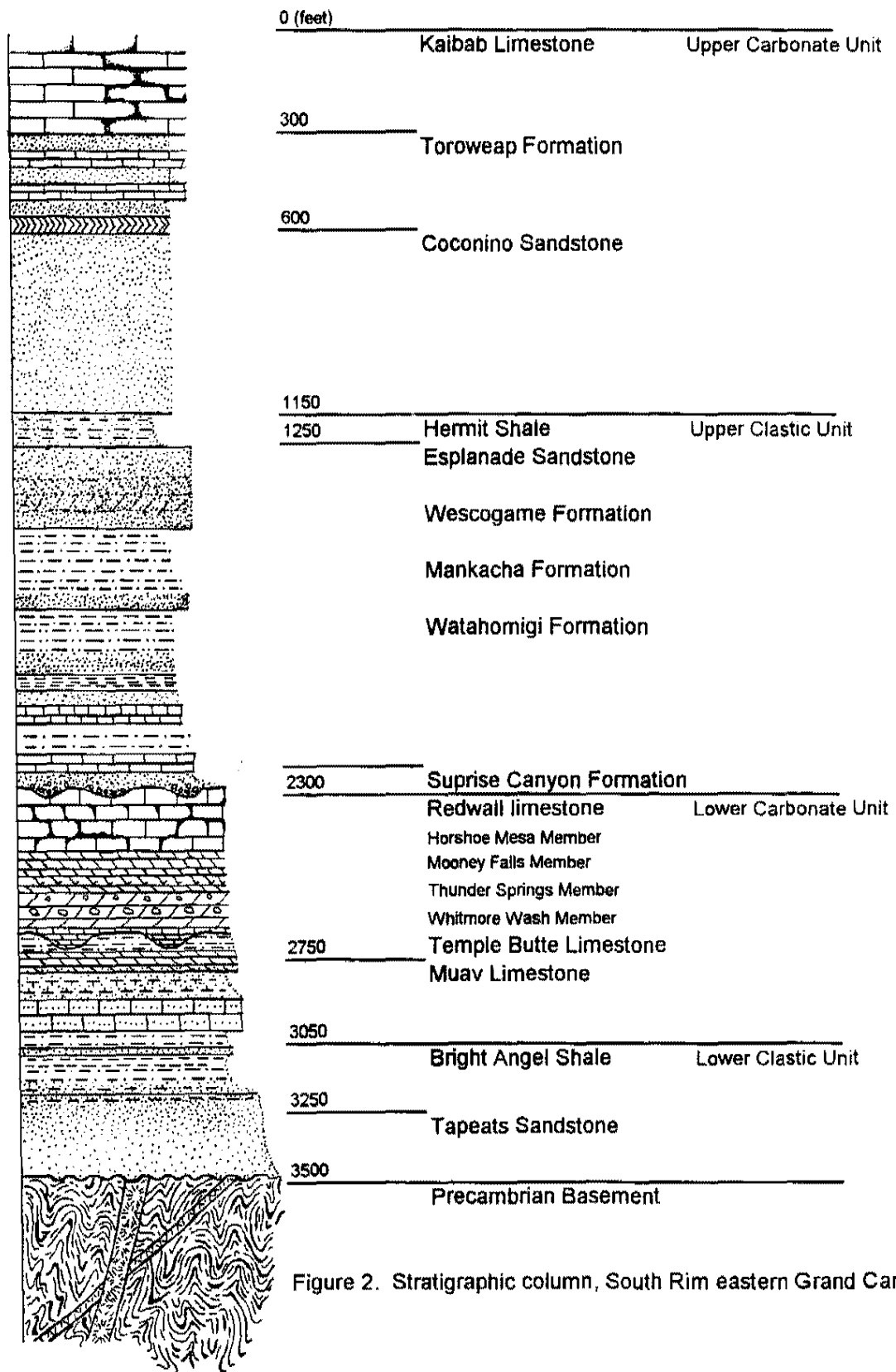


Figure 2. Stratigraphic column, South Rim eastern Grand Canyon.

Ga (Sears, 1990). Unroofed by erosion, these crystalline rocks form basement blocks that provide the foundation for siliciclastic and carbonate material deposited in the Paleozoic. The Great Unconformity, classified as a nonconformity, represents over 1 Ga of non-deposition and erosion, and separates the Precambrian basement from the Paleozoic sedimentary rocks (Sears, 1990) (Figure 2).

### **Tapeats Sandstone**

The Tapeats Sandstone consists of clastic material eroded from the Precambrian basement (Middleton and Elliott, 1990). Positive grading is present in the formation, with beds that are typically less than 1 meter (3.3 feet) thick (Middleton and Elliott, 1990). The sandstone contains feldspar and quartz and is lithified with a calcareous cement. Within the project area, the sandstone is approximately 77 meters (250 feet) thick (Figure 2).

### **Bright Angel Shale**

The Bright Angel Shale contains interbedded sandstone, siltstone, and shale with beds that pinch out to the west. The shale also grades into the underlying Tapeats Sandstone and the overlying Muav Limestone. Lithologically, the Bright Angel Shale contains quartz, rock fragments, a small percentage of feldspar, and authigenic glauconite.

The sandstone and siltstone beds are cemented with iron oxide and contain hematitic ooids. The shale member is dominantly illitic clay with trace amounts of kaolinite. In addition, fossils and sedimentary structures are abundant in the

formation (Middleton and Elliott, 1990). The thickness of the Bright Angel Shale within the study area is about 61 meters (200 feet) (Figure 2).

### **Muav Limestone**

Carbonate beds in the Muav Limestone are complexly interbedded with shale layers in the Bright Angel Shale. Regionally, the formation pinches out to the east of the project site (Middleton and Elliott, 1990). The formation consists of mottled dolomitic and calcareous mudstone and packstone (Middleton and Elliott, 1990). Small beds of micaceous shale and siltstone, and cliff forming fine-grained sandstone and silty limestone are interbedded in the formation. The thickness within the study area is 139 meters (450 feet) (Figure 2).

### **Temple Butte Limestone**

The Temple Butte Limestone is a thin, discontinuous formation that fills paleochannels scoured in the Muav Limestone. Lithologically, the Temple Butte Formation is dolomite with a small percentage of sandstone and limestone beds and is bound by unconformities (Beus, 1990). Within the project site, the Temple Butte Limestone is between 0 and 43 meters (140 feet) thick (Figure 2).

### **Redwall Limestone and Surprise Canyon Formation**

The Redwall Limestone is a thick carbonate formation with four prominent members deposited during Mississippian time. The four members of the Redwall Limestone in ascending order are the Whitmore Wash Member, Thunder Springs Member, Mooney Falls Member, and the Horseshoe Mesa Member (Figure 2). The

Redwall Limestone is the predominant Mississippian strata deposited over much of northern Arizona (Beus, 1990).

The Whitmore Wash Member of the Redwall Limestone consists of dolomite in the eastern Grand Canyon. Beus (1990) reports that the Whitmore Wash Member is almost pure carbonate with trace amounts of gypsum. In the vicinity of the project area the member is about 30 meters (100 feet) in thickness. Distinguished by thin beds of chert and dolomite, the Thunder Springs Member is about 30 meters (100 feet) thick in the eastern Grand Canyon. The thickest member of the Redwall Limestone is the Mooney Falls member (122 m (400 ft)), and it is composed of carbonate material (Beus, 1990). The Mooney Falls Member is conformably overlain by the Horseshoe Mesa Member which is only 14 meters (45 feet) thick in the eastern Grand Canyon (Beus, 1990) (Figure 2). The Horseshoe Mesa Member consists of limestone with small beds of chert.

The total thickness of the Redwall Limestone is about 200 meters (600 feet) in the eastern Grand Canyon (Figure 2). The Redwall Limestone is unconformably overlain by the Surprise Canyon Formation (Beus, 1990). The Surprise Canyon Formation consists of siliciclastic rocks which fill paleochannels and karst features in the Redwall Limestone (Beus, 1990).

#### **Supai Group and Hermit Formation**

The Supai Group unconformably overlies the Surprise Canyon Formation and Redwall Limestone. In ascending order, the four formations of the Supai Group are the Watahomigi, Manakacha, Wescogame, and Esplanade Sandstone (Figure 2). The

formations of the Supai Group are composed mainly of sandstone and siltstone, with thin limestone beds only present in the Watahomigi Formation. In addition, isolated evaporite minerals are contained within the Supai Group (Blakey, 1990).

The Hermit Shale has not been well studied in the past and current trends in Grand Canyon nomenclature suggest that the formation be subdivided in the Supai Group. The Hermit Formation, which commonly overlies the Supai Group, is called a shale, but this terminology is misleading because the formation is composed mainly of silty sandstone and sandy mudstone (Blakey, 1990). The contact with the overlying Coconino Sandstone is sharp, and desiccation cracks in the Hermit Formation are filled with sands found in the Coconino Sandstone (Blakey, 1990). The thickness of the Supai Group in the study area is over 308 meters (1000 feet), and the thickness of the Hermit Formation is about 31 meters (100 feet) (Figure 2).

#### **Coconino Sandstone**

The Coconino Sandstone was deposited in an aeolian environment in Permian time (EIS, 1985). The formation is regionally extensive and contains calcareously cemented cross-bedded sandstone. The thickness in the study area is 170 meters (550 feet) (Figure 2).

#### **Toroweap Formation**

The Toroweap Formation conformably overlies the Coconino Sandstone and thins to the south of the Grand Canyon, where it is interbedded with the upper Coconino Sandstone (EIS, 1985). The basal member of the formation is a gypsum

evaporite bed that is overlain by carbonate and siliciclastic rock. The thickness in the study area is 92 meters (300 feet) (Figure 2).

### **Kaibab Limestone**

The Kaibab Formation is the cap rock on the South Rim which is commonly exposed at the surface. This Triassic formation is a mix of carbonate and siliciclastic material (EIS, 1985). Approximately 92 meters (300 feet) thick in the project site, the formation has extensive karst development (Huntoon, 1974) (Figure 2).

### **Breccia Pipes**

The Colorado Plateau contains thousands of karst breccia pipes which have stopped upward in the Paleozoic strata since the Mississippian and Triassic (Wenrich, 1986). The typical breccia pipe has near vertical “ring fractures” that juxtapose the surrounding horizontal strata which suggests they collapse inward (Wenrich, 1986). Breccia pipes occur in clusters and follow linear trends across the Colorado Plateau and also tend to follow the cave systems developed in the Redwall Limestone during karst formation. Huntoon (1974) showed that the cave systems in the Redwall Limestone members have orientations that trend north-east and north-westerly. As a result, above cave systems, mineralized breccia pipes are commonly present (Wenrich, 1986). As many as eleven mineralized breccia pipes have been documented along north trending lineaments (Huntoon, 1974).

Karst development in the late Mississippian served as a nucleation point which facilitated the development of breccia pipes. Late Cretaceous (i.e., Laramide

Orogeny) uplift to the south of the modern Grand Canyon, created a rapidly flushing groundwater system which led to further cave formation in the Redwall and Muav Limestone. Wenrich (1986) suggested the latter features control present groundwater flow.

Wenrich (1985) found the breccia pipes in the Redwall Limestone to be heavily mineralized with sulfide and uranium minerals, while younger Triassic pipes tend to be unmineralized. Large amounts of Cu, U, Pb, Zn, Ni, Co, Mo, and As are mined from the mineralized breccia pipes. Moreover, anomalously high levels of Hg, V, As, and Se are present are found in the pipes. The paragenetic sequence of breccia pipe mineralization is summarized into five steps by Wenrich (1985): 1) deposition of calcite, dolomite, barite, siderite, anhydrite, and kaolinite by a saline brine similar to Mississippi Valley Type (MVT) deposits; 2) deposition of siegenite, bravoite, pyrite, arsenopyrite, and marcasite rich in Ni, Co, and As; 3) deposition of Cu-Fe-Pb sulfides; 4) deposition of uraninite by low temperature groundwater onto coarsely crystalline calcite matrix, in vugs, and detritus quartz grains; and 5) deposition of CuS minerals including malachite, azurite, and covellite.

The source and mechanism of uraninite precipitation in mineralized breccia pipes is not well understood. Wenrich (1986) suggested that silicic volcanic rocks of the Mogollon Highland, to the south of the Grand Canyon, could be source of uranium. From U-Pb age dates, Wenrich (1986) also suggested that uranium-rich groundwater flowed north along cave systems in the Redwall Limestone or in Surprise Canyon Formation. Under artesian pressure, the fluids were forced upward

through the breccia pipes. Precipitation of uraninite could have resulted from reduction due to sulfide minerals or degassing of CO<sub>2</sub> (Wenrich, 1986). The breccia pipes above cave formations are thought to be conduits for upward fluid flow in the past and downward flow in present (Wenrich, 1986).

### **Soils**

The soil zone than partially covers the South Rim, is a fine-sandy loam, thin (20 to 60 inches), with moderate soil permeability. The EIS (1985) reports 136,000 acres of soil zone in the Tusayan Ranger district. Lithic Ustochrept soils, typically 10 to 19 inches thick, are found at the northern edge of the South Rim and is produced in the forest. The latter soil has a low to moderate permeability rating, and it remains saturated 2 - 3 weeks a year during spring snow melt (EIS, 1985).

### **Inner Basins**

Tributaries to the Colorado River, which downcut the northern tip of the South Rim, are filled with debris eroded from the surrounding canyon walls. For the purpose of this investigation, the surface and groundwater drainage area within tributaries below the South Rim is classified as the inner basin. The volume of debris present in the inner-basin is a function surface-water drainage area below the rim. As this investigation will show, the inner basins at the base of the South Rim appear to have developed micro-aquifers which influence annual discharge and water chemistry of springs.



## STRUCTURAL GEOLOGY

The Colorado Plateau formed as a result of tectonic uplift and erosional events (Huntoon and Sears 1975). The initial deformation of the basement in the Proterozoic has controlled subsequent faulting, folding, karst formation, and collapse of the Paleozoic strata (Huntoon and Sears, 1975; Wenrich, 1986). The Precambrian crystalline basement was first deformed during the late Proterozoic when tectonic forces shortened the lithosphere and northeast trending thrust faults took up the compressional forces (Huntoon and Sears, 1975). Subsequent crustal extension facilitated the formation of northwest trending transverse normal faults, which are conjugate to the northeast oriented thrust faults. The scissors-like set of faults create a mosaic of Precambrian bedrock-blocks bounded on all sides by faults (Huntoon, 1974).

Erosion of the basement and deposition of Paleozoic sedimentary rocks preceded the folding caused by the Laramide Orogeny. Crustal compression during the Laramide Orogeny caused the horizontal Paleozoic rocks to buckle, and, as a result, reactivated the Precambrian faults in a reverse direction. Anticline and syncline folds developed in the originally flat lying Paleozoic sedimentary rocks with northwest oriented fold axes. The latter episode of deformation resulted in the formation of the Havasu Syncline, Supai Monocline, Ermita Monocline, Grandview Monocline, and East Kaibab Monocline which are all located in the study site. These folds are recognizable in modern surface topography of the Coconino Plateau. Basin and range crustal extension reactivated Precambrian faults in a reverse direction (Huntoon,

1974). Modern displacement along the Hermit, Bright Angel, Flash, McKee, and Vishnu Faults ranges from 10 to 200 feet within the project site (Huntoon, 1974) (Figure 1).

## **HYDROLOGY**

Because the South Rim has a semi-arid climate, thin soil zone, and paleo-karst formations, the majority of streams on the South Rim are intermittent (Huntoon, 1982). On the Coconino Plateau, the development of low and high order streams is controlled by the geomorphic features which are a function of the structural geology. Huntoon (1982) showed that most surface water drainage is along structural features which facilitate infiltration of water into the subsurface. Within the South Rim watershed (Figure 1), the surface topography slopes to the southwest and mimics the regional dip of the Paleozoic strata. Surface water drains west to the Havasu Downwarp (Figure 1). East of Cottonwood Spring, the Grandview Monocline causes surface water to drain southeast to the Little Colorado River (Figure 1).

## **HYDROGEOLOGY**

Hydrostratigraphic units are defined by a rock formations effective porosity, hydraulic conductivity, storage capacity, and do not coincide with traditional stratigraphic boundaries. Huntoon (1974) divided the Grand Canyon strata into five hydrostratigraphic units: 1) the Precambrian Basement; 2) Lower Clastic; 3) Lower Carbonate; 4) Upper Clastic; 5) Upper Carbonate Units (Figure 2). At present, there are no quantitative descriptions of the hydrostratigraphic properties available in the

literature. Qualitative descriptions, however, of the hydrostratigraphic units were published by Metzger (1961) and Huntoon (1974).

Precambrian rock is the lowest hydrostratigraphic unit where no significant groundwater flow occurs; therefore it is defined as an aquiclude (Metzger, 1961; Huntoon, 1982). Separated from the Precambrian Basement by the Great Unconformity, the Lower Clastic Unit is composed of the Tapeats Sandstone and Bright Angel Shale (Figure 2). Huntoon (1982) reports that the lithified sandstone and shale form a quasi-impermeable boundary (i.e. an aquitard).

Conformable, and complexly-interfingered with the shale beds in the Bright Angel Shale, carbonate rock in the Muav Limestone is the basal material in the Lower Carbonate Unit. This unit also incorporates the Temple Butte and Redwall Limestones (Figure 2). The Lower Carbonate Unit has high secondary porosity and is typically saturated at both regional and local scales. The Muav and Redwall Limestones form the major confined aquifer in the project site (i.e., South Rim Aquifer) (Huntoon, 1982).

The Upper Clastic Unit includes the Supai Group and Hermit Shale. Fine-grained siliciclastic material forms a semi-permeable boundary to vertical upward and downward flow (Huntoon, 1982). The Upper Carbonate Unit consists of the Coconino Sandstone, Toroweap Formation, and Kaibab Limestone (Figure 2). Perched aquifers, with limited lateral extent, are present in the Upper Clastic and Carbonate Units (Metzger, 1961; Huntoon, 1982).

### **Recharge and Intermediate Zones**

Physiographic features (i.e., faults, folds, and breccia pipes) on the South Rim capture precipitation and facilitate infiltration. The unsaturated zone above the South Rim Aquifer is extremely thick, and water must infiltrate 2500 feet before it reaches the saturated zone. Due to the lack of wells penetrating the South Rim Aquifer, groundwater boundaries are poorly defined. The aquifer, however, is bound to the north by the Colorado River gorge, where contact springs issue from the outcrop at various elevations.

The intermediate zone (i.e., vadose zone) is fractured and jointed by high-angle normal faults. Water is transmitted from the surface to the zone of saturation through fault and dissolution networks (Huntoon, 1982). Metzger (1961) suggested that brittle layers (e.g., Tapeats Sandstone, Redwall Limestone, and Coconino Sandstone) tend to transmit water vertically and ductile formations (e.g., Bright Angel Shale, Muav Limestone, and Supai Group) distribute flow laterally (Figure 2).

### **Saturated and Discharge Zones**

Owing to lithification, the Paleozoic sedimentary rock have low primary porosity that decreases with depth (Huntoon, 1982). Faults, joints, folds, karst features, and breccia pipes form a network of secondary porosity that concentrates zones of high hydraulic conductivity (Metzger, 1961; Huntoon, 1982; Allocco et al., 1989; Milanovic, 1981). High-angle normal faults in the study site tend to have sub-parallel sets of joints and fractures associated with the main slip plane (Huntoon, 1974). In the Lower Clastic Unit, faults commonly cut the quasi-plastic Bright Angel

Shale, but fractures and joints do not. Consequently, the subparallel joints and fractures may terminate in the plastic shale formation (Huntoon, 1974). According to Huntoon (1974), brittle formations in the Lower Carbonate Unit have high total porosity, but do not readily transmit water vertically, because they are sealed above and below by the quasi-plastic shale in the Watahomigi Formation and Bright Angel Shale respectively. Horizontal flow, therefore, tends to be concentrated along the aquitard (i.e., Bright Angel Shale). Major fracture networks in limestone are enhanced due to carbonate dissolution. As a result, the flow of groundwater is confined in the Lower Carbonate Unit (Metzger, 1961; Huntoon, 1982).

Fractures in the Paleozoic strata create the regional South Rim Aquifer. Havasu and Blue Springs are likely directly associated with these fracture systems (Huntoon, 1982), and these regional springs discharge at a constant annual rate (Metzger, 1961; Huntoon, 1982). Huntoon (1982) states that the constant discharge at Havasu and Blue Springs indicates the South Rim Aquifer is in dynamic equilibrium.

### **Regional Springs**

The Lower Carbonate Unit is the regional confined aquifer that delivers waters to the Havasu and Blue Springs. Issuing from faults, Havasu and Blue Springs flow at fairly constant rates and are the main discharge points from the South Rim Aquifer. However, they have different gross chemistry, calcium-magnesium-bicarbonate, and sodium-chloride respectively (Metzger, 1961; Huntoon, 1982; Foust and Hoppe, 1985) (Table 1).

The Havasu Springs are located along the Havasu Downwarp in the Havasupai Indian Reservation (Figure 1). Issuing from the Redwall Limestone at 3256 feet above mean sea level (amsl), the springs discharge 65 cfs (44,000 gpm) (Huntoon, 1982). Normal faults, that are transverse to the northwest plunging Havasu Monocline, are thought to be responsible for the location of the Havasu Springs (Metzger, 1961). The springs are calcium-magnesium-bicarbonate waters and are brackish (TDS > 1000 mg/l). Uranium-238 concentrations measured in the waters are low, whereas,  $^{234}\text{U}/^{238}\text{U}$  activity ratios are high (e.g. AR = 2.8) (EIS, 1985) (Table 1 A)).

Table 1. Historic data from Regional South Rim Springs (from EIS, 1985).

A)

Spring Name	Date	Elv	Q (gpm)	T (C)	pH	TDS(mg/l)	AR	1- $\sigma$
Havasus Springs	5/16/85	3250	44000	21.5	6.7	605	2.8	0.2
	5/16/85			21.5	6.7	614	1.9	0.9
	12/18/85			21	6.9	615	2.8	0.2
	12/18/85			21	6.9	552	2.5	0.2
Average				21.3	6.8	597	2.5	
Std Dev				0.3	0.1	30	0.4	
Max				21.5	6.9	615	2.8	
Min				21.0	6.7	552	1.9	

B)

Spring Name	Date	Elv	Q (gpm)	T (C)	pH	TDS(mg/l)	AR	1- $\sigma$
Blue Springs	5/16/85	3165	1E+05	20.5	6.3	2315	2.4	0.1
	5/16/85						3.1	0.8
	12/18/85			19.5	6.4	2455	2.3	0.2
	12/18/85						3.2	0.4
Average				20.0	6.4	2385	2.8	
Std Dev				0.7	0.1	99	0.5	
Max				20.5	6.4	2455	3.2	
Min				19.5	6.3	2315	2.3	

The Blue Springs are located on the south side of the Little Colorado River (Figure 1). The springs have a total discharge of 220 cfs (99,000 gpm) (Huntoon, 1982) (Table 1 B)). Water issues from the outcrop between 2,850 to 3,400 feet amsl,

and in the vicinity of the springs, the strata dip to the southeast. Groundwater discharges from the Tapeats Sandstone and the basal portion of the Supai Group, but the majority of water issues from the Mooney Falls Member of the Redwall Limestone (Huntoon, 1982). Blue Spring waters are sodium-chloride groundwater and have a low  $^{238}\text{U}$  concentration and high  $^{234}\text{U}/^{238}\text{U}$  activity ratios (e.g. AR = 2.4) (EIS, 1985) (Table 1).

### Existing Wells

Presently on the South Rim, five wells penetrate the South Rim Aquifer. The five wells, with depths greater than 2000 feet, include two Squire Inn Wells, the Canyon Mine Well, and two Valle Wells (Figure 1 and 3) (USGS, 1996). Well construction, lithologic log, and static water level data are available for only four of the five existing wells. Depth to water (i.e., potentiometric surface) on the South Rim ranges from about 2000 to 3000 feet (USGS, 1996). Figure 3 is a north south cross-section drawn through the Tusayan, Canyon Mine, and Valle Wells (Figure 1).

The Squire Inn Well is a pumping well located at 6900 feet amsl, and it has a total depth of approximately 3000 feet (Figure 3). The well fully penetrates the top two hydrostratigraphic units. The Redwall Limestone is first encountered at 2250 feet, the Muav Limestone is intersected from 2500 to 2850 feet, and the Bright Angel Shale is encountered at 2850 feet, but was not fully penetrated. The static water level in the well is about 2400 feet below the surface (USGS, 1996).

The Canyon Mine Well is a monitoring well located at 6500 feet amsl and it has a total depth of 3086 feet (Figure 3). The Redwall Limestone is encountered

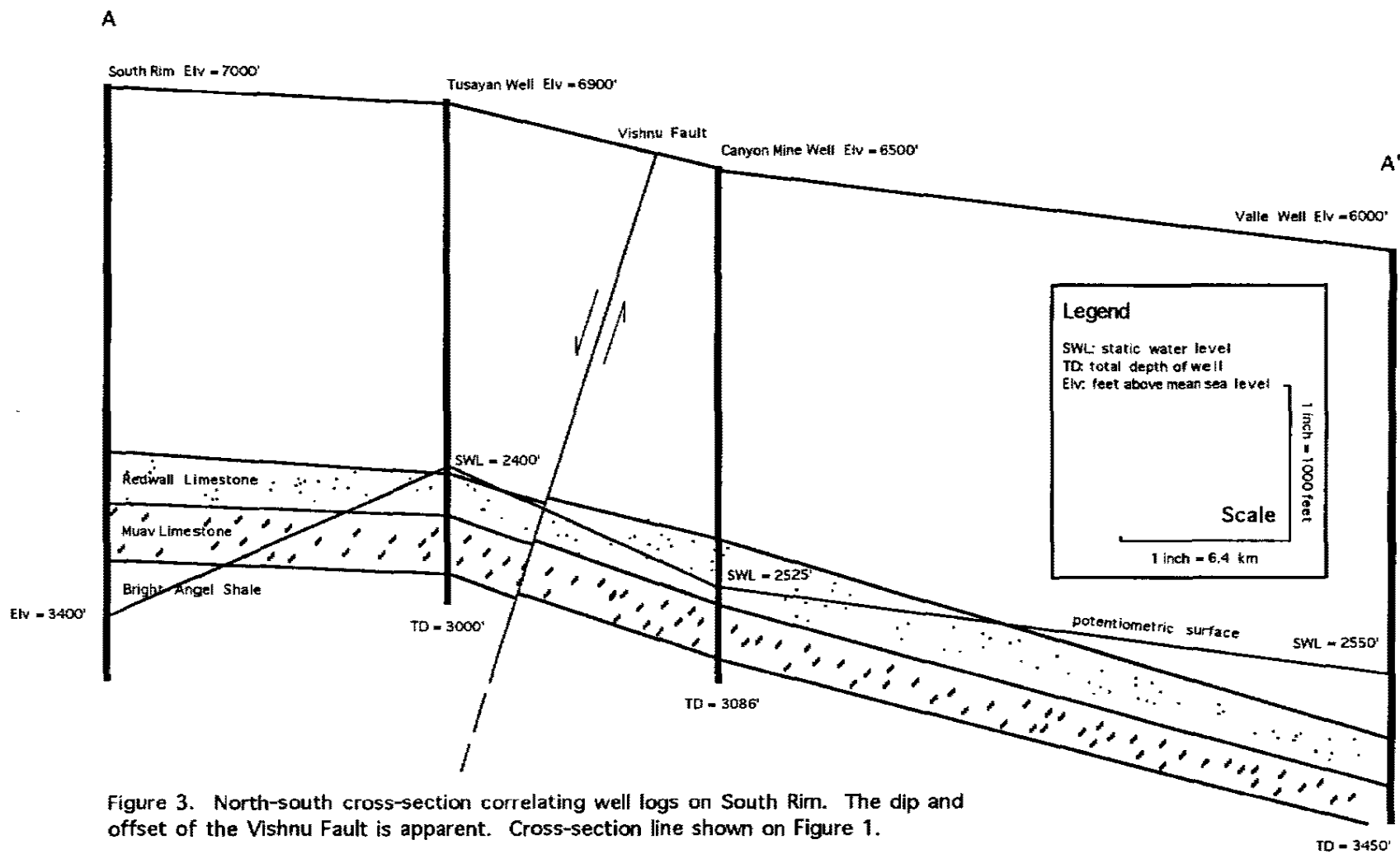


Figure 3. North-south cross-section correlating well logs on South Rim. The dip and offset of the Vishnu Fault is apparent. Cross-section line shown on Figure 1.



between 2242 and 2670 feet, the Muav Limestone is intersected from 2780 to 2980 feet, and the Bright Angel Shale was not fully penetrated. Exploration wells drilled at the Canyon Mine site had static water levels at about 2525 feet below the surface.

The Valle Well, which is a production well at an elevation of 6000 feet and has a total depth of 3450 feet (Figure 3), is located 40 miles south of Grand Canyon Village. Within the Valle Well, the Redwall Limestone is intersected at 2970 to 3240 feet, and the Muav Limestone is not fully penetrated. The static water level in the well is 2550 feet below the surface (USGS, 1996).

### **HYDROGEOCHEMISTRY**

Several research groups have investigated and established baseline water chemistry for many of the Grand Canyon Springs. Foust and Hoppe (1985), for example, conducted a 10-year hydrogeochemical survey of both North and South Rim springs. Graduate students from the University of Nevada, Las Vegas (UNLV) have studied South Rim spring water geochemistry since 1984. In 1985, Energy Fuels Incorporated, drafted an Environmental Impact Statement (EIS, 1985), which monitored major ion and radionuclides at the Canyon Mine Well, as well as, Indian Garden (i.e., Two Trees Spring), Havasu, and Blue Springs.

Foust and Hoppe (1985) established baseline physiochemistry, major ion, and trace metal concentrations for the majority of Grand Canyon Springs. The study found most Grand Canyon Spring waters have basic pH, are oxidizing, fixed  $P_{CO_2}$ , and are heavily mineralized (i.e., high calcium-magnesium bicarbonate concentrations). The latter findings are in agreement with other studies (Metzger, 1961; Goings, 1985;

EIS, 1985; Zukosky, 1995). Dolomite and limestone lithologies in the Lower Clastic and Carbonate Units are likely responsible for Grand Canyon Spring water geochemistry (Metzger, 1961; Huntoon, 1974; Foust and Hoppe, 1985).

Foust and Hoppe (1985) also found that baseline gross-constituents in spring waters, analyzed during periods of low flow, will provide the most accurate representation of spring chemistry. The exceptions are dissolved fluoride and bromide, where their concentration remained constant regardless of flow volume. In addition, trace-constituents were determined to provide accurate water type “fingerprints” of various Grand Canyon spring water types (Foust and Hoppe, 1985).

Zukosky (1995) collected water samples from South Rim Springs for stable hydrogen and oxygen isotopes and heavy and light rare earth elements (HREE and LREE). Zukosky (1995) concluded that stable isotope plots indicate a common source of recharge to the South Rim Aquifer with minimal evaporation in the vadose zone.

## **CHAPTER 3 GEOCHEMICAL THEORY**

### **INTRODUCTION**

Environmental isotopes were used in this study to interpret the relative ages of groundwaters; therefore a description of their chemistry, occurrence, and application is provided in this chapter. The understanding and validation of environmental isotope geochemical methods, stem from integrated research conducted by geologists, hydrologists, and chemists (e.g. Fritz and Fontes, 1980; Buttlar and Libby, 1954; Ivanovich and Harmon, 1992; Cowart, 1974; Kaufman, 1974; Osmond, 1980; Gaspar, 1987; and Holloway, 1993; Kronfeld et al., 1994).

### **TRITIUM**

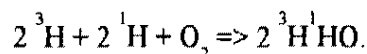
Tritium is used in hydrogeochemistry as a relative age dating method for both surface and groundwaters. High-yield thermonuclear testing in the 1950's and 1960's exponentially elevated the level of tritium in the atmosphere. In the mid-1960s, termination of above ground thermonuclear testing stopped large anthropogenic inputs of tritium to the atmosphere. As a result, this bomb-pulse "peak" is used as a reference point to relative age date waters on the basis of their tritium concentration.

The tritium isotope has a half life of  $12.42 \pm 0.05$  years and is expressed as an

abundance ratio (Tritium Ratio = TR), relative to stable hydrogen.

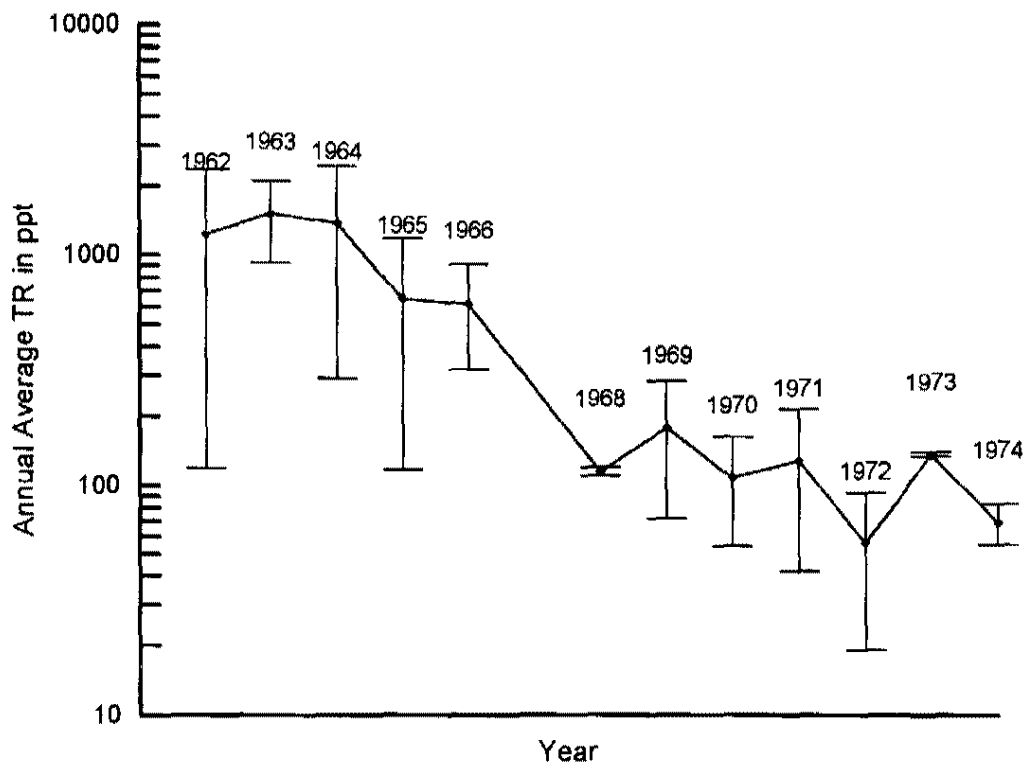
$$1 \text{ TR} = {}^3\text{H}/10^{18} \text{ H}.$$

Atmospheric tritium, similar to  $^{14}\text{C}$ , is naturally produced in the atmosphere by cosmic ray spallation (Buttlar and Libby, 1954). Tritium assumes three molecular forms in the atmosphere that are listed here in order of abundance: 1) tritiated water; 2) hydrogen gas; and 3) methane (Murphy, 1993). The oxidation of  ${}^3\text{H}$  atoms, and subsequent hydrogen bonding with oxygen, is described by the following (Fontes, 1980):

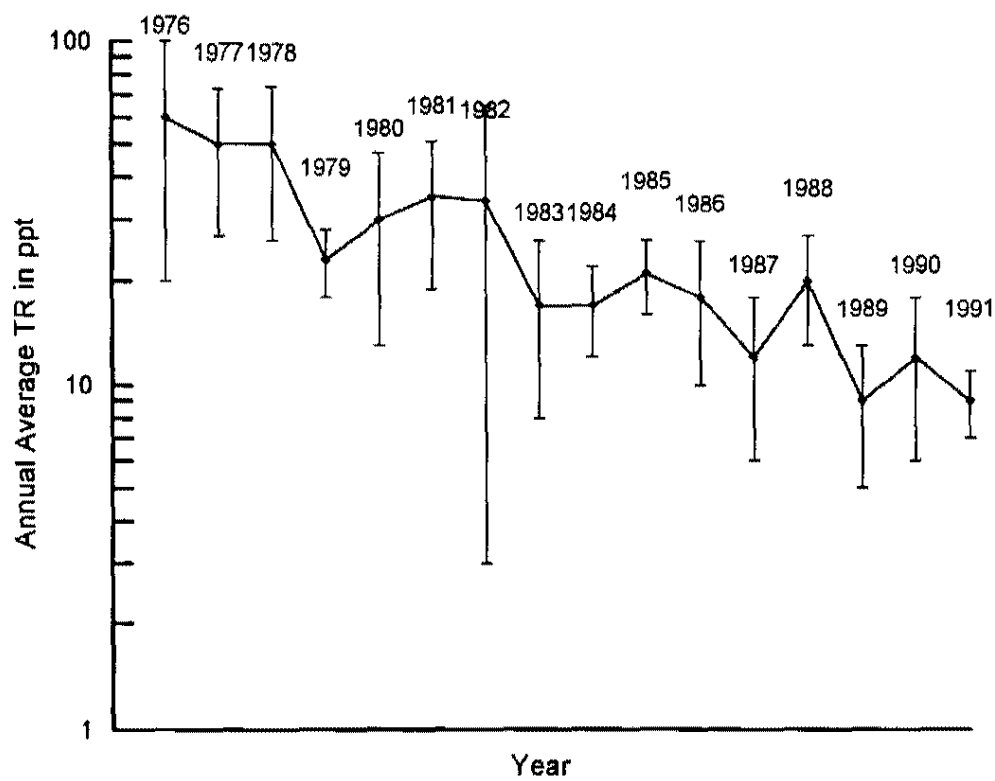


In the troposphere, tritiated water molecules have a residence time of 21 to 41 days, where they rapidly oxidize, resulting in precipitation of tritiated water (Murphy, 1993). The residence time of  ${}^3\text{H}$  in the atmosphere is short owing to rapid beta decay of N and O gases, which results in autocatalysis and subsequent spontaneous oxidation of  ${}^3\text{H}$  to the liquid phase (Gaspar, 1987; Murphy, 1993).

The volume of natural tritiated water in the troposphere varies spatially and temporally. In effect, longitude in the northern hemisphere influences the  ${}^3\text{H}$  concentration in precipitation, where the TR is unity near the ocean and increases inward toward the continent (Buttlar and Libby, 1954). Turbulence and turnover in the atmosphere causes  ${}^3\text{H}$  concentration to vary annually, such that, the natural  ${}^3\text{H}$  in meteoric water tends to be high in the summer and low in the winter (International Atomic Energy Agency, 1960-1974; Holloway, 1993). The natural level of tritiated water in precipitation is estimated to be between 5-20 TR (Buttlar and Libby, 1954;



A)



B)

Figure 4. Historic environmental isotope data ( $^3\text{H}$ ) collected by the IAEA (1960-1991) in A) Flagstaff, Arizona and B) Albuquerque, New Mexico

Holloway, 1993). Prior to 1951, few tritium analyses were performed on precipitation (Holloway, 1993).

The advent of above ground thermonuclear testing in 1952, resulted in an increase in the volume of  $^3\text{H}$  in the atmosphere. Since 1952 the International Atomic Energy Agency (IAEA) has monitored the concentration of tritium in precipitation. Over Ottawa Canada, bomb-pulse  $^3\text{H}$  in precipitation peaked at 10,000 TR in 1963 (International Atomic Energy Agency, 1963). Figure 4 is a plot illustrating the variation of the average monthly anthropogenic  $^3\text{H}$  concentration relative to the average monthly precipitation at Flagstaff, Arizona, from 1962 to 1974 and Albuquerque, New Mexico, from 1976 to 1991. During high-yield thermonuclear testing (i.e., 1952 to 1964), the  $^3\text{H}$  concentration did not fluctuate as a function of precipitation, whereas, after thermonuclear testing (i.e., 1964), the abundance of tritiated water became more dependent on the amount of precipitation (Figure 4).

After termination of above ground nuclear testing in the 1960s, the TR in precipitation exponentially decreased (Figure 4), and is presently thought to be approaching natural levels (Holloway, 1993). In this investigation  $^3\text{H}$  data collected in Flagstaff, Arizona from 1962 to 1974, and Albuquerque, New Mexico from 1976 to 1991, has been used to establish the historic and modern annual average baseline TR in precipitation over the project site (Figure 4).

As previously stated, condensation of tritiated water molecules delivers  $^3\text{H}$  to the terrestrial stage of the hydrologic cycle. Tritiated water enters the soil zone as a gas and/or liquid (Murphy, 1993). Within the A-soil horizon, plants and

microorganisms use a small fraction of tritiated water, but relative to capillary and gravity forces acting on tritiated water, organic activity is negligible (Murphy, 1993). Therefore, although the volume of soil water will change, the TR will not change. In addition, once soil water infiltrates below the upper weathered zone, aqueous  $^3\text{H}$  is not effected by soil zone processes (Murphy, 1993).

### URANIUM-SERIES DISEQUILIBRIUM

Uranium-series disequilibrium is useful in hydrogeochemistry due to fractionation that occurs between  $^{238}\text{U}$  and  $^{234}\text{U}$  in aqueous solution. The  $^{234}\text{U}/^{238}\text{U}$  activity ratio (AR) is used by hydrogeochemists to fingerprint water types, interpret rock-water interactions, and estimate groundwater residence time. Because of the various complexities involved in the evolution and fractionation of uranium isotopes in groundwater systems, the following section describes the concert of chemical reactions which affect uranium sequentially from the weathered zone to discharge zone.

The naturally occurring isotopes of uranium are  $^{238}\text{U}$ ,  $^{235}\text{U}$ , and  $^{234}\text{U}$ .  $^{238}\text{U}$  decays to  $^{206}\text{Pb}$  through a series of progeny, by alpha and beta decay.  $^{238}\text{U}$  has a long half life ( $t_{1/2} = 4.47 \times 10^9$  years) relative to the first three progeny in the decay series,  $^{234}\text{Th}$  ( $t_{1/2} = 24.1$  days) and  $^{234}\text{U}$  ( $t_{1/2} = 2.48 \times 10^5$  years) which facilitates the use of isotopic fractionation between  $^{234}\text{U}$  and  $^{238}\text{U}$ . In the solid or mineral phase, the  $^{234}\text{U}/^{238}\text{U}$  activity ratio (AR) is assumed to be in secular equilibrium (i.e.,  $\text{AR} \sim 1$ ) where their respective rates of decay are equal; this is under the assumption that there

is no addition or loss of uranium from the solid. The  $^{234}\text{U}/^{238}\text{U}$  activity ratio (i.e.,  $\lambda N_{234}/\lambda N_{238}$ ) is mathematically defined as:

$$\text{AR} = \lambda N_{234} / \lambda N_{238}$$

where  $\lambda$  is the decay constant and  $N$  is the neutron number.

In natural waters, the  $^{238}\text{U}$  concentration typically falls in a range between 0.1 to 10  $\mu\text{g/l}$  (ppb), and the  $^{234}\text{U}/^{238}\text{U}$  activity ratio usually ranges from 0.7 to 5.0 AR (Osmond and Cowart, 1976). The wide range of AR in groundwater is due to fractionation processes that occur in the subsurface. The  $^{234}\text{U}/^{238}\text{U}$  activity ratio in solution changes or “fractionates” when fluids interact with the solid phase.

In oxidized aqueous solution, dissolved  $\text{U}^{6+}$  is chemically conservative, whereas in reduced solution,  $\text{U}^{4+}$  is highly insoluble (Osmond and Cowart, 1976). As with most metals, uranium complexation in aqueous solution is a function of initial uranium concentration, mineralogy, pH, and  $P_{\text{CO}_2}$  of the system. At low pH, the metal remains a free cation ( $\text{M}^{n+}$ ), but as pH increases, the metal will become complexed. In a carbonate groundwater system, hydroxyl and carbonate uranium complexes are common and occur as a function of solution pH and alkalinity (Morse et al., 1983).

At low pH the uranyl complex ( $\text{UO}_2^{2+}$ ) is stable in solution; as pH increases, the uranyl species tend to adsorb to carbonate minerals, and as a result, uranium is removed from solution (Morse et al., 1984). Additionally, sorbed uranium hydroxyl complexes form a coating over the carbonate mineral surface (i.e., carbonate complex) as carbonate minerals are precipitated (Morse et al., 1984; Ivanovich and Harmon, 1992).



Meteoric precipitation typically has a negligible uranium concentration and an acidic pH  $\sim 5.65$  at steady state conditions. As water infiltrates through the weathered zone, acid-base and redox reactions dissolve uranium, thus “fingerprinting” the water with a characteristic  $^{234}\text{U}/^{238}\text{U}$  activity ratio and total  $^{238}\text{U}$  concentration. The amount of uranium leached is a function of pH, oxidation state, solid mineral composition, and crystal surface area (Osmond and Cowart, 1976; Osmond, 1980). As part of the large ion lithophile group of elements, uranium is highly incompatible in magmatic systems and becomes enriched in the liquid phase during partial melting as well as fractional crystallization. Therefore, at the surface, where uranium minerals are unstable, the uranium isotopes are susceptible to chemical weathering processes.

Rock-water interactions in the weathered zone result in leaching of uranium from the solid. In general, uranium minerals will typically have higher uranium content than the liquid (Cowart et al., 1978; Osmond and Cowart, 1976). Uranium dissolution and precipitation follow the law of mass balance, the relative  $^{234}\text{U}/^{238}\text{U}$  activity ratio in the solid is expected to decrease, while  $^{234}\text{U}/^{238}\text{U}$  activity ratio in the liquid is increased and, therefore, the  $^{234}\text{U}/^{238}\text{U}$  activity ratio and total  $^{238}\text{U}$  concentration are inversely proportional in solution (Osmond and Cowart, 1976; Ivanovich and Harmon, 1992).

Once infiltrating water enters the saturated zone, the uranium “fingerprint” will either remain conservative or non-conservative as a function of geologic and geochemical environment. There are three basic types of groundwater systems with respect to uranium: 1) steady state; 2) augmenting; and 3) decaying. The steady

state system typically has high buffering capacity, high  $P_{O_2}$ , and high  $P_{CO_2}$ .

Consequently, the carbonate species is stable, and the  $^{234}U/^{238}U$  activity ratio and total  $^{238}U$  concentration remain constant (Morse et al., 1984; Ivanovich and Harmon, 1992).

The augmenting system is geochemically closed as a result of changes in pH, redox potential, and  $P_{CO_2}$ . Most documented augmenting systems contain a reducing zone which converts  $U^{6+}$  to  $U^{4+}$ , consequently causing the precipitation of uraninite ( $UO_2$ ) (Osmond and Cowart, 1976). Decaying systems are also closed, but have long ground residence times allowing the  $^{234}U$  activity to decrease due to radioactive decay (Osmond and Cowart, 1976). It necessarily follows that in a decaying system, the longer the groundwater residence time, the lower the  $^{234}U/^{238}U$  activity ratio will become. If the system is decaying, the groundwater velocity is slow relative to the  $^{234}U$  half life ( $t_{1/2} = 2.48 \times 10^5$  years), the  $^{234}U/^{238}U$  activity ratio will decrease, and the total  $^{238}U$  (i.e.,  $t_{1/2} = 4.47 \times 10^9$  years) will remain constant. (Ivanovich and Harmon, 1992; Osmond and Cowart, 1976; Kronfeld et al. 1994).

In a closed augmenting or decaying system, the abundance of uranium oxide and degree of isotopic fractionation are a function of rock geochemistry. Isotopic fractionation in the saturated zone results from two processes: 1) alpha recoil; and 2) selective leaching of  $^{234}U$ . Osmond and Cowart (1976) report that alpha recoil is the primary mechanism of fractionation in reducing aquifers. Alpha recoil is the sudden reactive movement of progeny through a distance of a few hundred angstrom units, when an alpha particle is expelled in the opposite direction (Ivanovich and Harmon,

1992). Alpha recoil, a product of  $^{238}\text{U}$  decay, can result in the progeny ( $^{234}\text{Th}$ ), escaping the crystal lattice and, therefore, causing  $^{234}\text{Th}$  to transfer across the solid-liquid interface. Due to the short half-life of  $^{234}\text{Th}$  (24.1 days),  $^{234}\text{U}$  is rapidly produced and, consequently, increases the  $^{234}\text{U}/^{238}\text{U}$  activity ratio in solution.

The second isotopic fractionation mechanism is selective leaching which rests on the inference that  $^{234}\text{Th}$  and  $^{234}\text{U}$  are both more “susceptible” to dissolution as a result of the “recoil effect.” In this case, instead of directly transferring the progeny to aqueous solution, alpha recoil displaces progeny to the outer margins of the crystal lattice. Subsequent rock-water interactions selectively leach the  $^{234}\text{Th}$  and/or  $^{234}\text{U}$  from the rock (Osmond and Cowart, 1976).

Kronfeld et al. (1994) pose an alternate avenue for elevated  $^{234}\text{U}/^{238}\text{U}$  activity ratios resulting from alpha recoil in an oxidizing system. Alpha recoil typically occurs in a reducing system where precipitation of  $\text{UO}_2$  is occurring. Kronfeld et al. (1994) have shown that in an oxidized carbonate systems, ion exchange and/or sorption of uranium complexes on carbonate mineral surfaces provide an effective source of  $^{238}\text{U}$  which will increase  $^{234}\text{U}$  in solution as a result alpha recoil. Kronfeld et al. (1994) also found that the amount of radiogenic fractionation is a function groundwater residence time, such that the longer the groundwater residence time, the higher the  $^{234}\text{U}/^{238}\text{U}$  activity ratio.

## **CHAPTER 4 MATERIALS AND METHODS**

### **THEORETICAL DESIGN**

Hydrogeologic and hydrogeochemical methods were used in this investigation to estimate the residence time of South Rim spring waters. Individual springs were grouped into populations based on discharge and geology. Differences and similarities between spring populations were used to interpret the residence time and geochemical evolution of groundwater; including: 1) location; 2) elevation; 3) position in strata; 4) lithology; 5) structure; 6) flow volume; 7) temperature; 8) pH; 9) alkalinity; 10) conductivity 11) total dissolved solids 12) major-ion concentrations; and 13) environmental isotopes (i.e., tritium and uranium).

### **MATERIALS**

A variety of analytical equipment was used in the field to measure the latter field parameters (e.g. pH, alkalinity, conductivity). A standardized field equipment packing list was developed to maintain sampling consistency throughout the duration of the study. Because Grand Canyon springs are typically reached by foot, basic backpacking equipment was used to transport equipment and samples.

Topographic maps were used for land navigation and as base maps for hydrogeologic mapping. The 7.5 minute quadrangles that cover the project site are Grandview Point, Cape Royal, Phantom Ranch, Tusayan East, and Tusayan West Quadrangles. The geologic maps drafted by Huntton et al. (1980) and Metzger (1961) were used to correlate the hydrology to stratigraphy and geologic structure. The Arizona State Geologic Map was used to relate the project site to the regional geology and hydrology. A Global Positioning System (GPS) was used to approximate the longitude and latitude of sample stations. The altitude of sample stations was derived from the topographic maps.

Field portable instruments were used to measure basic field parameters. The instruments used in the field included a thermometer, pH meter, conductivity-TDS meter, and alkalinity titration kit.

## **METHODS**

Water samples were collected from springs, seeps, creeks, and wells on the North and South Rims of the eastern Grand Canyon. The majority of the springs that drain into the Colorado River basin have been sampled for gross dissolved constituents, tritium, and uranium. Geologic and hydrologic characteristics and properties of springs were recorded in a field notebook and plotted on a topographic base map. The field descriptions include sample location, altitude, weather, vegetation, stratigraphy, structure, discharge, physiochemistry, and any other notable characteristic.

Discharge at Hermit, Two Trees, Pipe, and Cottonwood Springs is measured by stream gages installed by the USGS (Figure 5). Stream gages at Hermit, Pipe, and Cottonwood Spring are located down stream from the spring orifice. Consequently, the latter gages measure total discharge from the spring and inner basin alluvium. For the remaining springs, discharge was measured volumetrically.

Water samples from South Rim springs were collected, handled, and analyzed following currently accepted quality assurance procedures (Wood et al., 1993; Osmond and Cowart, 1976). Springs were sampled, as much as possible, from the point of issuance. For “outcrop” type springs (i.e., contact springs), water samples were collected at the same location, whereas, samples collected from inner basin alluvium, were sampled where the water first surfaced. Because of sample location restrictions, the alluvium samples were often collected at different locations within the same inner basin (i.e., Chapter 2).

Major ion samples were collected in 120 ml precleaned polyethylene bottles. The water sample was filtered through a 0.45  $\mu\text{m}$  filter, using a hand-held peristaltic pump. Cation samples were acidified to  $\text{pH} < 2$ , with ultra-pure, concentrated nitric acid. Traditionally, anion samples are preserved by keeping them cool and performing the analyses within 48 hours of sample collection. Due to the remote sample locations, the anion samples collected in this study had variable temperatures and were stored in their sample bottles for seven days. Because of these limiting factors, the  $\text{PO}_4^{2-}$  species, which can be affected by temperature and long storage, were not considered in the anion analysis.

Tritium samples were collected as “grab” samples in one-liter glass bottles. A 500 ml sample is needed for isotopic enrichment analysis (Wood et al., 1993), but a 1000 ml sample was collected at each site.

Uranium samples were collected in one liter, acid precleaned, polyethylene bottles. One liter, “grab” samples for uranium were collected at each spring. Samples were filtered through a 0.45  $\mu\text{m}$  filter, and acidified in the field to  $\text{pH} < 2$ , with ultra-pure, concentrated nitric-acid. Filtered and unfiltered samples were both collected depending on the turbidity of the water at each sample site. Past research indicates that filtering uranium water samples is typically not necessary, with the exception of high turbidity surface water (Osmond and Cowart, 1976).

### **SAMPLE ANALYSIS**

Major ion samples were analyzed at the Harry Reid Center for Environmental Studies (HRC). The four major cations (i.e., sodium, magnesium, calcium, and potassium) were measured by atomic adsorption spectroscopy (AA). The detection limit of the AA method is approximately  $0.01 \pm 0.05$  mg/l. Dilution correction factors were used to statistically support the accuracy and precision of the average sample concentration. Anion samples were analyzed using a Dionex ion chromatography (IC) system. Similar to the cation accuracy, the detection limit of IC is  $0.01 \pm 0.05$  mg/l.

Tritium analyses were performed at the Desert Research Institute, Reno (DRI), and at the Environmental Protection Agency, Las Vegas (EPA). Both labs use the same method and have similar limits of detection of 1 to 2 TR. The water sample

is enriched by electrolysis and then placed into a liquid scintillation counter which records beta decay in disintegrations per unit time. If electrolytically enriched before liquid scintillation, the method has a detection limit of 2 TR or 6 pCi/l (Moser et al., 1988).

Uranium samples were analyzed at the Trace Metals Lab, University of Nevada Las Vegas (UNLV). Uranium disequilibrium analysis, described below, was conducted using the anion-exchange method described by the US EPA (1979). First,  $^{232}\text{U}$  is added to the samples as a tracer to quantify the percentage of uranium isotope recovery. Uranium is then removed from solution by coprecipitating uranium isotopes with ferric hydroxide. The precipitate is then dissolved in hydrochloric acid, and the solution is passed through columns to separate uranium isotopes from other metals. Ion exchange is achieved by flushing the columns with acid and collecting the analyte. The uranium is then plated on a stainless steel planchets by electrodeposition, and a high resolution solid-state alpha particle spectrometer is used to count the alpha emissions. The samples are counted for 1000 minutes, and the resultant disintegrations per unit time are used to calculate the concentration of uranium in solution. Blanks are run through the entire laboratory analysis and provide a correction factor for counting background. The minimum detection limit for uranium isotopes is less than 0.01  $\mu\text{g/l}$ , with a 1-sigma error =  $\pm 5\%$  for uranium concentration and  $\pm 3\%$  for AR (Ivanovich and Harmon, 1980).



## **CHAPTER 5 RESULTS**

### **INTRODUCTION**

Results reported in this chapter include seasonal sampling, sample limitations, spring outcrop geology, field physiochemistry, and major ion, tritium, and uranium analyses. Major ion samples were collected in July 1995, tritium samples were collected from January 1994 to February 1996, and uranium samples were collected from March 1994 to November 1995. Appendix I is composed of field data sheets which summarize all data collected during the investigation. Additionally, Appendix II lists the results from water sample analyses for tritium, major ions, and uranium. Discharge measurement for the 1994-1995 water year are tabulated in Appendix III.

### **SEASONAL DATA**

In order to establish seasonal variations in environmental isotope concentrations, tritium samples were collected periodically. Table 2 A) and B) list the annual average tritium and uranium concentrations in spring waters and their variance from the sample mean. Both tritium and uranium concentrations in spring water had minimal variability during 1994 and 1995 (Table 2 A) and B)). Samples collected

directly at the spring orifices show minimal variability in their tritium and uranium concentrations throughout the year, whereas samples collected from inner basin sediment exhibit a higher degree of variance.

**Table 2. A) Seasonal sampling results for tritium measurements**

Spring Name	Date	TR	2- $\sigma$
Page Spring	11/11/94	1.08	0.83
	5/12/95	1.25	1.88
	7/16/95	1.88	1.88

Average 1.41

Std Dev 0.42

Spring Name	Date	TR	2- $\sigma$
Cottonwood Creek	11/11/94	1.44	0.93
	11/12/94	1.06	1.08
	2/25/95	2.23	1.88
	7/16/95	1.57	2.19

Average 1.57

Std Dev 0.48

Spring Name	Date	TR	2- $\sigma$
Pipe Creek	4/29/94	0.94	3.13
	11/14/94	1.99	0.87
	9/26/94	1.45	0.89

Average 1.46

Std Dev 0.52

Spring Name	Date	TR	2- $\sigma$
Two Trees Spring	4/30/94	0.82	0.85
	9/29/94	0.99	0.87
	11/26/94	0.66	1.57
	4/30/95	-0.47	3.13
	5/18/95	-0.09	2.19

0.38 1.72

0.63 0.97

Spring Name	Date	TR	2- $\sigma$
Horn Creek	4/30/94	2.32	2.19
	6/5/95	4.39	1.88

Average 3.35

Std Dev 1.46

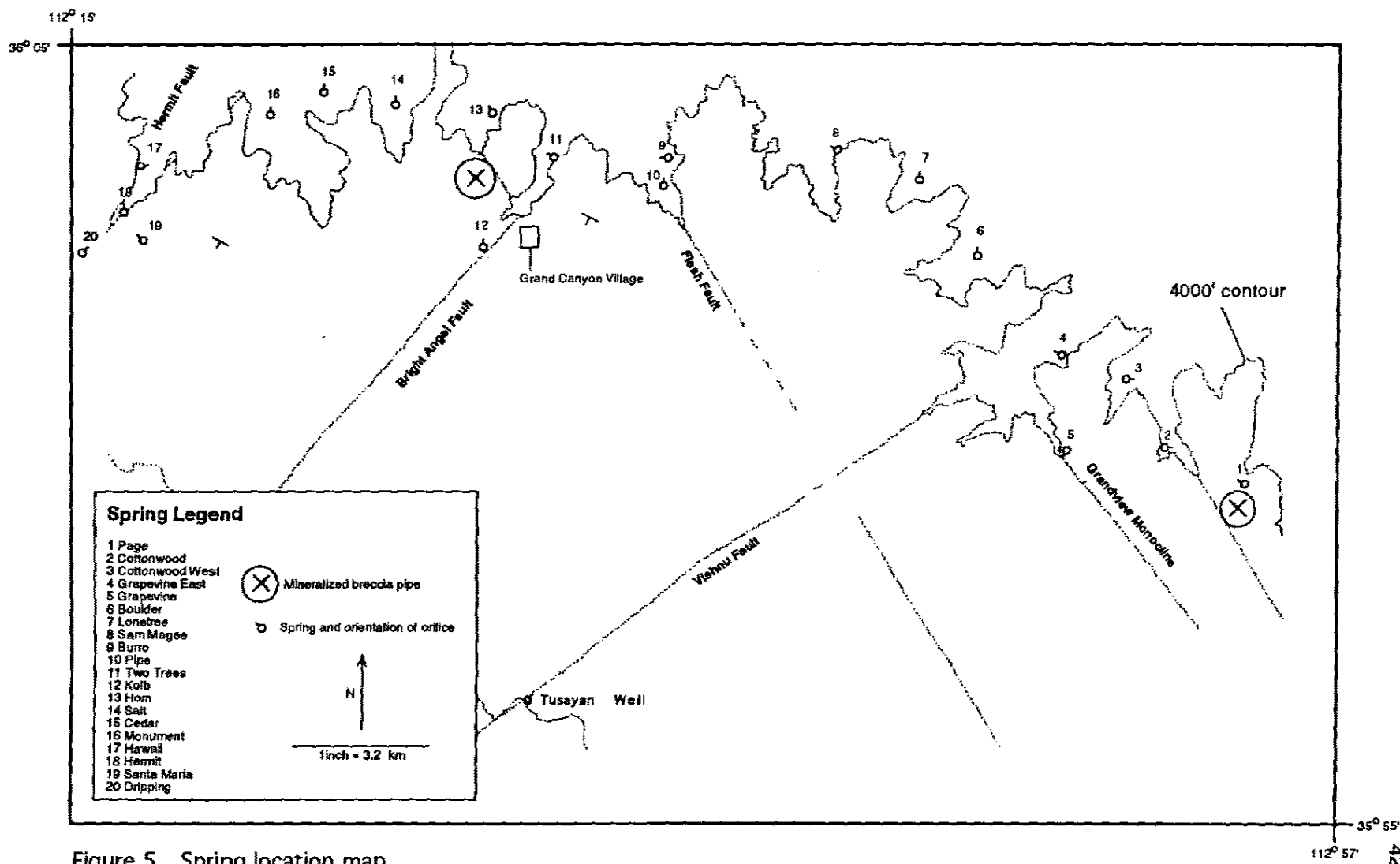


Figure 5. Spring location map.

Table 2. B) Seasonal sampling results for uranium measurements

Spring Name	Date	UT*(ppb)	1- $\sigma$	AR	1- $\sigma$
Page Spring	5/12/95	3.9	0.1	1.6	0.139
	9/9/95	3.7	0.2	1.6	0.111
Average		3.8		1.60	0.13
Std Dev		0.1		0.00	0.02
Spring Name	Date	UT*(ppb)	1- $\sigma$	AR	1- $\sigma$
Pipe Creek	4/29/94	2.0	0.2	2.8	0.52
	6/4/95	2.4	0.1	2.7	0.157
Average		2.2		2.75	0.34
Std Dev		0.3		0.07	0.26
Spring Name	Date	UT*(ppb)	1- $\sigma$	AR	1- $\sigma$
Two Trees Spring	4/30/94	0.6	0.2	3.5	0.654
	6/5/95	0.6	0.2	3.7	0.31
Average		0.6		3.60	0.48
Std Dev		0.0		0.14	0.24
Spring Name	Date	UT*(ppb)	1- $\sigma$	AR	1- $\sigma$
Horn Creek	4/30/94	24.7	0.3	0.94	0.032
	3/19/95	92.7	0.2	0.8	0.011
	6/5/95	27.6	0.3	1	0.023
Average		48.3		0.91	0.02
Std Dev		38.5		0.10	0.01

\* UT = total  $^{238}\text{U}$  (ppb)

### SAMPLE LIMITATIONS

Contact springs discharging directly from the rock outcrop are ideal sampling locations because the geology that the groundwater issues from can be directly observed, and there is minimal risk of chemical changes in water chemistry. Ideally, the sample is collected directly from the rock outcrop, but in the Grand Canyon sample location is limited by the presence of inner-basin sediment described in Chapter 2. At several sample sites modern alluvium has buried the spring orifice, and water that flows from the Paleozoic rock and into alluvium interacts with sediment and modern meteoric water. Cottonwood, Grapevine, Pipe, Horn, and Monument

Springs all discharge from inner basin sediment (Figure 5). Additional sample error could arise from evaporation and/or mixing with modern precipitation at the spring orifice. For example, in the case of tritium, the TR is expected to be higher if evapotranspiration and/or mixing occurs.

Major ion samples were not collected from all South Rim springs. As discussed in Chapter 2, Foust and Hoppe (1985) suggested that major ion water samples should be collected during low-flow conditions to accurately represent the dissolved constituents in spring waters. Intermittent springs were dry during the time of major ion sampling, and perennial springs were assumed to be at low flow conditions (Foust and Hoppe, 1985; Goings, 1985). Consequently, intermittent springs were not sampled for major ions but were sampled for tritium and uranium.

Several of the springs sampled in this study have not previously been sampled; therefore no historic discharge or hydrogeochemical data exists for comparison. Springs that lack historic data include Page, Cottonwood, Cottonwood West, Grapevine Hell, Grapevine East, Grapevine, Boulder, Lonetree, Sam Magee, Cremation, Kolb, Cedar, and Matkatamiba Springs (Figure 5).

### **SPRING OUTCROP GEOLOGY**

Spring waters that were sampled from the Paleozoic carbonate rock outcrop include Page, Cottonwood West, Grapevine-Hell, Grapevine East, Lonetree, Sam Magee, Burro, Kolb, Two Trees, Salt, Cedar, Hawaii, Hermit, Santa Maria, and Dripping Springs (Figure 5). Cottonwood, Grapevine, Pipe, Horn, and Monument

Springs are locations where water flows through inner basin sediment before surfacing; therefore samples were collected from inner basin sediment.

The majority of contact springs (i.e., Paleozoic orifice) discharge from the Bright Angel Shale-Muav Limestone contact. Dripping, Santa Maria, and Kolb Springs issue from the Upper Clastic Unit and are associated with perched aquifers (Metzger, 1961; Huntoon, 1982) (Figure 2). The remaining contact springs issue from the outcrop between the Thunder Springs Member of the Redwall Limestone and the Tapeats Sandstone (Figure 2).

### **SPRING DISCHARGE**

Discharge from springs that issue from the South Rim walls of the eastern Grand Canyon is fairly constant (USGS, 1996; Metzger, 1961; Huntoon, 1982). Appendix III lists the measured discharge from South Rim springs for the 1994-1995 water year. In general, outcrop springs have relatively constant discharge. However, spring water which flows through alluvium tends to have a seasonally variable discharge. Diurnal fluctuations in stream discharge were observed at Grapevine Spring where surface-water flow ceases at night.

Several of the springs sampled in this study flow intermittently which include Cottonwood West, Grapevine Hell, Boulder, Cremation, Kolb, and Cedar Springs (Appendix III). Intermittent springs are classified as seeps because their maximum discharge is less than 1 liter per minute. The latter springs typically cease flowing during the summer months and begin flowing in January-March.

## FIELD PHYSIOCHEMISTRY

Standard water quality parameters were measured each time a spring was sampled for environmental isotopes. Table 3 lists the results of field physiochemical measurements for all springs sampled. In summary, South Rim springs are below standard state temperature (i.e., 25 °C), have high buffering capacity ( $\text{pH} > 6$ ), and abundant dissolved solids (Table 3).

## MAJOR ION CONCENTRATIONS

Owing to lithology, most South Rim springs are heavily mineralized and of poor water quality. The major ion data collected in July 1995 is plotted on a Piper-diagram in order to display chemical variation between spring waters (Table 4) (Figure 6). In general, anion species in South Rim waters vary, whereas cation concentrations do not significantly differ (Figure 6). North Rim water, sampled from the Indian Garden Pump Station, is a calcium-bicarbonate water (Figure 6). South Rim spring waters, however, are predominantly calcium-magnesium-bicarbonate waters, although some are calcium-magnesium-sulfate waters (Figure 6). In South Rim waters, bicarbonate and sulfate concentrations are variable while chloride is semi-constant. Additionally, the magnesium to calcium ratio is 1 for the majority of South Rim springs (Table 4) (Figure 6).

## TRITIUM

Springs and wells sampled from the South Rim Aquifer had minimal variation in their  $^3\text{H}$  concentrations (Table 2 A)). Twelve of the sample locations have tritium ratios between -1 and 2 TR which include Page, Cottonwood, Grapevine East,

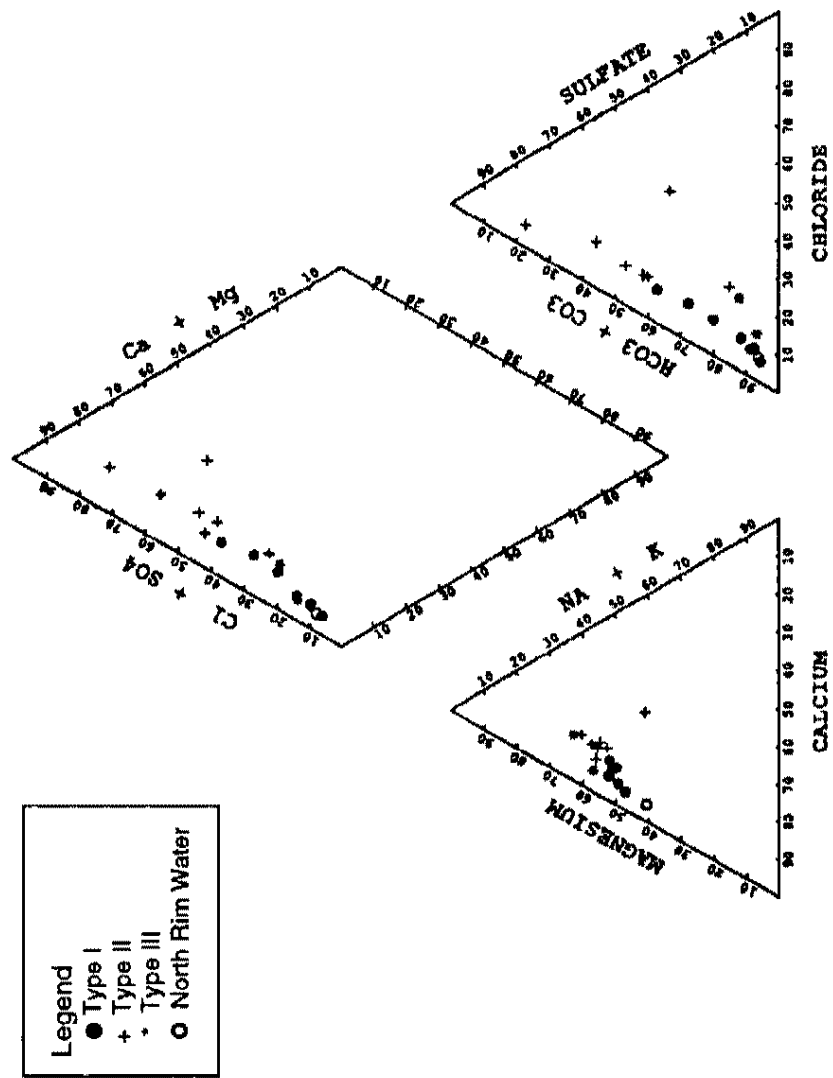


Figure 6. Piper diagram plot of eastern Grand Canyon springs.



Grapevine, Sam Magee, Burro, Pipe, Two Trees, Hawaii, Hermit, Dripping Springs, the Canyon Mine, and the Squire Inn Wells (Figure 7) (Table 5 A)). The remaining South Rim springs (i.e., Cottonwood West, Boulder, Lonetree, Kolb, Horn, Cedar, Monument, and Santa Maria Springs) had tritium concentrations that are between 2 to 5 TR (Figure 7) (Table 5 A)).

## URANIUM

In general, South Rim springs showed a large variance in their  $^{234}\text{U}/^{238}\text{U}$  activity ratio and total  $^{238}\text{U}$  concentration. For example, Horn Spring, located just east of Two Trees Spring (Figure 5), had a very high total  $^{238}\text{U}$  concentration and an average  $^{234}\text{U}/^{238}\text{U}$  activity ratio of 1 AR (Table 2 B)). Conversely, Cottonwood, Grapevine, Two Trees, and Dripping Springs have dilute total  $^{238}\text{U}$  concentrations and  $^{234}\text{U}/^{238}\text{U}$  activity ratios that fall between 3 and 4 AR (Table 5 B)). Burro, Pipe, Hawaii, and Hermit Springs have intermediate total  $^{238}\text{U}$  concentrations and  $^{234}\text{U}/^{238}\text{U}$  activity ratios at approximately 3 AR (Table 5 B)). The remaining springs (i.e., Cottonwood West, Grapevine Hell, Boulder, Lonetree, Sam Magee, Salt, Cedar, Monument, and Santa Maria Springs), have high total  $^{238}\text{U}$  concentrations and  $^{234}\text{U}/^{238}\text{U}$  activity ratios that range between 1.5 and 2.5 AR (Table 5 B)).

Table 3. Field measured physiochemistry data (1994-1995).

Sample Station	Date	T (C)	pH	TDS(g/l)	Alk (mg/l)
Dripping Spring	3/17/95	14.6	7	0.152	145
	7/22/95	16.8	8.5	0.169	134
Santa Maria Spring	3/17/95	14	7	0.145	194
	7/22/95	16	8.63	0.237	167
Hawaii Spring	3/18/95	18	6		210
	7/21/95	19.8	8.15	0.26	190
	11/25/95	17.9	8	0.07	206
Hermit Source Spring	3/18/95	17.5	7		208
	7/21/95	19.6	8.59	0.216	194
Monument Creek	3/18/95	18	7	0.989	218
	7/20/95	23.5	7.58	0.663	234
	11/25/95	17.9	8	0.492	200
Cedar Spring	3/18/95	15	7	0.466	250
	11/26/95	10	8	0.401	221
Salt Creek	3/19/95	13.3	7	0.758	191
	7/20/95	20.9	7.90	0.811	na
	11/26/95	10.1	8	0.705	194
Horn Creek	3/19/95	13.5	6	0.527	198
	6/5/95	17.2	7.09	0.522	235
	7/19/95	21.5	7.47	0.503	280
	11/26/95	14	7	0.312	272
Two Trees Spring	11/14/94	18.2		0.210	
	7/19/95	18.7	7.65	0.222	176
	11/26/95	18.3	7	0.211	184
	6/5/95	18.3	7.54	0.115	
	7/19/95	22.7	7.44	0.236	196
Pipe Creek	11/14/94	11.5		0.3	
	6/4/95	16.6	7.14	0.333	190
	7/19/95	22.6	8.04	0.321	206
	1/11/94	8.3	6	0.27	
	4/29/94	13	7	0.3	215
Burro Spring	11/14/94	11.5		0.28	
	7/19/95	20	8.36	0.321	220
	6/4/95	18.7	7.12	1.072	84
	11/14/94	9.5		0.23	
Cremation Creek	6/3/95	17	7.6	0.394	138
Sam Magee Spring	7/19/95	19.8	8.1	0.377	138
	1/10/94	2.9	6	0.63	
	11/13/94	9.8		0.7	
Lonetree Spring	6/3/95	19.7	6.95	0.607	360
	7/18/95	24.6	7.21	0.72	450
	6/3/95	21.5	7.08	0.898	90
	1/9/94	5.6	6	0.33	
Boulder Creek	1/10/94	2.7	6	0.32	
Grapevine Creek	11/12/94	11.7		0.36	
	5/13/95	12.8	7.2	0.279	265
	7/17/95	19	7	0.157	256
Grapevine East Spring	11/12/94	10.1		0.24	
	5/13/95	20	8.1	0.344	150
	7/17/95	26.2	7	0.453	272
Grapevine-Hell Spring	5/13/95	22.7	8.44	0.892	301
Cottonwood Creek	11/11/94	13.4		0.35	
	5/12/95	13	7.49	0.34	300
	7/16/95	19	7.97	0.398	390
Cottonwood West Spring	5/13/95	21.8	7.8		420
Page Spring	1/8/94	8		0.214	
	11/11/94	13.1		0.206	
	5/12/95	12.6	8.2	0.191	142
	7/16/95	16.5	8.23	0.218	125
	9/9/95	17.4	8.27		

Table 4. Major ion concentrations (mg/l) in South Rim Springs, collected in July, 1995.

Sample Station	Ca	2- $\sigma$	Mg	2- $\sigma$	Na	2- $\sigma$	K	2- $\sigma$	SO <sub>4</sub>	2- $\sigma$	HCO <sub>3</sub>	Cl	2- $\sigma$	F	2- $\sigma$	Br	2- $\sigma$	NO <sub>3</sub>	NO <sub>4</sub>	2- $\sigma$
Page Spring	24.56	0.29	33.77	0.35	0	NA	3.82	0.02	42.7	0.28	125	23	0.33	0		0.197	0.01	5.64	1.27	0.068
Cottonwood Spring	81.62	1.79	62.13	1.23	12.22	0.31	4.41	0.02	31	0.175	390	20	0.03	0		0.166	0.008	0.102	0.02	0.002
Grapevine East Spring	77.59	1.8	74.72	2.19	19.2	0.09	7.03	0.09	173	2.61	272	35	0.132	0.141	0	0.236	0.006	0.145	0.03	0.01
Grapevine Spring	62.68	0.95	36.87	0.24	6.24	0.1	1.86	0.08	12.4	0.041	256	9.17	0.091	0.093	0.002	0.09	0.003	0.369	0.083	0.002
Lonetree Spring	115.69	3.03	121.17	0.09	50.86	1.24	14.37	0.06	303.5	1.44	450	57	0.06	0		0.451	0.012	0.087	0.02	0.003
Sam Magee Spring	55.45	0.84	57.09	0.6	20.54	0.16	6.63	0.17	186	0.134	138	29.9	0.3	0.5	0.025	0.269	0.007	15.4	3.48	0.159
Burro Spring	56.95	0.56	47.11	1.23	15.84	0.04	4.29	0.002	75.9	0.087	220	20.1	0.094	0		0.157	0.006	1.79	0.404	0.012
Pipe Spring	65.52	0.64	50.48	1.25	14.59	0.11	4.69	0.08	110.5	0.018	206	19.6	0.137	0		0.126	0	1.734	0.392	0.033
Two Trees Spring	46.46	0.71	34.77	0.86	7.43	0.02	1.51	0.04	22.2	0.002	196	12.5	0.23	0		0.113	0.005	2.09	0.47	0.003
IGS	42.01	0.92	33.86	1.1	7.25	0.05	1.74	0.06	21.8	0.001	176	12.7	0.198	0.094	0.004	0.11	0.006	2.81	0.63	0.01
IGPS	37.23	0.65	17.61	0.32	1.28	0.006	0.58	0.01	3.72	0.011	150	3.31	0.032	0.1	0.005	0		0.862	0.195	0.021
Horn Spring	87.78	1.71	81.99	1.06	32.51	0.18	13.66	0.21	239.1	0.701	280	39.3	0.203	0		0.207	0.01	0.549	0.124	0.002
Salt Spring	126.99	3.16	143.8	0.38	47.73	0.21	19.16	0.24	674.3	0.695	190	38.1	0.365	0		0.16	0.006	4.38	0.989	0.058
Monument Spring	89.48	2.37	72.91	0.56	92.63	6.99	8.48	0.24	199.8	4.37	234	162.9	0.572	0		0.482	0.015	9.66	2.18	0.316
Hawaii Spring	49.30	0.003	36.3	0.53	12.29	0.34	2.54	0.003	42	0.012	190	14.9	0.129	0		0.11	0.002	2.79	0.63	0.021
Hermit Spring	49.00	0.39	31.5	1.18	6.36	0.13	1.5	0.02	13.5	0.003	194	10.9	0.14	0.099	0.001	0.087	0.003	2.9	0.655	0.064
Santa Maria Spring	27.71	0.4	41.22	0.68	12.83	0.08	3.85	0.02	23	0.06	167	26.7	0.051	0		0.228	0	6.24	1.41	0.021
Dripping Spring	30.50	0.62	27.65	0.97	4.57	0.03	1.08	0.01	8.72	0.05	134	11.8	0.189	0.154	0.003	0.13	0.001	5.7	1.29	0.024

Table 5. A) Tritium results from South Rim springs.

Sample Station	Date	pCi/l	2- $\sigma$	TR	2- $\sigma$
Indian Garden Pump Station	4/30/94	20	6	6.27	1.88
Canyon Mine Well	5/14/94	-1.4	8	-0.44	2.51
Pipe Spring	9/26/94	4.629	2.845	1.43499	0.89
Indian Garden Spring	9/26/94	3.222	2.777	0.99882	0.87
Page Spring	11/11/94	3.446	2.636	1.06826	0.83
Cottonwood Spring	11/11/94	4.581	2.974	1.42011	0.93
Cottonwood Spring	11/12/94	3.391	3.449	1.05121	1.08
Grape East Spring	11/12/94	5.118	2.986	1.58658	0.94
Cottonwood West Spring	11/12/94	7.25	2.71	2.2475	0.85
Grapevine Spring	11/12/94	6.112	2.854	1.89472	0.89
Lonetree Spring	11/13/94	11.627	3.073	3.60437	0.96
Sam Magee Spring	11/14/94	2.791	3.344	0.86521	1.05
Pipe Spring	11/14/94	6.337	2.776	1.96447	0.87
Squire Inn Well	11/15/94	2.767	3.315	0.85777	1.04
Indian Garden Pump Station	11/26/94	2.1	5	0.66	1.57
Indian Garden Pump Station	11/26/94	13.613	3.032	4.22003	0.95
Two Trees Spring	11/26/94	2.577	2.703	0.79887	0.85
Kolb Spring	11/27/94	10.555	2.713	3.27205	0.85
Lab Blank "Fossil Water"	12/20/94	4.432	3.468	1.37392	1.09
South-rim rain-water	2/25/95	34.1	7	10.69	2.19
Cottonwood Spring	2/25/95	7.1	6	2.23	1.88
Santa Maria Spring	3/17/95	9.4	6	2.95	1.88
Dripping Spring	3/17/95	0.5	7	0.16	2.19
Upper Hermit Creek	3/17/95	19.9	7	6.24	2.19
Hermit Spring	3/17/95	3.6	8	1.13	2.51
Hawaii Spring	3/18/95	1.6	8	0.50	2.51
Monument Creek	3/18/95	9.1	7	2.85	2.19
Cedar Spring	3/18/95	8.8	6	2.76	1.88
Salt Creek	3/19/95	18	9	5.64	2.82
Burro Spring	4/29/95	6.1	9	1.91	2.82
Pipe Spring	4/29/95	3	10	0.94	3.13
Bright Angel Creek	4/30/95	19	13	5.96	4.08
Two Trees Spring	4/30/95	-1.5	10	-0.47	3.13
Horn Creek	4/30/95	7.4	7	2.32	2.19
Page Spring	5/12/95	4	6	1.25	1.88
Squire Inn Well	5/17/95	-1.3	10	-0.41	3.13
Two Trees Spring	5/18/95	-0.3	7	-0.09	2.19
Boulder Spring	6/3/95	12	5	3.76	1.57
Cremation Spring	6/4/95	23	8	7.21	2.51
Page Spring	7/16/95	6	6	1.88	1.88
Cottonwood Spring	7/16/95	5	7	1.57	2.19
Indian Garden Pump Station	7/19/95	6.6	10	2.07	3.13
Fence Fault Spring (S)	7/31/95	9	8	2.82	2.51
Fence Fault Spring (N)	7/31/95	8	9	2.51	2.82
Vacy's Paradise Spring	8/1/95	16	8	5.02	2.51
Monkey Flower Spring	8/1/95	14	8	4.39	2.51
Deer Spring South	8/4/95	9	8	2.82	2.51
Tapeats Creek	8/4/95	16	10	5.02	3.13
Matkatiamiba Spring	8/5/95	4	8	1.25	2.51
Ledges Spring	8/5/95	<1		0	

Table 5. B) Uranium results from South Rim springs.

Sample Station	Date	238 (pCi/l)	1- $\sigma$	238 (ug/l)	234 (pCi/l)	AR	1- $\sigma$
Dripping Spring	3/17/95	0.47	0.05	1.3	1.65	3.5	0.946
Santa Maria Spring	3/17/95	2.21	0.03	6.2	4.3	1.9	0.083
Hawaii Spring	3/18/95	0.94	0.02	2.6	2.68	2.8	0.21
Hermit Source Spring	3/18/95	1.01	0.02	2.8	2.89	2.9	0.18
Monument Creek	3/18/95	3.24	0.04	9	6.71	2.1	0.066
Cedar Spring	3/18/95	5.57	0.05	15.6	10.59	1.9	0.052
Salt Creek	3/19/95	5.23	0.05	14.6	8.03	1.5	0.041
Horn Creek	4/30/94	8.76	0.09	24.7	8.22	0.94	0.032
	3/19/95	33.21	0.12	92.7	27.82	0.8	0.011
	6/5/95	9.9	0.08	27.6	9.48	1	0.023
Two Trees Spring	4/30/94	0.643	0.05	1.81	2.26	3.5	0.654
	6/5/95	0.59	0.02	1.6	2.16	3.7	0.31
Pipe Creek	4/29/94	0.723	0.05	2.04	2.04	2.8	0.52
	6/4/95	0.85	0.02	2.4	2.33	2.7	0.157
Burro Spring	4/29/94	0.861	0.08	2.43	2.23	2.6	0.59
Cremation Creek	6/4/95	2.72	0.06	7.6	5.35	2	0.108
Sam Magee Spring	6/3/95	1.35	0.02	3.8	2.2	1.6	0.083
Lonetree Spring	6/3/95	1.71	0.03	4.8	2.71	1.6	0.071
Boulder Creek	6/3/95	2.46	0.03	6.9	4.84	2	0.084
Grapevine Spring	5/13/95	0.42	0.01	1.2	1.54	3.6	0.286
Grapevine East Spring	5/13/95	1	0.05	2.8	1.68	1.7	0.198
Grapevine-Hell Spring	5/13/95	2.5	0.06	7	4.94	2	0.117
Cottonwood Spring	5/12/95	0.41	0.01	1.1	1.47	3.6	0.42
Cottonwood West Spring	5/13/95	1.6	0.03	4.5	3.53	2.2	0.095
Page Spring	5/12/95	1.41	0.05	3.9	2.24	1.6	0.139
	9/9/95	1.31	0.03	3.7	2.09	1.6	0.111
Indian Garden Pump Station	4/30/94	0.074	0.06	0.21	0.356	4.8	9.25
Bright Angel Creek (N. Rim)	4/30/94	0.154	0.08	0.055197	0.819	3.8	5.32

## **CHAPTER 6 DISCUSSION**

### **INTRODUCTION**

Various lithologies and structures in the Paleozoic strata are controlling groundwater flow and ultimately the residence time and resultant water chemistry of South Rim spring waters. For the purpose of discussion, springs are grouped on the basis of their associated geology and annual average discharge. This latter dichotomy permits a comparison of springs that is dependent on spring geology, and not geochemistry. Five groups of springs are thus classified under this convention.

In general, Type I through IV springs discharge from the South Rim of the Grand Canyon, and Type V springs issue from the southern and eastern edges of the North Rim (Figure 1 and 5). Type I springs generally have moderate discharge and are associated with high-angle normal faults (Table 6); Type II springs have low discharge and issue from hydrogeologically isolated canyon mesas (Figure 5) (Table 7); Type III have low discharge and issue from the Upper Clastic Unit (Table 8); Type IV are geologically similar to Type II springs but have intermittent flow (Table 9); and Type V springs have highly variable discharge and issue from the North Rim Aquifer (Table 10).

## SPRING TYPES

### Type I Springs

The Type I springs typically surface near the head waters of tributaries to the Colorado River. Spring waters discharge from the Lower Clastic and Carbonate Units, between the Bright Angel Shale and the basal members of the Redwall Limestone (Figure 2). Major faults and/or folds in the Paleozoic strata appear to dictate the flow path of Type I spring waters (Figure 5).

Table 6. South Rim spring data, collected (1994-1995) from Type I springs.

Spring Name	Eiv <sup>a</sup>	Q (gpm)	T (°C)	pH	TDS	TR	2-σ	AR	1-σ	U ppb <sup>**</sup>	1-σ
Hawaii Spring	4240	3	19.8	8.3	260	0.5	2.5	2.8	0.2	2.6	0.05
Hermit Spring	4320	314*	19.6	8.5	216	1.1	2.5	2.9	0.2	2.8	0.06
Two Trees Spring	3760	221*	22.7	7.4	236	0.2	0.9	3.6	0.3	1.7	0.04
Pipe Spring	3680	104*	22.6	8.4	321	1.5	0.9	2.8	0.2	2.2	0.13
Burro Spring	3700	4	20	8.4	321	1.9	2.8	2.6	0.6	2.4	0.22
Grapevine Spring	4000	5	19	7.2	320	1.9	0.9	3.6	0.3	1.2	0.04
Cottonwood Spring	3680	5.4*	19	7.9	396	1.6	0.9	3.6	0.4	1.1	0.04
Average		109	20.6	8.0	279	1.2		3.0		2.2	
Std Dev		132	1.6	0.2	47.7	0.7		0.4		0.6	
Max		314	22.7	8.4	396.0	1.9		3.6		2.8	
Min		3	19.0	7.2	216.0	0.2		2.6		1.1	

Field measurements are average values for individual springs

<sup>a</sup> Elevation, feet above mean sea level

<sup>\*\*</sup> Total uranium-238

<sup>\*</sup> USGS, oral communication 1995

The fact that Hermit, Hawaii, Two Trees, Pipe, Burro, Grapevine, and Cottonwood Springs are associated with the Hermit, Bright Angel, Flash, Vishnu, and McKee Faults, respectively, is strong evidence that geologic structures are controlling groundwater flow to Type I springs (Figure 5).

For the 1995 water year, high flow occurred from January to February and low discharge was in July (Appendix IV). Averaging flow from Type I springs, produces a mean annual discharge of 109 gpm, though individual spring flow varied by  $\pm 132$  gpm (Table 6). Hermit and Two Trees Springs had the highest flow rates, 314 and 221 gpm, respectively (USGS, 1995). As stated in Chapter 5, springs that issue directly from the outcrop tend to discharge at a fairly constant annual rate. Conversely, springs that discharge from inner basin alluvium, tend to fluctuate in flow diurnally and annually. Hawaii, Two Trees, and Burro Springs flow at a fairly constant rates, whereas, Hermit, Pipe, Grapevine and Cottonwood Springs have variable discharge.

The average water temperature and pH measured for Type I springs were 20 °C and 8.0, respectively, and the average TDS value was 263 mg/l (Table 6). Type I springs are  $\text{Ca}^{2+}$  -  $\text{Mg}^{2+}$  -  $\text{HCO}_3^-$  waters that have a  $[\text{Mg}^{2+}]/[\text{Ca}^{2+}]$  ratio typically less than 1. Additionally, sulfate values are low relative to bicarbonate (Figure 6).

Tritium concentrations in Type I springs are low relative to modern precipitation levels (Table 5 A)). The mean concentration for the spring population is 1.2 TR and varies by  $\pm 0.2$  TR. Burro and Grapevine Springs exhibited the greatest  $^3\text{H}$  concentration (1.9 TR), and Two Trees Spring water contained the least amount of  $^3\text{H}$  (0.2 TR) (Table 5 A)).

Trace amounts of  $^{238}\text{U}$  were measured in Type I springs, with an average concentration of 2.0 ppb (Table 5 B)). Hermit and Cottonwood Spring waters had the highest and lowest  $^{238}\text{U}$  concentrations respectively (Table 5 B)). Type I Springs



were found to have high AR, with a mean  $^{234}\text{U}/^{238}\text{U}$  activity ratio of 3.1 AR. Two Trees, Grapevine, and Cottonwood Springs had the highest  $^{234}\text{U}/^{238}\text{U}$  activity ratio (3.6 AR) (Table 5 B)), whereas Hermit, Hawaii, Pipe, and Burro Springs had lower ARs, which range from 2.6 to 2.9 AR.

### **Type II Springs**

Type II springs issue from Grand Canyon mesas, which extend out from the South Rim and generally dip toward the Colorado River gorge (Figure 5) (Table 7). Originating from the Lower Clastic and Lower Carbonate hydrostratigraphic units, Type II springs discharge between the Tapeats Sandstone and the Redwall Limestone (Figure 2). Groundwater typically flows from siliciclastic beds in the Bright Angel Shale. Monument, Salt, Horn, Lonetree, and Grapevine East Springs all issue from the upper portion of the Tapeats Sandstone, whereas Sam Magee and Page Spring flow from the contact between the Muav and Redwall Limestones (Figure 2).

Type II springs are not located in the proximity of large faults but are associated with northwest trending Grandview Monocline (Figure 5). Sam Magee, Lonetree, Grapevine East, and Page discharge along the fold axis of the Grandview Monocline. In addition, mineralized breccia pipes, that extend vertically into the Redwall Limestone, are present on the South Rim, above the majority of Type II spring orifices (Figure 5).

Discharge from Type II springs is low and almost constant diurnally and annually. During the 1995 water year, the average flow for Type II springs was 1.5

gpm. Monument Spring had the highest average discharge of 5 gpm, and the remaining springs discharged less than 2 gpm. (Table 7).

Table 7. South Rim spring data, collected (1994-1995) from Type II springs.

Spring Name	EIV <sup>A</sup>	Q (gpm)	T(°C)	pH	TDS	TR	2-σ	AR	1-σ	U ppb <sup>**</sup>	1-σ
Monument Spring	3300	5	23.5	7.6	668	2.9	2.19	2.1	0.1	9.0	0.11
Salt Spring	3900	0.3	20.9	7.9	811	5.6	2.82	1.5	0	14.6	0.13
Horn Spring	3900	0.5	21.5	7.5	503	3.4	1.88	0.9	0.1	48.3	0.22
Sam Magee Spring	4000	0.25	19.8	8.1	377	0.9	1.05	1.6	0.1	3.8	0.07
Lonetree Spring	3680	0.75	24.6	7.2	720	3.7	0.96	1.6	0.1	4.8	0.08
Grapevine E Spring	3640	2	26.2	7.6	453	1.6	0.94	1.7	0.2	2.8	0.14
Page Spring	4320	1.5	16.5	8.2	218	1.4	0.8	1.6	0.1	3.8	0.07
Matkatamiba Spring	2800	1	25			1.3	2.5				
Average		1.5	21.9	7.7	536	2.6		1.6		12.4	
Std Dev		1.7	3.2	0.5	209	1.6		0.4		16.3	
Max		5	26.2	8.2	811	5.6		2.1		48.3	
Min		1	16.5	6.7	218	0.9		0.9		2.8	

Field measurements are average values for individual springs

<sup>A</sup> Elevation, feet above mean sea level

<sup>\*\*</sup> Total uranium-238

Type II springs have an average water temperature of 22 °C and average pH of 7.7. The spring waters are abundant in dissolved salts, with an average TDS of 536 mg/l (Table 7). Type II springs are classified as intermediate  $Mg^{2+}$  -  $Ca^{2+}$  -  $HCO_3^-$  -  $SO_4^{2-}$  waters and show a large variation in anionic species (Figure 6). The  $[Mg^{2+}]/[Ca^{2+}]$  ratio is greater than 1, and bicarbonate concentrations appear to be inversely proportional to sulfate concentrations. In Salt and Sam Magee Springs, the sulfate concentration is greater than bicarbonate, and Monument Spring contains high levels of chloride (Figure 6) (Table 7). In general, for Type II springs, the TDS values are on average a factor of 2 greater than Type I springs. The higher TDS in

Type II springs could be due to one of two processes: 1) long groundwater residence time or 2) high mineral concentration due to small flow volume.

The concentration of tritiated groundwater in Type II springs is low relative to modern levels, but is higher than Type I springs. The average  $^3\text{H}$  concentration found in Type I spring waters is  $2.6 \pm 1.6$  TR over the spring population (Table 7).

Lonetree Spring had the highest  $^3\text{H}$  concentration (5.6 TR), and Sam Magee had the lowest  $^3\text{H}$  concentration (0.9 TR).

Total  $^{238}\text{U}$  concentrations in Type II spring waters were extremely high. The average  $^{238}\text{U}$  concentration for the population was 11.7 ppb and varied by 16.3 ppb. During March 1995 a  $^{238}\text{U}$  concentration of 48.3 ppb was measured in Horn Spring water. Of Type II springs, Grapevine East Spring had the lowest  $^{238}\text{U}$  concentration (2.8 ppb) (Table 7). The average  $^{234}\text{U}/^{238}\text{U}$  activity ratio in Type II waters was  $1.6 \pm 0.4$  AR. Monument Spring had the highest  $^{234}\text{U}/^{238}\text{U}$  activity ratio (2.1 AR), and Horn Creek, had the lowest  $^{234}\text{U}/^{238}\text{U}$  activity ratio, which was equal to unity.

### Type III Springs

Santa Maria and Dripping Springs are separated from other South Rim springs because they discharge from the Upper Clastic hydrostratigraphic unit (Figure 2). Both springs are located in the eastern portion of the study area, and they are in the vicinity of the Hermit Fault. Santa Maria Spring issues from the Esplanade Sandstone Formation in the Supai Group, and Dripping Spring discharges from the Hermit Shale-Coconino Sandstone contact (Figure 2). Santa Maria Spring discharges laterally along sandstone beds, whereas at Dripping Spring, flow is concentrated

along fractures in the Coconino Sandstone, below the north dipping Ermita Monocline (Figure 5).

Table 8. South Rim spring data, collected (1994-1995) from Type III springs.

Spring Name	Elv <sup>^</sup>	Q (gpm)	T(°C)	pH	TDS	TR	2-σ	AR	1-σ	U ppb <sup>**</sup>	1-σ
Dripping Spring	6400	1	16.8	7.8	169	0.2	2.2	3.5	0.9	1.3	0.13
Santa Maria Spring	5400	0.5	16	7.8	273	2.9	1.88	1.9	0.1	6.2	0.09
Average		0.8	16.4	7.8	221.0	1.6		2.7		3.8	
Std Dev		0.4	0.6	0.0	73.5	2.0		1.1		3.5	
Max		1.0	16.8	7.8	273.0	2.9		3.5		6.2	
Min		0.5	16.0	7.8	169.0	0.2		1.9		1.3	

Field measurements are average values for individual springs

<sup>^</sup> Elevation, feet above mean sea level

<sup>\*\*</sup> Total <sup>238</sup>U

Santa Maria and Dripping Springs have low discharge rates relative to Type I and V springs (Table 8). Discharge from Santa Maria Spring varies annually, with high flow occurring in spring, whereas Dripping Spring discharges at a fairly constant annual rate.

The average temperature and pH measured during the investigation were 16.4 °C and 7.8, respectively. Dissolved salts in solution averaged about 200 mg/l for Type III springs (Table 8).

Dripping and Santa Maria Springs have different abundances of tritium and uranium isotopes. Both springs were sampled for tritium and uranium in March 1995. Santa Maria Spring had a <sup>3</sup>H concentration of  $3.0 \pm 1.9$  TR, and Dripping Spring had a <sup>3</sup>H concentration of  $0.2 \pm 2$  TR. Uranium samples had a <sup>234</sup>U/<sup>238</sup>U activity ratio of  $1.9 \pm 0.1$  and  $3.5 \pm 0.9$  for Santa Maria and Dripping Springs, respectively. Santa Maria Spring contained 6.2 ppb of <sup>238</sup>U, in contrast to Dripping Spring, which

contained 1.3 ppb  $^{238}\text{U}$  (Table 8). From the latter information, it is apparent that Santa Maria and Dipping Springs waters are both geologically and geochemically unrelated.

### Type IV Springs

Similar to Type II springs, Type IV springs typically discharge from canyon mesas within the Lower Clastic Unit. The Type IV spring waters, however, have intermittent discharge. Kolb Spring discharges from the Coconino Sandstone and is in the vicinity of the Bright Angel Fault (Figure 5). Discharge from Type IV springs generally terminates during summer and begins in Spring. All the Type IV springs are classified as “intermittent seeps”, because their high flow rate is less than 1 lpm.

Table 9. South Rim spring data, collected (1994-1995) from Type IV springs.

Spring Name	Elv <sup>A</sup>	Q (gpm)	T(°C)	pH	TDS	TR	2-σ	AR	1-σ	U ppb <sup>**</sup>	1-σ
Cedar Spring	3450	int	15	7.5	433.5	2.8	1.9	1.9	0.1	15.6	0.13
Kolb Spring	6000	int				3.4	0.9				
Cremation Spring	3600	int	18.7	7.12	1072	7.2	2.5	2.0	0.1	7.6	0.16
Boulder Spring	3520	int	21.5	7.08	898	3.8	1.6	2.0	0.1	6.9	0.09
Grapevine Hell Spring	3760	int	22.7	8.44	892			2.0	0.1	7	0.15
Cottonwood W Spring	3840	int	21.8	7.8		2.4	0.00	2.2	0.1	4.5	0.08
Average			19.9	7.6	823.9	3.9		2.0		8.3	
Std Dev			3.1	0.6	273.3	1.9		0.1		4.2	
Max			22.7	8.4	1072.0	7.2		2.2		15.6	
Min			15.0	7.1	433.5	2.4		1.9		4.5	

Field measurements are average values for individual springs

<sup>A</sup> Elevation, feet above mean sea level

<sup>\*\*</sup> Total uranium-238

The Type IV springs have an average water temperature of 20 °C and a pH of 7.6. Salty to brackish waters discharge from Type IV springs which have a mean TDS of 824 mg/l (Table 9). One of the brackish springs, Cremation Spring, had a

TDS value of 1072 mg/l in May 1995. The Type IV springs have a relatively high tritium concentrations, with an average of  $3.9 \pm 2.0$  TR. The average  $^{234}\text{U}/^{238}\text{U}$  activity ratio is  $2.0 \pm 0.1$  AR, and the average  $^{238}\text{U}$  concentration is  $8.7 \pm 4.2$  ppb (Table 9).

### Type V Springs

The North Rim springs (i.e., Type V springs), discharge water from the Kaibab Plateau. Huntton (1974), developed a hydrogeologic model of the North Rim Aquifer. Much like South Rim springs, Type V springs discharge from the Lower Carbonate and Clastic hydrostratigraphic units, and groundwater circulation is associated with faults and folds. Conversely, groundwater flow from the North Rim

Table 10. North Rim spring data, collected (1994-1995) from Type V springs.

Spring Name	Elev <sup>A</sup>	Q (gpm)	T(°C)	pH	TDS	TR	2-σ	AR	1-σ	U ppb <sup>**</sup>	1-σ
Fence Fault Spring (S)						2.8	2.5				
Fence Fault Spring (N)						2.5	2.8				
Vacy's Paradise Spring						5.0	2.5				
Monkey Flower Spring						4.4	2.5				
Bright Angel Creek			15.3	6	117	6.0	4.1	3.8	5.3	0.43	0.22
Indian Garden Pump Station		3740	24.1	8.02	152	2.5	47.6	4.8	9.3	0.21	0.18
Deer Spring South						2.8	2.5				
Tapeats Creek						5.0	3.1				
Ledges Spring						ND					
Average						19.7	7.0	135	3.5	4.3	0.3
Std Dev							1.4	24.7	1.8	0.7	0.2
Max							8.0	152.0	6.0	4.8	0.4
Min							6.0	117.0	0.0	3.8	0.2

Field measurements are average values for individual springs

<sup>A</sup> Elevation, feet above mean sea level

<sup>\*\*</sup> Total uranium-238

migrates rapidly through large fractures as a function of large effective fracture porosity (Huntton, 1974). Total discharge from the North Rim is not well

documented, but discharge fluctuates significantly on an annual basis (Huntoon, 1974; Brown and Moran, 1974).

North Rim water samples were collected along the Colorado River and from the Indian Garden Pump Station. Unlike the South Rim Aquifer, historic data indicates that North Rim water chemistry varies significantly on an annual basis (Hoppe and Foust, 1985). Milanovic (1981) suggests that variable water chemistry in carbonate aquifers (i.e., North Rim Aquifer) is an indication of rapidly flushing groundwater system. The Type V waters are  $\text{Ca}^{2+}$  -  $\text{HCO}_3^-$  waters (Figure 6), and have an average tritium concentration of  $3.5 \pm 1.8$  TR. The springs that were measured for uranium had high  $^{234}\text{U}/^{238}\text{U}$  activity ratios and very dilute amounts of  $^{238}\text{U}$  (Table 10).

## **GROUNDWATER RESIDENCE TIME**

### **Relative Age Date [ $^3\text{H}$ ]**

Using historic precipitation data from Flagstaff, Arizona and Albuquerque, New Mexico, the ages of spring waters (i.e. the travel time of groundwater) in the South Rim Aquifer were estimated to be greater than 40 years or pre-thermonuclear testing. Pre-thermonuclear testing data from Buttlar and Libby (1954), and the IAEA (1960-1991), provide baseline annual  $^3\text{H}$  levels in precipitation over the project site (Figure 4) (Table 11 and 12). These data sets indicate the following: 1) water recharged prior to 1940 should have little to no  $^3\text{H}$ ; 2) water recharged between 1940 and 1951 may have between 0.2 and 2 TR (Buttlar and Libby, 1954); 3) water recharged between 1951 and 1966 will have a  $^3\text{H}$  concentration greater than 100 TR

(Table 12); 4) water recharged between 1967 and 1978 may have between 20 and 60 TR (Table 12) and; 5) post 1980 water should have  $^3\text{H}$  concentrations greater than 10 TR.

South Rim precipitation had a  $^3\text{H}$  concentration of  $10.69 \pm 2.19$  TR in January 1995 (Table 5 A)). For the purpose of interpretation, the 1995 rainwater sample is assumed to represent the average concentration of tritium in modern precipitation over the South Rim. Storm runoff at Hermit Creek and Cremation Creek both have a tritium concentration between 7-14 TR which indicate current  $^3\text{H}$  levels in modern meteoric water are around 10 TR (Table 5 A)). Further, the  $^3\text{H}$  concentration in precipitation over Albuquerque, New Mexico was 10 TR in 1991 (Figure 4) (International Atomic Energy Agency, 1991).

In order to relative age date groundwater using tritium, two sets of assumptions were made. First, precipitation is the only source of  $^3\text{H}$ , the TR remains conservative within the subsurface, and the only loss of tritium is through radioactive decay. Second, within the soil and vadose zones, there is limited evaporation, negligible organic activity, and no significant dilution caused by mixing of old and modern precipitation.

Because  $^3\text{H}$  is bonded in the water molecule, it is a safe to assume that  $^3\text{H}$  remains chemically conservative in the subsurface (Murphy, 1993). Soil characteristics and surface-water drainage patterns on the South Rim strongly support the second set of assumptions discussed above. The soil zone for example is thin (20 to 60 inches), has moderate permeability, and remains saturated 2- 3 weeks per year



(EIS, 1985); therefore wet deposition will have a short residence time in the soil zone. Additionally, once soil water enters the Kaibab Limestone, infiltration is rapid due to dissolution cavities enhanced by faults and folds (Metzger, 1961; Huntoon, 1974; Milanovic, 1981). The lack of perennial streams on the South Rim is another indication that wet deposition rapidly infiltrates into the vadose zone (Metzger, 1961). Zukosky (1995), using stable oxygen and hydrogen isotopes, suggested that limited evaporation occurs in the vadose zone. The consistently different, yet internally constant,  $^{238}\text{U}/^{234}\text{U}$  activity ratio “fingerprints” of Type I through IV spring waters, help support the assumption that there is limited mixing of old and modern water in the unsaturated zone.

Table 11. Possible levels of tritium in South Rim precipitation prior to thermonuclear testing. Decay corrected tritium level (PTR) to 1996 relative to a given time (e.g. 1942).

Year	Natural level		Range of values	
	TR	TR	PTR <sup>a</sup>	PTR <sup>a</sup>
1940	5	20	0.2	0.9
1941	5	20	0.2	0.9
1942	5	20	0.2	1.0
1943	5	20	0.3	1.0
1944	5	20	0.3	1.1
1945	5	20	0.3	1.2
1946	5	20	0.3	1.2
1947	5	20	0.3	1.3
1948	5	20	0.3	1.4
1949	5	20	0.4	1.5
1950	5	20	0.4	1.5
1951	5	20	0.4	1.6

<sup>a</sup> Decay corrected present tritium ratio (PTR)

Under the second group of assumptions, it follows that precipitation which enters the South Rim during a particular time period serves as a reference point indicating when the groundwater residence time “clock” starts. The reported data

suggest that the TR in spring waters will reflect the following relative age correlations (Table 11 and 12).

- Waters with less than 0.5 TR are older than 1940.
- Waters with 0.5 to 2 TR were likely recharged between 1940 and 1950.
- Waters with 2 to 10 TR are post 1951 or a mix of old and modern water.

Table 12. Historic precipitation isotope data from the IAEA.

Flagstaff, Arizona			Albuquerque, New Mexico		
Year	TR	PTR <sup>A</sup>	Year	TR	PTR <sup>A</sup>
1962	952	143.3	1975	60	18.6
1963	1415	225.2	1976	60.3	19.8
1964	980	164.9	1977	49.7	17.2
1965	455	80.9	1978	45.4	16.7
1966	572	107.6	1979	22.9	8.9
1967	344	68.3	1980	23.3	9.6
1968	115	24.2	1981	35.7	15.5
1969	153	34.0	1982	28.9	13.3
1970	97	22.8	1983	16.2	7.9
1971	100	24.8	1984	16.5	8.5
1972	47	12.3	1985	19.7	10.7
1973	136	37.8	1986	17.3	9.9
1974	68	20.0	1987	11.2	6.8
			1988	18.9	12.1
			1989	10	6.8
			1990	11.4	8.2
			1991	8.6	6.5
			1995**	10.7	10.1

\* Time from present (1995)

<sup>A</sup> Decay corrected present tritium ratio (PTR)

\*\* Ppt sample from the eastern Grand Canyon, collected 2/95

The concentration of tritiated water measured in South Rim springs is below the concentration of  $^3\text{H}$  in 1995 precipitation (Figure 7) (Table 12). In addition, South Rim springs contain no obvious bomb-pulse  $^3\text{H}$  recharged between 1951 and 1971 (Table 12). The Canyon Mine and Squire Inn Wells have less than 0.5 TR which may mean that groundwater south of the Colorado River gorge (i.e., Grand

Canyon) is likely to be greater than 51 years old (Figure 7) (Table 5 A)). Moreover, Dripping, Hawaii, and Two Trees Springs also contain less than 0.5 TR, indicating their waters are greater than 51 years old (Table 5 A)).

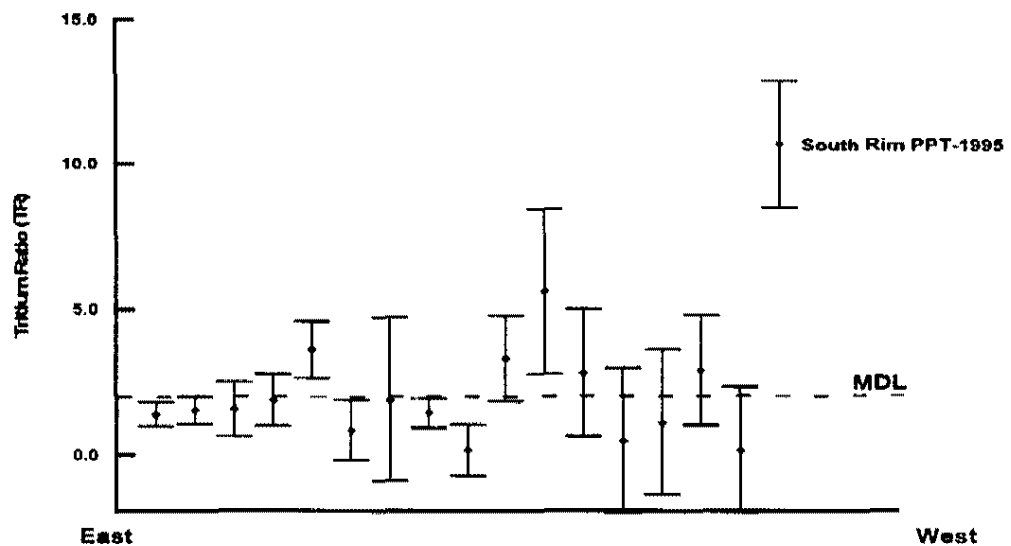


Figure 7. Measured  $^3\text{H}$  concentrations in eastern Grand Canyon springs.

Hermit, Pipe, Burro, Sam Magee, Grapevine, Grapevine East, Cottonwood, and Page Springs have less than 2 TR, meaning their waters were deposited on the South Rim between 1940 and 1950 (Figure 7) (Table 5 A)).

Spring waters with  $^3\text{H}$  concentrations greater than 2 TR may be a mix of old and modern waters (Figure 7) (Table 5 A)). This hypothesis is especially valid for springs that discharge from inner basin alluvium as discussed in Chapter 2 (e.g.,

Monument, Salt, Horn, and Lonetree Springs). Under this hypothesis, pre-bomb pulse  $^3\text{H}$  in groundwater, which discharges from the Lower Clastic and Carbonate hydrostratigraphic units and subsequently percolates through quaternary alluvium, would mix with modern precipitation captured in the inner basin sediment.

An example of effective mixing with modern precipitation is Lonetree Spring which is spatially and stratigraphically related to Sam Magee Spring (Figure 2), yet their TRs vary substantially (Table 7). This inconsistency could be due to analytical error, mixing with modern rainwater, and/or evaporation at the spring orifice. The  $^{234}\text{U}/^{238}\text{U}$  activity ratio fingerprint is a good indicator of mixing when compared with tritium levels, because the AR does not change when mixed with a solution containing no uranium (Osmond and Cowart, 1976). Lonetree Spring sample has a higher TR than Sam Magee Spring while their  $^{234}\text{U}/^{238}\text{U}$  activity ratio remains constant. Modern precipitation may have mixed with groundwater at the spring orifice which contains no uranium. Lonetree Spring was sampled in November 1995, while it was raining; therefore mixing with modern rainwater at Lonetree Spring is the probable cause for the TR anomaly that exists between Lonetree and Sam Magee Springs.

Santa Maria Spring, which is associated with a perched aquifer (i.e., Type III spring) (Metzger, 1961), appears to be younger than waters that discharge from the lower hydrostratigraphic units. Dripping Spring, which is also a Type III spring, is stratigraphically higher than Santa Maria Spring, yet has one of the lowest measured TR in the project site (0.2 TR) (Table 5 A)). Perched water west of Hermit spring basin appears to be pre-bomb water, whereas perched water east of Hermit spring

basin contains post-1951  $^3\text{H}$  (Figure 7). This inconsistency illustrates the variety of groundwater bodies present in the South Rim. In addition, the geology present at Type III springs does not positively correlate with water chemistry unlike Type I and II springs

### **Hydrogeochemical Evolution**

Dedolomitization may occur in aquifers containing limestones, dolostones, in combination with sulfate minerals (i.e., gypsum and anhydrite) (Plummer et al., 1990); this process results from the irreversible dissolution of gypsum and subsequent saturation of the solution with respect to the mineral calcite. Dedolomitization is defined as a chemical process where dolomite dissolves while calcite precipitates as a result of gypsum dissolution.

Water chemistry trends in spring waters indicate that dedolomitization is occurring in the South Rim Aquifer. Gypsiferous layers are present in the Lower Carbonate Unit (Chapter 2), and both Type I and II waters have  $[\text{Mg}^{2+}]/[\text{Ca}^{2+}]$  ratios that are about unity (Figure 8). Additionally, past research suggest that lithology is controlling water chemistry (Foust and Hoppe, 1985; Metzger, 1961). Based on the results from measured major ion concentrations in spring waters and generated output from the geochemical model PHREEQE (Parkhurst et al., 1993), data suggest that calcite is precipitating while dolomite is dissolving, as a result of irreversible gypsum dissolution in the South Rim Aquifer.

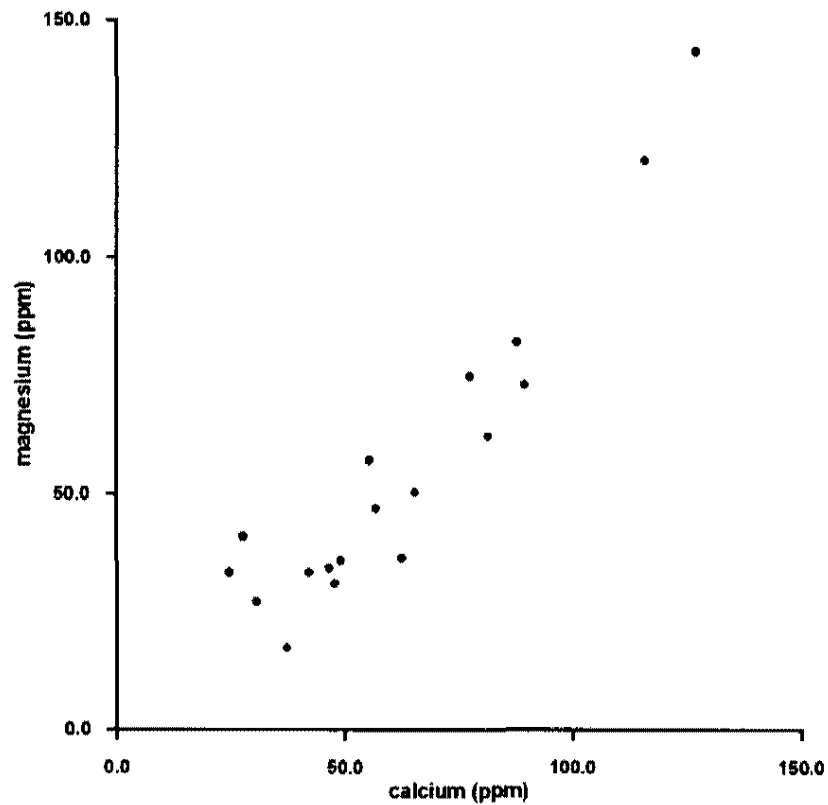
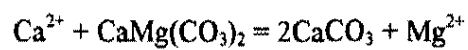


Figure 8. Scatter plot illustrating a general linear relationship between  $\text{Ca}^{2+}$  and  $\text{Mg}^{2+}$  concentrations in all measured South Rim spring waters.

Dedolomitization occurs in a closed carbonate aquifer (i.e., fixed  $P_{\text{CO}_2}$ ) which contains calcite and dolomite minerals, where the  $[\text{Ca}^{2+}]/[\text{Mg}^{2+}]$  ratio evolves toward unity.



$$K_{\text{rn}} = [\text{Mg}^{2+}]/[\text{Ca}^{2+}].$$

At equilibrium, dolomite is highly insoluble relative to calcite and the  $[Mg^{2+}]/[Ca^{2+}]$  ratio remains fixed (Appelo and Postma, 1994). However, if gypsum or anhydrite are present, dissolution of dolomite can occur where the  $SO_4^{2-}$  concentration increases coeval with the  $[Mg^{2+}]/[Ca^{2+}]$  ratio. The disassociation of gypsum reacts as follows:



$$K_{gyp} = [Ca^{2+}][SO_4^{2-}][H_2O]^2.$$

Through substitution, the equilibrium constants can be combined to form:

$$K_{4.22} = [Mg^{2+}]/[Ca^{2+}] = K_{dol} / K_{cal}^{1/2} = 10^{-17.09} / (10^{-8.48})^2 = 0.8.$$

As gypsum dissolves, the  $Ca^{2+}$  concentration in solution increases to the point of calcite saturation which results in the precipitation of calcite. Consequently, the total alkalinity decreases by consumption of carbonate, which in turn facilitates the dissolution of dolomite; thus increases the  $Ca^{2+}$  and  $Mg^{2+}$  concentrations in solution. The  $[Mg^{2+}]/[Ca^{2+}]$  ratio remains close to unity in accord with equilibrium between calcite and dolomite, but the  $SO_4^{2-}$  concentration increases (Appelo and Postma, 1993; Plummer et al., 1990).

The magnesium concentration in South Rim spring water increases coincident with the  $SO_4^{2-}$  concentration (Figure 9). Dissolution of gypsum lowers the pH which results in enhanced dissolution of dolomite. Moreover, the consumption of  $CO_3^{2-}$  species by precipitation of calcium carbonate reduces the buffering capacity of groundwater. The end result is a constant  $[Mg^{2+}]/[Ca^{2+}]$  of  $\sim 0.8$  and precipitation of calcium carbonate.

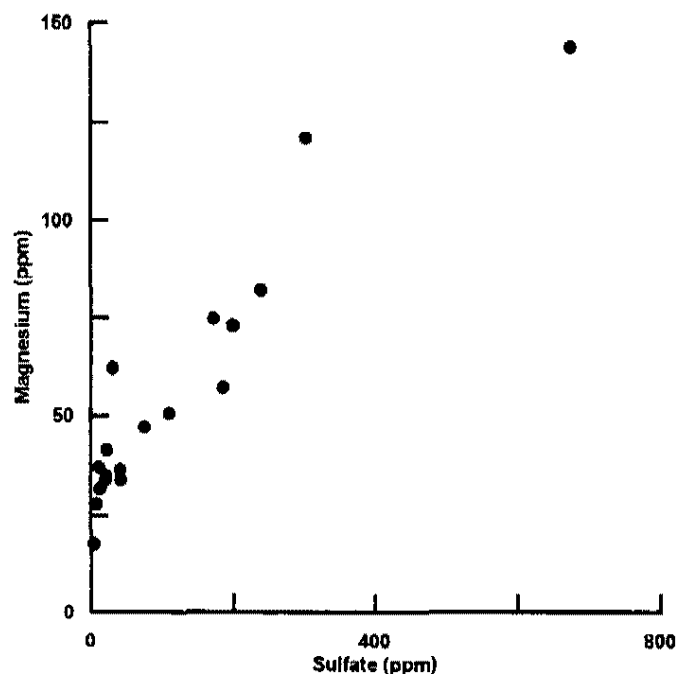


Figure 9. Magnesium versus sulfate concentrations in all measured South Rim springs.

Figure 10 is a plot of calcite and gypsum saturation indices (SI) versus sulfate concentration. Calcite clusters around equilibrium regardless of  $\text{SO}_4^{2-}$  concentration, whereas the SI of gypsum approaches equilibrium with increases in  $\text{SO}_4^{2-}$  concentration. The chemical trends indicate most spring waters are over-saturated with respect to calcite, whereas the solution approaches gypsum saturation with increases in sulfate concentration (Figure 10).

A comparison of measured and modeled concentrations of  $\text{Ca}^{2+}$ ,  $\text{Mg}^{2+}$ ,  $\text{HCO}_3^-$ , and  $\text{SO}_4^{2-}$  in Type I and II spring waters also supports the hypothesis that dedolomitization is occurring in the South Rim Aquifer (Table 13). A two step computer simulation was conducted to depict the evolution of South Rim groundwaters.



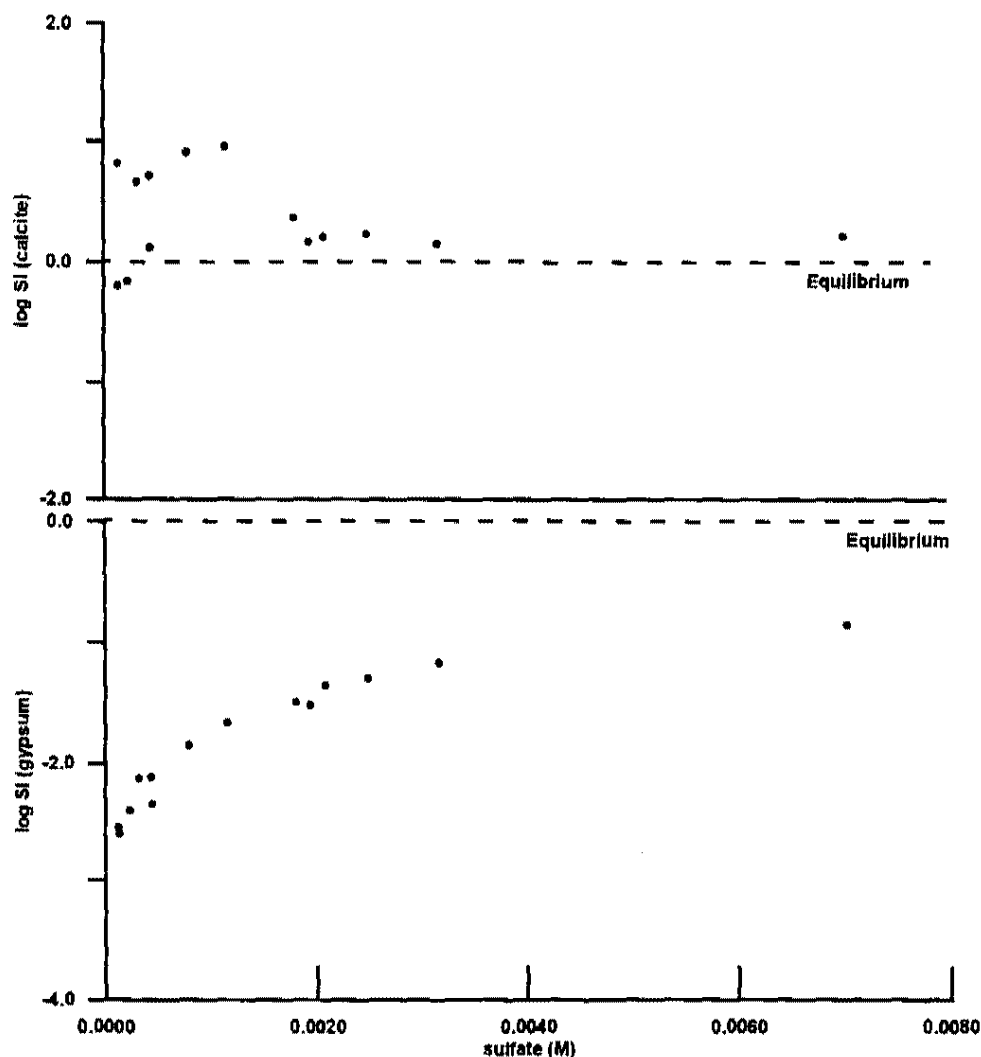


Figure 10. Scatter plots of mineral saturation index as a function of sulfate concentration.

Target solutions, which contain the average measured major ion concentrations in Type I and II springs, were equilibrated with calcite, dolomite, and gypsum, in order to calculate their respective SI. The second step attempted to predict the average major ion concentration in groundwater using the average annual pH and dissolved constituents in South Rim precipitation (NPS, 1996).

For Type I and II springs PHREEQE predicted measured pH values and major ion concentrations with errors of 0 to 20 % of modeled values (Table 13). Since the

measured values are averaged over the spring populations, the percent differences between model output and measured data are probably not statistically significant.

PHREEQE calculated negative  $\Delta$  phase values for the mineral calcite for both Type I and II springs. The model predicts calcite is precipitating.

Table 13. A) and B): Type I and II springs average measured parameters compared to modeled output.

Parameter	Measured	Modeled	% Error	$\Delta$ Phase**
	Molality	Molality		
pH	8.0	8.0	0	
Calcium	0.001463	0.001162	21	-0.00077
Magnesium	0.001757	0.001397	20	0.0014
Bicarbonate	0.003656	0.0040482	-11	
Sulfate	0.000457	0.0005398	15	0.000535

\*\* negative  $\Delta$  phase values indicate precipitation of mineral.

Parameter	Measured	Modeled	% Error	$\Delta$ Phase**
	Molality	Molality		
pH	7.7	7.7	0	
Calcium	0.00206	0.0017867	13	-0.004408
Magnesium	0.0034418	0.0031622	8	0.0031609
Bicarbonate	0.0034931	0.0039286	-12	
Sulfate	0.0027063	0.0030349	11	0.0030298

\*\* negative  $\Delta$  phase values indicate precipitation of mineral.

The following lines of evidence strongly support the hypothesis that dedolomitization is occurring in the South Rim Aquifer: 1) water chemistry trends previously discussed (Figure 8 and 9); 2) gypsiferous beds are present in the Lower Carbonate Unit (i.e., Chapter 2); and 3) PHREEQE output predicts a dependence on sulfate concentration and precipitation of calcite (Figure 9) (Table 13). These results show that groundwater chemistry is dependent on rock mineralogy (i.e., carbonates) and groundwater residence time.

### Uranium-series Disequilibrium

Uranium data indicate that the  $^{234}\text{U}/^{238}\text{U}$  activity ratios in South Rim springs are not conservative and may increase in solution with increases in rock-water interaction. In addition, the South Rim Aquifer appears to be an open-augmenting system (Chapter 3), where dissolved uranium is not conservative as a result of dedolomitization. Plotting uranium isotope data on 2-D scatter plots in accordance with standard methods (Osmond and Cowart, 1974), reveals consistent trends between  $^{234}\text{U}/^{238}\text{U}$  activity ratios and total  $^{238}\text{U}$  in South Rim spring waters. Due to the dedolomitization process, calcium carbonate precipitated on the aquifer matrix may be capturing uranium complexes; therefore producing an effective medium for the transfer of  $^{234}\text{U}$  into solution through alpha recoil (Chapter 3). As a result, the longer the groundwater residence time, the higher the  $^{234}\text{U}/^{238}\text{U}$  activity ratio. A similar trend in uranium chemistry was recognized by Kronfeld et al. (1994) who suggested that the  $^{234}\text{U}/^{238}\text{U}$  activity ratio in solution increases with increased rock-water interactions.

A positive correlation ( $r = 0.80$ ), was calculated between individual  $^{234}\text{U}/^{238}\text{U}$  activity ratio and  $S$  ( $1/\text{total } ^{238}\text{U}$  (ppb)) in spring waters (Figure 11). The latter correlation coefficient is statistically significant and conforms to the relationship noted by Osmond and Cowart (1976), such that as the total  $^{238}\text{U}$  concentration increases, the  $^{234}\text{U}/^{238}\text{U}$  activity ratio decreases. Two important conclusions can be made from this relationship: 1) the data is of good analytical quality; and 2) the South Rim Aquifer can be compared to similar groundwater systems.

Figure 12 is a plot of excess  $^{234}\text{U}$  as a function of total  $^{238}\text{U}$  concentration and reveals the presence of a common uranium mineral source with an  $^{234}\text{U}/^{238}\text{U}$  activity ratio of  $\sim 1$  AR for all South Rim springs. This uranium “fingerprint” is a result of acidic waters infiltrating through the weathered zone which leach uranium and other metals from the solid phase (Chapter 3). A possible source of uranium on the South Rim could be uraninite deposited in breccia pipes (Chapter 2). From the  $^{234}\text{U}$  excess graph (Figure 12), Type I springs group along the same linear trend with Havasu and Blue Springs, while Type II springs plot separately.

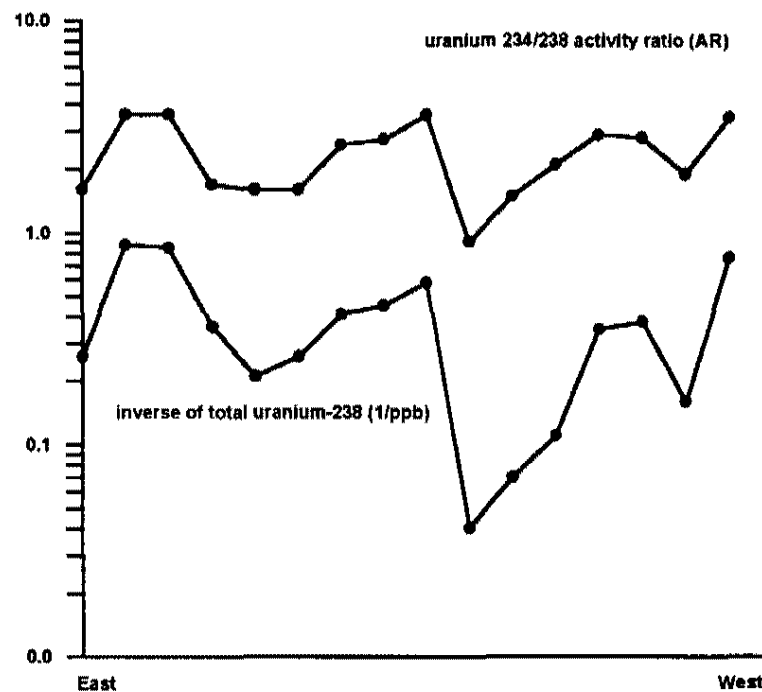


Figure 11. Plot illustrating a positive correlation ( $r = 0.80$ ) between  $^{234}\text{U}/^{238}\text{U}$  activity and  $1/\text{total } [^{238}\text{U}]$  (S).

Type II springs, in the eastern portion of the project site, also plot along a linear trend, but may be unrelated to Type I springs. Page, Grapevine East, Lonetree,

and Sam Magee Springs are all hydrostratigraphically and structurally related and plot along a distinctive linear trend (Figure 12). On the other hand, Type I springs plot along a linear trend with Havasu and Blue Springs. These trends indicate uranium is not conservative within the South Rim Aquifer.

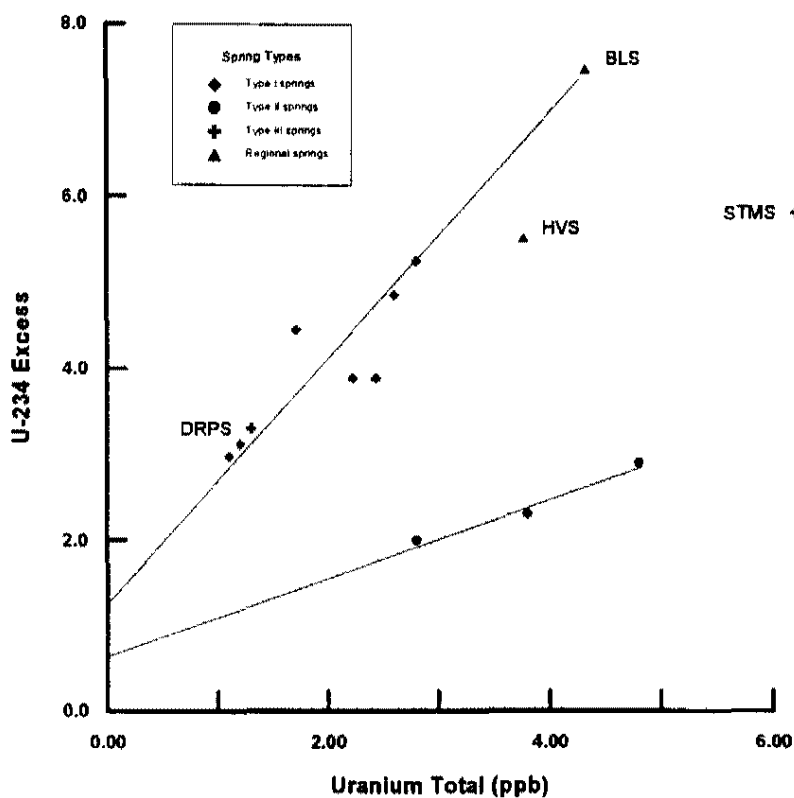


Figure 12.  $^{234}\text{U}$  excess versus total  $^{238}\text{U}$  concentration diagram, which illustrates possible geochemical evolution of groundwater in the South Rim Aquifer.

Figure 13 illustrates  $^{234}\text{U}/^{238}\text{U}$  activity ratio versus  $S$  which further supports the latter hypothesis that uranium is not conservative in the South Rim Aquifer. Two groups of South Rim springs are apparent in Figure 12: 1) Type I springs have high

$^{234}\text{U}/^{238}\text{U}$  activity ratios; 2) on the other hand, Type II and IV springs have low  $^{234}\text{U}/^{238}\text{U}$  activity ratios.

Type I springs plot as two distinct groups (Figure 13), where Type I<sub>A</sub> springs have  $^{234}\text{U}/^{238}\text{U}$  activity ratios  $> 3.5$  AR and total  $^{238}\text{U} < 2$  ppb (i.e.,  $S = 0.5$ ). Type I<sub>B</sub> springs have lower  $^{234}\text{U}/^{238}\text{U}$  activity ratios and lower total  $^{238}\text{U}$  values (Figure 13). Type II springs also plot into two distinct groups: 1) Type II<sub>A</sub> springs have  $^{234}\text{U}/^{238}\text{U}$  activity ratios of 1.6 AR and total  $^{238}\text{U} < 5$  ppb (i.e.,  $S = 0.2$ ); 2) Type II<sub>B</sub> springs plot separately with total  $^{238}\text{U} > 15$  ppb (i.e.,  $S = 0.06$ ) (Figure 13). Type III springs do not appear to be related to one another.

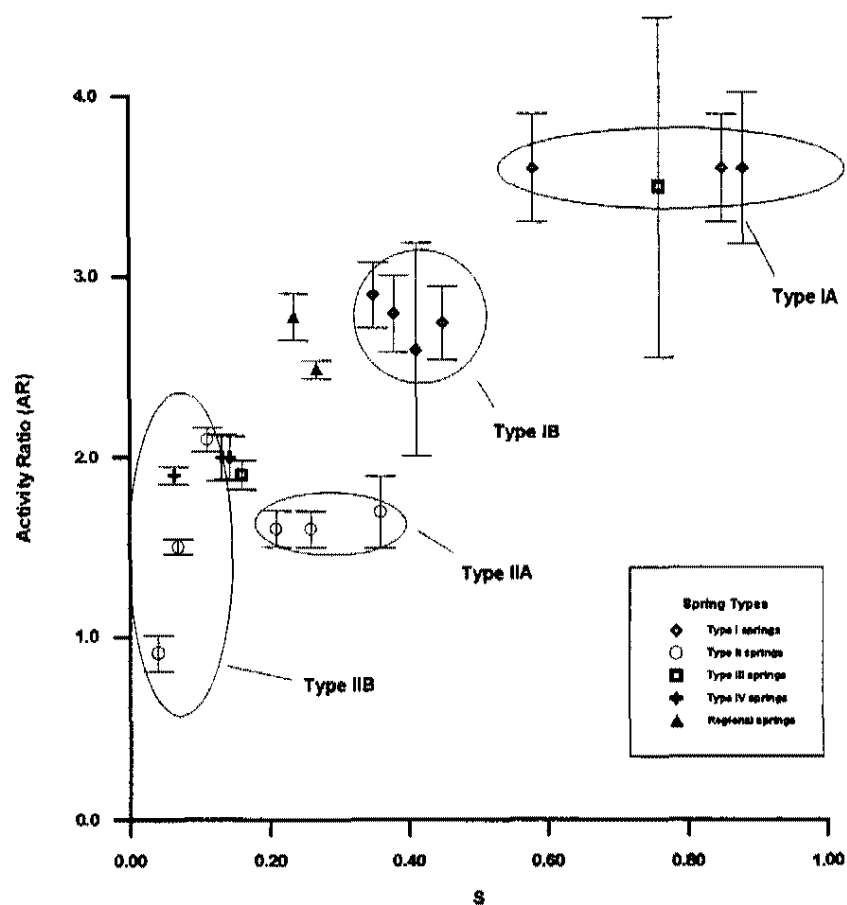


Figure 13. Plot of  $^{234}\text{U}/^{238}\text{U}$  activity ratio versus S, which illustrates different types of South Rim springs.

Figure 14, a plot of  $^{234}\text{U}/^{238}\text{U}$  activity ratio as a function of the tritium ratio, illustrates a sympathetic inverse relationship between Type I and II springs. Based on the relative ages determined with tritium, the preceding negative correlation indicates that higher  $^{234}\text{U}/^{238}\text{U}$  activity ratios may be a result of longer groundwater residence times. The latter conclusion is in agreement with Kronfeld et al. (1994) which correlated groundwater residence time to  $^{234}\text{U}/^{238}\text{U}$  activity ratio. The two spring clusters in Figure 14 may indicate that Type I springs have a longer subsurface residence time than Type II springs. In addition, Type I<sub>A</sub> springs have higher  $^{234}\text{U}/^{238}\text{U}$  activity ratios and lower  $^3\text{H}$  concentrations than Type I<sub>B</sub> springs which may be due to an even longer travel time (Figure 14).

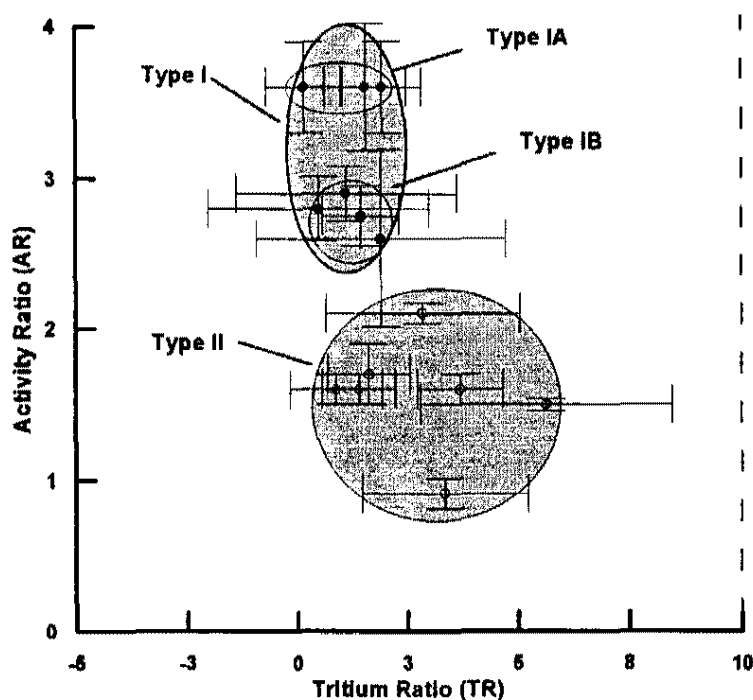


Figure 14. Scatter plot of  $^{234}\text{U}/^{238}\text{U}$  activity ratio as a function of the tritium ratio (i.e. age of spring water). Two clusters are recognizable and plot as Type I and II springs. Graph may indicate that older waters have higher activity ratios.

### Short Residence Time Aquifer

Horn Spring is located directly below a mineralized breccia pipe west of Two Trees Spring (Figure 5) and discharges from the Bright Angel Shale and inner basin sediment. Data suggest that base flow from Horn Spring is a product of spring discharge from Paleozoic carbonate rocks, whereas high flow results from groundwater which discharges from inner basin sediment. Seasonal water chemistry data at Horn Spring (Table 2) also suggest that at high flow Horn Spring waters are derived from a short lived groundwater system (i.e., short residence time). The latter, in turn, provides a key piece of evidence that supports the conclusion that South Rim spring waters have a long groundwater residence time (i.e., > 40 years). Counterintuitive to common hydrogeochemical expectations, total  $^{238}\text{U}$  was present in greater abundance in Horn Spring waters during high flow regimes than during low flow periods (Table 2).

Discharge at base flow has a fixed  $\text{P}_{\text{CO}_2}$ , high buffer capacity, and an average  $^{238}\text{U}$  concentration of  $24 \pm 0.3$  ppb. Water discharging during high flow has a pH of 6, and a  $^{238}\text{U}$  concentration of  $92.7 \pm 0.1$  ppb. The Horn Spring inner basin aquifer is unconfined and open system, so that at high flow regimes, theoretically, there is an infinite reservoir of  $\text{CO}_2$  gas available. As a result, the solution pH is slightly acidic (pH = 6), which can actively leach uranium from the mineral phase; therefore the solution contains high total  $^{238}\text{U}$  concentration and  $^{234}\text{U}/^{238}\text{U}$  activity ratio < 1 during high flow.



Since Horn Spring waters have a  $^3\text{H}$  concentration  $> 2$  TR and the dissolution and transport of uranium may occur over a short-time scale, this system may represents the rapid geochemical evolution of groundwaters. By comparing Horn Spring at high flow to other South Rim springs, it is evident that the Horn Spring has a significantly different groundwater residence time.

### GEOLOGIC CONTROL

The majority of South Rim springs discharge from the Lower Clastic and Carbonate hydrostratigraphic units (Figure 2), and contact springs are associated with the Bright Angel Shale and Muav Limestone. Major ion data indicates that various lithologies in the Paleozoic strata are influencing spring chemistry on a local scale which is in agreement with Foust and Hoppe (1985). Monument Spring is an example of the latter, where high concentrations of  $\text{Na}^+$  and  $\text{Cl}^-$  were measured (Figure 6); this may be due to local evaporite beds (KCl or NaCl) in the Supai Group (Foust and Hoppe, 1985).

Deformation and dissolution features in the Paleozoic carbonate rocks control the infiltration and circulation of water into and through the South Rim Aquifer (Metzger, 1961; Huntoon, 1974). As noted previously, secondary porosity created by South Rim faults, dissolution features, and folds have controlled the transmission of water through the Colorado Plateau since 190 to 200 Ma (Wenrich, 1986; Metzger 1961; Huntoon, 1974). The three types of structures controlling groundwater flow through the South Rim Aquifer are northeast and northwest trending normal faults,

dissolution features/breccia pipes, and north-west trending folds (Metzger, 1961; Wenrich, 1986; Huntoon, 1974).

The preceding relationship and location of South Rim springs may indicate that northwest trending faults and folds may be conduits for groundwater flow, whereas northeast trending faults may act as partial groundwater boundaries (Figure 15). An example of a potential boundary are faults transverse to the Bright Angel Fault (Figure 15). The static water level in the Tusayan Well indicates that the potentiometric surface of the South Rim Aquifer slopes toward the Colorado river with a gradient  $\sim 0.01$  (Figure 3). The Bright Angel Fault has 200 feet of offset (Huntoon and Sears, 1975) and places the Muav Limestone next to the Bright Angel Shale. Since the hydraulic gradient east of the Bright Angel Fault appears to be generally to the north-northwest, the Bright Angel Fault may act as a lateral boundary to groundwater flow east of the fault (Figure 15). Therefore, lateral boundaries created by structures could potentially isolate various groundwater bodies which evolve a unique array of chemistry (e.g., Type I and II springs).

Different groundwater flow patterns are also apparent in various plots of spring geochemical components as a function of latitude (Figure 16). This line-plot illustrates positive and negative correlations between major faults and spring chemistry. The Vishnu, Bright Angel, and Hermit Faults may be groundwater boundaries to groundwater flow, whereas, transverse faults and folds (not illustrated in cross-section) facilitate circulation east and west.

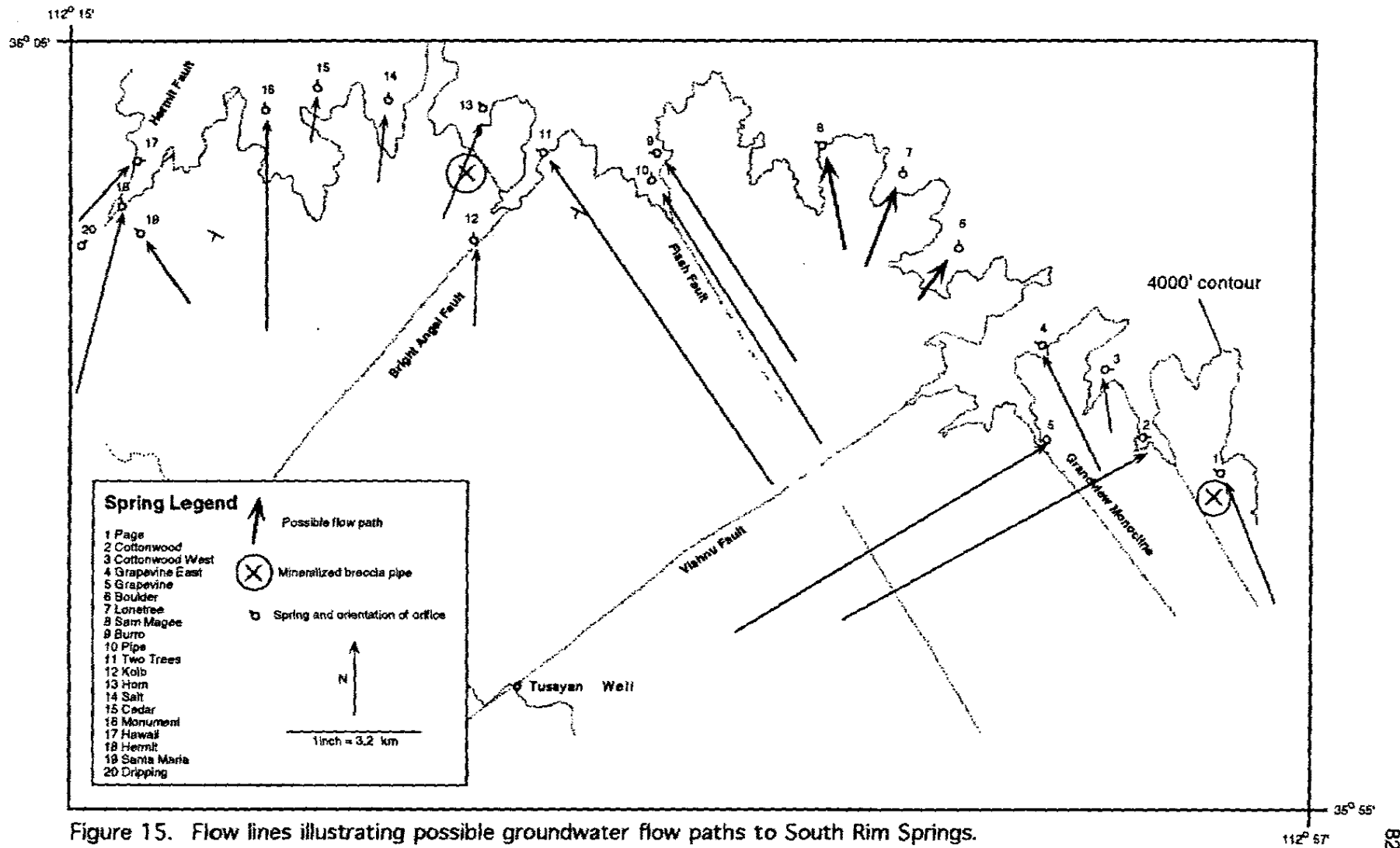


Figure 15. Flow lines illustrating possible groundwater flow paths to South Rim Springs. Length of arrow corresponds to the amount of discharge, where the longer the arrow, the greater the flow rate.

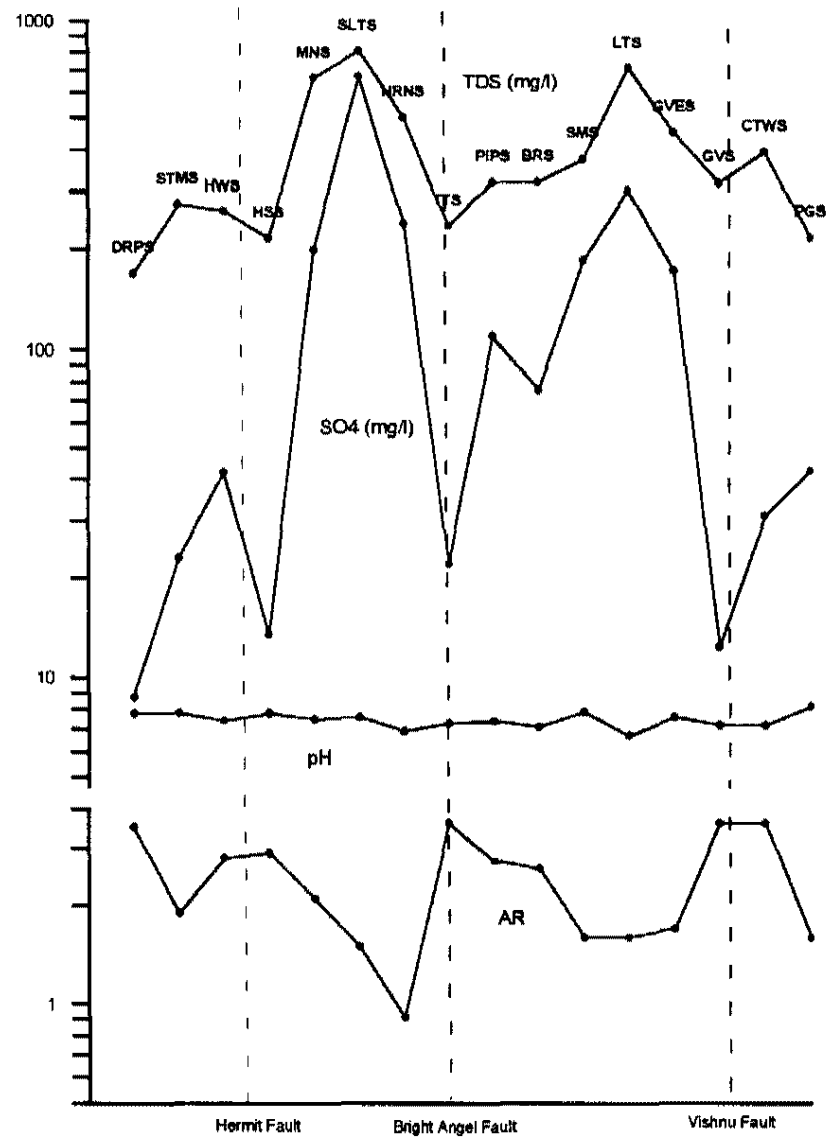


Figure 16. Cross-section plot illustrates changes in spring chemistry relative to high-angle normal faults and breccia pipes.

## CHAPTER 7 CONCLUSIONS

The purpose of this study was to determine the residence time of groundwaters discharging from the South Rim Aquifer using in-situ environmental isotopes (i.e., tritium and uranium); these results indicate subsurface residence times are greater than 40 years. This primary conclusion is supported by three lines of evidence which resulted from different facets of the study: 1) relative age of groundwaters is indicated to be greater than forty years by low  $^3\text{H}$  concentrations in South Rim waters; 2) the geochemistry of groundwaters reflect the process of dedolomitization; and 3) Uranium-series disequilibrium in spring waters indicates that uranium is not chemically conservative in the South Rim Aquifer as a result of dedolomitization, because uranium can be sorbed to calcite, indirectly increasing the  $^{234}\text{U}/^{238}\text{U}$  activity ratio in solution. Further, uranium data suggest that long groundwater residence times are associated with high  $^{234}\text{U}/^{238}\text{U}$  activity ratios in solution.

On a larger scale, this investigation suggests that Type I and II spring waters are the product of regional and local recharge respectively. High  $^{234}\text{U}/^{238}\text{U}$  activity ratios in Type I springs may be the result of longer groundwater residence time, where Type II springs have low  $^{234}\text{U}/^{238}\text{U}$  activity ratios and high  $^{238}\text{U}$  concentrations,

indicating shorter subsurface residence time. From the data collected in this investigation, it is apparent that groundwater is not rapidly transmitted through the Paleozoic strata; therefore the conclusion that the  $^{234}\text{U}/^{238}\text{U}$  activity ratio increases with longer travel times is strongly supported.

### **FURTHER RESEARCH**

With respect to development on the South Rim, this study indicates that increases in pumping from the South Rim Aquifer could reduce aquifer yield to the point where small seeps would dry-up or become intermittent. Further monitoring and research would further constrain this conclusion. Since this investigation is based on reconnaissance data and a small window of sampling time, South Rim springs should be periodically monitored for physiochemistry, major ions, uranium, and discharge. Future studies should include the use of chlorine-36 to determine the absolute age of groundwaters. Additionally, radium-226 and radon-222 are radionuclides which could be used to further investigate the geochemical evolution of uranium in the aquifer.

## APPENDIX I: Spring Data Sheets

### Dripping Spring

Spring Elevation 5600'

Geology Hermit Shale—Coconino Sandstone contact

Longitude/Latitude 36-03"98' 112-14"78'

#### Hydrochemical Data

Date of sample	pH	EC(ms/cm)	TDS(g/l)	T (C)	T air (C)	Alk (mg/l)	Q (l/m)
3/17/95	7	0.302	0.152	14.6	18.6	145	1
7/22/95	8.5	0.338	0.169	16.8	21.5	134	0.75
Average	7.8	0.320	0.161	15.7	20.1	140	0.9
Std Dev	1.1	0.025	0.012	1.6	2.1	8	0.18

Date of sample	TR	2-σ	AR	2-σ	J-238 (ug/l)	2-σ
3/17/95	0.16	2.19	3.5	0.946	1.3	0.01

Chemical Facies calcium-magnesium bicarbonate

**Comments:** Dripping Springs flows from the outcrop at the Hermit Shale-Coconino Sandstone.  
The spring orifice faces south-east, and fractures in the out crop are vertical.  
Discharge constant, water-samples collected from main drip above rock pool.

### Santa Maria Spring

Spring Elevation 5120'

Geology Esplanade Sandstone

Longitude/Latitude 36-03"57' 112-13"19'

#### Hydrochemical Data

Date of sample	pH	EC(ms/cm)	TDS(g/l)	T (C)	T air (C)	Alk (mg/l)	Q (l/m)
3/17/95	7	0.290	0.145	14	27.1	194	1
7/22/95	8.63	0.475	0.237	16	19.7	167	0.5
Average	7.8	0.383	0.191	15.0	23.4	181	0.8
Std Dev	1.2	0.131	0.065	1.4	5.2	19	0.35

Date of sample	TR	2-σ	AR	2-σ	J-238 (ug/l)	2-σ
3/17/95	2.95	1.88	1.9	0.083	6.2	0.02

Chemical Facies magnesium-calcium bicarbonate

**Comments:** Santa Maria Spring issues from sandstone beds in the Esplanade Formation.  
No associated structure but spring continuous laterally along bedding planes.  
Discharge varies annually, high flow during March.  
Water samples collected from the outcrop, above the rock shelter.  
During wet season springs abundant in laterally equivalent Esplanade Sandstone

## Hawaii Spring

Spring Elevation 3600'

Geology Muav Limestone

Longitude/Latitude 36-04"30' 112-13"06'

### Hydrochemical Data

Date of sample	pH	EC(ms/cm)	TDS(g/l)	T (C)	T air (C)	Alk (mg/l)	Q (l/m)
3/18/95	6			18	13.6	210	3
7/21/95	8.15	0.522	0.260	19.8	21.9	190	3
11/25/95	8	0.250	0.070	17.9	15.6	206	3
Average	7.4	0.386	0.17	18.6	17.0	202	3.0
Std Dev	1.2	0.192	0.13	1.1	4.3	11	

Date of sample	TR	2-σ	AR	2-σ	U-238 (ug/l)	2-σ
3/18/95	0.50	2.51	2.8	0.21	2.6	0.01

Chemical Facies magnesium bicarbonate

Comments: Discharge constant throughout duration of investigation.

## Hermit Source Spring

Spring Elevation 4320'

Geology Redwall Limestone

Longitude/Latitude NA

### Hydrochemical Data

Date of sample	pH	EC(ms/cm)	TDS(g/l)	T (C)	T air (C)	Alk (mg/l)	Q (l/m)
3/18/95	7			17.5	15	208	3
7/21/95	8.59	0.439	0.216	19.6	20.4	194	0.125
Average	7.8			18.6	17.7	201	1.6
Std Dev	1.1			1.5	3.8	10	2.0

Date of sample	TR	2-σ	AR	2-σ	U-238 (ug/l)	2-σ
3/18/95	1.13	2.51	2.9	0.18	2.8	0.010

Chemical Facies calcium-magnesium bicarbonate

Comments: Discharge constant throughout duration of investigation. Initial flow from the Temple Butte Limestone. No significant stream flow above the Redwall Limestone.



## Monument Spring

Spring Elevation 3280'

Geology Tapeats Sandstone-Bright Angel Shale

Longitude/Latitude 36-04°94' 112-11°14'

### Hydrochemical Data

Date of sample	pH	EC(mS/cm)	TDS(g/l)	T (C)	T air (C)	Alk (mg/l)	Q (l/m)
3/18/95	7	1.978	0.989	18	26	218	1
7/20/95	7.58	1.327	0.663	23.5	34.5	234	3
11/25/95	8	0.988	0.492	17.9	14.2	200	5
Average	7.5	1.4	0.7	19.8	24.9	217	3.0
Std Dev	0.5	0.5	0.3	3.2	10.2	17	2.0

Date of sample	TR	2-σ	AR	1-σ	U-238 (ug/l)	1-σ
3/18/95	2.85	2.19	2.1	0.07	9	0.1

Chemical Facies calcium-sodium chloride

Comments: Samples collected from inner-basin sediment. Significant influx and deposition of sediment during the study.

## Cedar Spring

Spring Elevation 3450'

Geology Tapeats Sandstone-Bright Angel Shale

Longitude/Latitude 36-05°15' 112-08°66'

### Hydrochemical Data

Date of sample	pH	EC(mS/cm)	TDS(g/l)	T (C)	T air (C)	Alk (mg/l)	Q (l/m)
3/18/95	7	0.934	0.466	15	20.7	250	0.5
7/20/95							DRY
11/26/95	8	0.799	0.401	10	13.3	221	0.5
Average	7.5	0.8665	0.4335	12.5	17	236	0.5
Std Dev	0.71	0.10	0.05	3.54	5.23	21	0.00

Date of sample	TR	2-σ	AR	1-σ	U-238 (ug/l)	1-σ
3/18/95	2.76	1.88	1.9	0.052	15.6	0.04

Chemical Facies

Comments: Dry in the summer months, when discharging only small pools present.  
High levels of dissolved uranium noted.

## Salt Creek

Spring Elevation 3760'

Geology Tapeats Sandstone-Bright Angel Shale

Longitude/Latitude 36-05"12' 112-09"71'

### Hydrochemical Data

Date of sample	pH	EC(ms/cm)	TDS(g/l)	T (C)	T air (C)	Alk (mg/l)	Q (l/m)
3/19/95	7	1.52	0.758	13.3	12.7	191	0.25
7/20/95	7.90	1.623	0.811	20.9	20.7		0.25
11/26/95	8	1.41	0.705	10.1	20.4	194	0.25
Average	7.6	1.518	0.758	14.8	17.9	193	0.3
Std Dev	0.6	0.107	0.053	5.5	4.5	2	0.0

Date of sample	TR	2-σ	AR	1-σ	U-238 (ug/l)	1-σ
3/19/95	5.64	2.82	1.5	0.04	14.6	0.03

Chemical Facies intermediate sulfate

Comments: Seeps flow from the Tapeats Sandstone mainly from opening in cross-bedding.

## Horn Spring

Spring Elevation 3600'

Geology Bright Angel Shale-Muav Limestone

Longitude/Latitude 36-05"15' 112-08"66'

### Hydrochemical Data

Date of sample	pH	EC(ms/cm)	TDS(g/l)	T (C)	T air (C)	Alk (mg/l)	Q (l/m)
3/19/95	6	1.049	0.527	13.5	14	198	1.5
6/5/95	7.09	1.03	0.522	17.2	26.3	235	0.25
7/19/95	7.47	1.005	0.503	21.5	25.4	280	0.25
11/26/95	7			14	17.8	272	0.25
Average	6.89	1.028	0.517	16.6	20.9	246	0.56
Std Dev	0.63	0.022	0.013	3.7	6.0	38	0.6

Date of sample	TR	2-σ	AR	1-σ	U-238 (ug/l)	1-σ
4/30/94	2.32	2.19	0.94	0.03	24.7	0.01
3/19/95			0.8	0.01	92.7	0.21
6/5/95	4.39	1.88	1	0.02	27.6	0.06
Average	3.4		0.9		48.3	
Std Dev	1.5		0.1		38.5	

	δO	δH
4/30/94	-11.8	-89

Chemical Facies calcium-magnesium sulfate

Comments: Samples collected from inner-basin sediment. At high flow regimes samples collected about 3/4 mile up the drainage from the Tonto Trail. Samples collected 200 feet from the trail at low flow. Western drainage typically dry.

## Two Trees Spring

**Spring Elevation** 3760'

**Geology** Bright Angel Shale—Muav Limestone

**Longitude/Latitude** 36-04'69"/112-07'54'

36-04,52"/112-07'60'

### Hydrochemical Data

Date of sample	pH	EC(mS/cm)	TDS(g/l)	T (C)	T air (C)	Alk (mg/l)	Q (l/m)
1/11/94	7	0.430	0.210	18.1	4.4		gage
11/14/94		0.440	0.210	18.2	9.3		
7/19/95	7.65	0.444	0.222	18.7	26.4	176	
11/26/95	7	0.423	0.211	18.3	14.8	184	
6/5/95	7.54	0.491	0.115	18.3	27.9		
7/19/95	7.44	0.472	0.236	22.7	25.8	196	
Average	7.3	0.450	0.201	19.1	18.1	185.3	
Std Dev	0.3	0.026	0.043	1.8	10.0	10.1	

Date of sample	TR	2-σ	AR	1-σ	U-238 (ug/l)	1-σ
4/30/94	0.82	0.85	3.5	0.7	0.64	0.05
9/29/94	0.99	0.87				
11/26/94	0.66	1.57				
4/30/95	-0.47	3.13				
5/18/95	-0.09	2.19				
6/5/95			3.7	0.31	0.59	0.02
Average	0.38	1.72	3.60		0.64	
Std Dev	0.63	0.97	0.14		0.04	

	δO	δH
1/11/94	-12.2	-93
4/30/94	-12.3	-91
4/30/94	-12.4	-91

**Chemical Facies** calcium-magnesium bicarbonate

**Comments:** An alternative name for this spring are 1) Pump House Spring;  
2) Indian Garden Spa. Discharge gage often failed during this investigation. Samples collected from below two trees on eastern canyon wall.

## Pipe Spring

Spring Elevation 3840'

Geology Bright Angel Shale—Muav Limestone

Longitude/Latitude 36-04,24' 112-05,89'

### Hydrochemical Data

Date of sample	pH	EC(mS/cm)	TDS(g/l)	T (C)	T air (C)	Alk (mg/l)	Q (l/m)
1/11/94		0.47	0.23	4	3.2		gage
4/29/94	7	0.567	0.285	16	13	142	
11/14/94		0.62	0.3	11.5	9.2		
11/26/94							
6/4/95	7.14	0.671	0.333	16.6	39.5	190	
7/19/95	8.04	0.637	0.321	22.6	37.7		
Average	7.4	0.6	0.3	14.1	20.5	166	
Std Dev	0.6	0.1	0.0	6.9	16.9	34	
Date of sample	TR	2-σ	AR	1-σ	U-238 (ug/l)	1-σ	
4/29/94	0.94	3.13	2.8	0.52	2.04	0.01	
11/14/94	2.02	0.87					
11/26/94	1.48	0.89					
6/4/95			2.7	0.157	0.85	0.00315	
Average	1.5	1.6	2.8	0.3	0.9	0.0	
Std Dev	0.5	1.3	0.1	0.3			
	δO	δH					
1/11/94	-12.4	-92					
4/29/94	-12.4	-91					

Chemical Facies calcium-magnesium bicarbonate-sulfate

Comments: Samples collected from inter-basin sediment. Flow fluctuates, higher during March through May.

## Burro Spring

Spring Elevation 3760'

Geology Bright Angel Shale—Muav Limestone

Longitude/Latitude 36-04"61' 112-06"06'

36-04,60' 112-06,01'

### Hydrochemical Data

Date of sample	pH	EC(mS/cm)	TDS(g/l)	T (C)	T air (C)	Alk (mg/l)	Q (l/m)
1/11/94	6	0.55	0.27	8.3	11		
4/29/94	7	0.6	0.3	13	20	215	
11/14/94		0.57	0.28	11.5	16.5		3
7/19/95	8.36	0.643	0.321	20	26.2	220	5
Average	7.1	0.591	0.293	13.2	18.4	218	4
Std Dev	1.2	0.040	0.023	4.9	6.4	4	1
Date of sample	TR	2-σ	AR	1-σ	U-238 (ug/l)	1-σ	
4/29/94	1.91	2.82	2.6	0.59	2.43	0.02	
	δO	δH					
1/11/94	-12.2	-92					
4/29/94	-12.2	-90					

Chemical Facies calcium-magnesium bicarbonate

Comments: Abundant vegetative growth around the spring orifice. Constant annual discharge.

## Cremation Creek

Spring Elevation 3500'  
 Geology Tapeats Sandstone  
 Longitude/Latitude

### Hydrochemical Data

Date of sample	pH	EC(mS/cm)	TDS(g/l)	T (C)	T air (C)	Alk (mg/l)	Q (l/m)
11/14/94							DRY
6/4/95	7.12	2.16	1.072	18.7	25.2		POOL DRY
Date of sample	TR	2-σ	AR	1-σ	U-238 (ug/l)	1-σ	
6/4/95	7.20	2.50	2	0.108	7.6	0.022	

Comments: Spring dry the majority of the time. Abundant salt precipitate in creek bed.

## Sam Magee Spring

Spring Elevation 4000'  
 Geology Bright Angel Shale—Muav Limestone  
 Longitude/Latitude 36-04"73' 112-03"90'

### Hydrochemical Data

Date of sample	pH	EC(mS/cm)	TDS(g/l)	T (C)	T air (C)	Alk (mg/l)	Q (l/m)
11/14/94		0.460	0.230	9.5	7.9		0.25
6/3/95	7.6	0.788	0.394	17	20	138	0.25
7/19/95	8.1	0.754	0.377	19.8	22.8	138	0.25
Average	7.9	0.667	0.334	15.4	16.9	138	0.25
Std Dev	0.4	0.180	0.090	5.3	7.9		
Date of sample	TR	2-σ	AR	1-σ	U-238 (ug/l)	1-σ	
11/14/94	0.89	1.05					
6/3/95			1.6	0.083	3.8	0.012	

Chemical Facies calcium-magnesium sulfate

Comments: Very low rate of discharge. Spring located at the Bright Angel Shale-Muav Limestone contact.

## Lonetree Spring

Spring Elevation 3680'

Geology Tapeats Sandstone--Bright Angel Shale

Longitude/Latitude 36-04°27' 112-02°73'

### Hydrochemical Data

Date of sample	pH	EC(mS/cm)	TDS(g/l)	T (C)	T air (C)	Alk (mg/l)	Q (l/m)
1/10/94	6	1.28	0.630	2.9	13.9		
11/13/94		1.43	0.700	9.8	14.4		0.2
6/3/95	6.95	1.21	0.607	19.7	36.8	360	2
7/18/95	7.21	1.441	0.720	24.6	34.2	450	1
Average	6.7	1.340	0.664	14.3	24.8	405	1.1
Std Dev	0.6	0.114	0.054	9.8	12.4	64	0.9

Date of sample	TR	2-σ	AR	1-σ	U-238 (ug/l)	1-σ
11/13/94	3.71	0.96				
6/3/95			1.6	0.071	4.8	0.014

Chemical Facies calcium-magnesium sulfate

Comments: Actual spring orifice buried by modern sediment.

Tritium sample collected while raining.

## Boulder Creek

Spring Elevation 3520'

Geology Tapeats Sandstone

Longitude/Latitude 36-00°97' 112-00°37'

### Hydrochemical Data

Date of sample	pH	EC(mS/cm)	TDS(g/l)	T (C)	T air (C)	Alk (mg/l)	Q (l/m)
11/13/95							DRY
6/3/95	7.08	1.797	0.898	21.5	30		0.1
7/18/95							DRY

Date of sample	TR	2-σ	AR	1-σ	U-238 (ug/l)	1-σ
6/3/95	3.76	1.57	2	0.084	6.9	0.019

Comments: Dry the majority of the time. Spring water flows from the Tapeats Sandstone.

## Grapevine Spring

Spring Elevation 4000'

Geology Bright Angel Shale—Muav Limestone

Longitude/Latitude 36-01°39' 112-00°79'

### Hydrochemical Data

Date of sample	pH	EC(ms/cm)	TDS(g/l)	T (C)	T air (C)	Alk (mg/l)	Q (l/m)
1/9/94	6	0.67	0.33	5.6	12		
1/10/94	6	0.66	0.32	2.7	-1.6		
11/12/94		0.73	0.36	11.7	11.5		5
5/13/95	7.2	0.559	0.279	12.8	18	265	5
7/17/95	7	0.315	0.157	19	34.4	256	3
Average	6.6	0.6	0.3	10.4	14.9	261	4.3
Std Dev	0.6	0.2	0.1	6.4	13.1	6	1.2

Date of sample	TR	2-σ	AR	1-σ	U-238 (ug/l)	1-σ
11/12/94	1.95	0.89				
5/13/95			3.6	0.29	1.2	0.03

	δO	δH
1/9/94	-10.1	-80
1/10/94	-12.4	-92

Chemical Facies calcium-magnesium bicarbonate

Comments: Spring orifice buried by modern sediment. Flow fluctuates on a diurnal basis.  
Sample location 1 to 3 miles above Tonto Trail.

## Grapevine East Spring

Spring Elevation 3680

Geology Bright Angel Shale

Longitude/Latitude 36-02°57' 112-00°81'

### Hydrochemical Data

Date of sample	pH	EC(ms/cm)	TDS(g/l)	T (C)	T air (C)	Alk (mg/l)	Q (l/m)
11/12/94		0.85	0.24	10.1	21.3		3
5/13/95	8.1	0.687	0.344	20	33.3	150	
7/17/95	7	0.906	0.453	26.2	42.1	272	3
Average	7.6	0.814	0.346	18.8	32.2	211	
Std Dev	0.8	0.114	0.107	8.1	10.4	86	

Date of sample	TR	2-σ	AR	1-σ	U-238 (ug/l)	1-σ
11/12/94	1.63	0.94				
5/13/95			1.7	0.2	2.8	0.03

	δO	δH
1/10/94	-11.6	-88

Chemical Facies calcium-magnesium sulfate

Comments: Discharge constant, heavy vegetation growth around spring orifice.

**Grapevine Hell Spring**

Spring Elevation 3760'

Geology Bright Angel Shale

Longitude/Latitude

**Hydrochemical Data**

Date of sample	pH	EC(mS/cm)	TDS(g/l)	T (C)	T air (C)	Alk (mg/l)	Q (l/m)
11/12/94							DRY
5/13/95	8.44	1.783	0.892	22.7	26.7	301	
7/17/95							DRY

Date of sample	TR	2-σ	AR	1-σ	U-238 (ug/l)	1-σ
5/13/95			2	0.12	7	0.01

Comments: Dry the majority of the year. Abundant salt deposits around orifice

**Cottonwood West Spring**

Spring Elevation 3680'

Geology Tapeats Sandstone--Bright Angel Shale

Longitude/Latitude

**Hydrochemical Data**

Date of sample	pH	EC(mS/cm)	TDS(g/l)	T (C)	T air (C)	Alk (mg/l)	Q (l/m)
11/12/94		1.13	0.57	12.7	16.4		0.02
5/13/95	7.8	1.293	0.647	21.8	26.7	420	0.02
7/17/95							DRY
Average		1.212	0.609	17.3	21.6		
Std Dev		0.115	0.054	6.43	7.28		

Date of sample	TR	2-σ	AR	1-σ	U-238 (ug/l)	1-σ
11/12/94	2.32	0.87				
5/13/95			2.2	0.1	4.5	0.01

Comments: Intermittent discharge, when flowing very small volume from the Tapeats Sandstone.



**Cottonwood Spring**

Spring Elevation 3920'

Geology Bright Angel Shale—Muav Limestone

Longitude/Latitude 36-01"30' 111-59"30'

**Hydrochemical Data**

Date of sample	pH	EC(mS/cm)	TDS(g/l)	T (C)	T air (C)	Alk (mg/l)	Q (l/m)
1/9/94	6	0.48	0.240				gage
11/11/94		0.701	0.350	13.4	16.3		
11/12/94		1.13	0.570	12.7	16.4		
5/12/95	7.49	0.681	0.340	13	21.3	300	
7/16/95	7.97	0.798	0.396	19	27.8	390	
Average	7.2	0.758	0.379	14.5	20.5	345	
Std Dev	1.0	0.238	0.121	3.0	5.4	64	
Date of sample	TR	2-σ	AR	1-σ	U-238 (ug/l)	1-σ	
11/11/94	1.46	0.93					
11/12/94	1.08	1.08					
5/12/95			3.6	0.42	1.1	0.006	
7/16/95	1.57	2.19					
Average	1.4						
Std Dev	0.3						
	δO	δH					
1/9/94	-12.5	-93					

Chemical Facies calcium-magnesium bicarbonate

**Comments:** Samples collected at USGS stream gage. Abundant riparian vegetation and plant waste in stream bed. Springs on the east side go dry during summer. More discharge below USGS gage from the Bright Angel Shale.

**Page Spring**

Spring Elevation 4320'

Geology Muav Limestone—Bright Angel Shale

Longitude/Latitude 36-00"97' 111-58"38'

**Hydrochemical Data**

Date of sample	pH	EC(mS/cm)	TDS(g/l)	T (C)	T air (C)	Alk (mg/l)	Q (l/m)
1/8/94		0.420	0.214	8	11.4		
11/11/94		0.418	0.206	13.1	19		1
5/12/95	8.2	0.383	0.191	12.6	20.1	142	1
7/16/95	8.23	0.436	0.218	16.5	21.7	125	1
9/9/95	8.27	0.460		17.4			1
Average	8.2	0.423	0.207	13.5	18.1	134	1.0
Std Dev	0.04	0.028	0.012	3.72	4.57	12	
Date of sample	TR	2-σ	AR	1-σ	U-238 (ug/l)	1-σ	
11/11/94	1.10	0.83					
5/12/95	1.28	1.88	1.6	0.14	3.9	0.013	
7/16/95	1.92	1.88					
9/9/95			1.6	0.11	3.7	0.012	
Average	1.4	1.529	1.600	0.1	3.8		
Std Dev	0.43	0.608	0.000	0.02	0.14		
	δO	δH					
1/8/94	-12.2	-93					

Chemical Facies calcium bicarbonate

**Comments:** Page Spring was sampled directly from the outcrop. Flow constant throughout the duration of investigation.

## APPENDIX II: Geochemical Data

Results from tritium analysis listed in chronological order.

Sample Station	Date	pCi/l	2- $\sigma$	TR	2- $\sigma$	MDL(pCi/l)	Lab
Indian Garden Pump Station	4/30/94	20	6	6.27	1.88		DRI
Canyon Mine Well	5/14/94	-1.4	8	-0.44	2.51		DRI
Pipe Spring	9/26/94	4.629	2.845	1.43499	0.89	4.533	EPA
Indian Garden Spring	9/26/94	3.222	2.777	0.99882	0.87	4.467	EPA
Page Spring	11/11/94	3.446	2.636	1.06826	0.83	4.227	EPA
Cottonwood Spring	11/11/94	4.581	2.974	1.42011	0.93	4.748	EPA
Cottonwood Spring	11/12/94	3.391	3.449	1.05121	1.08	5.568	EPA
Grape East Spring	11/12/94	5.118	2.986	1.58658	0.94	4.75	EPA
Cottonwood West Spring	11/12/94	7.25	2.71	2.2475	0.85	4.226	EPA
Grapevine Spring	11/12/94	6.112	2.854	1.89472	0.89	4.499	EPA
Lonetree Spring	11/13/94	11.627	3.073	3.60437	0.96	4.683	EPA
Sam Magee Spring	11/14/94	2.791	3.344	0.86521	1.05	5.416	EPA
Pipe Spring	11/14/94	6.337	2.776	1.96447	0.87	4.364	EPA
Squire Inn Well	11/15/94	2.767	3.315	0.85777	1.04	5.369	EPA
Indian Garden Pump Station	11/26/94	2.1	5	0.66	1.57		DRI
Indian Garden Pump Station	11/26/94	13.613	3.032	4.22003	0.95	4.555	EPA
Two Trees Spring	11/26/94	2.577	2.703	0.79887	0.85	4.366	EPA
Kolb Spring	11/27/94	10.555	2.713	3.27205	0.85	4.127	EPA
Lab Blank "Fossil Water"	12/20/94	4.432	3.468	1.37392	1.09	5.566	EPA
South-rim rain-water	2/25/95	34.1	7	10.69	2.19		DRI
Cottonwood Spring	2/25/95	7.1	6	2.23	1.88		DRI
Santa Maria Spring	3/17/95	9.4	6	2.95	1.88		DRI
Dripping Spring	3/17/95	0.5	7	0.16	2.19		DRI
Upper Hermit Creek	3/17/95	19.9	7	6.24	2.19		DRI
Hermit Spring	3/17/95	3.6	8	1.13	2.51		DRI
Hawaii Spring	3/18/95	1.6	8	0.50	2.51		DRI
Monument Creek	3/18/95	9.1	7	2.85	2.19		DRI
Cedar Spring	3/18/95	8.8	6	2.76	1.88		DRI
Salt Creek	3/19/95	18	9	5.64	2.82		DRI
Burro Spring	4/29/95	6.1	9	1.91	2.82		DRI
Pipe Spring	4/29/95	3	10	0.94	3.13		DRI
Bright Angel Creek	4/30/95	19	13	5.96	4.08		DRI
Two Trees Spring	4/30/95	-1.5	10	-0.47	3.13		DRI
Horn Creek	4/30/95	7.4	7	2.32	2.19		DRI
Page Spring	5/12/95	4	6	1.25	1.88		DRI
Squire Inn Well	5/17/95	-1.3	10	-0.41	3.13		DRI
Two Trees Spring	5/18/95	-0.3	7	-0.09	2.19		DRI
Boulder Spring	6/3/95	12	5	3.76	1.57		DRI
Cremation Spring	6/4/95	23	8	7.21	2.51		DRI
Page Spring	7/16/95	6	6	1.88	1.88		DRI
Cottonwood Spring	7/16/95	5	7	1.57	2.19		DRI
Indian Garden Pump Station	7/19/95	6.6	10	2.07	3.13		DRI
Fence Fault Spring (S)	7/31/95	9	8	2.82	2.51		DRI
Fence Fault Spring (N)	7/31/95	8	9	2.51	2.82		DRI
Vacy's Paradise Spring	8/1/95	16	8	5.02	2.51		DRI
Monkey Flower Spring	8/1/95	14	8	4.39	2.51		DRI
Deer Spring South	8/4/95	9	8	2.82	2.51		DRI
Tapeats Creek	8/4/95	16	10	5.02	3.13		DRI
Matkatimiba Spring	8/5/95	4	8	1.25	2.51		DRI
Ledges Spring	8/5/95	<1		0			DRI

Major ion concentrations (mg/l) in South Rim Springs, collected in July, 1995.

Sample Station	Ca	2- $\sigma$	Mg	2- $\sigma$	Na	2- $\sigma$	K	2- $\sigma$	SO4	2- $\sigma$	HCO3	Cl	2- $\sigma$	F	2- $\sigma$	Br	2- $\sigma$	NO3	NO4	2- $\sigma$
Page Spring	24.56	0.29	33.77	0.35	0	NA	3.82	0.02	42.7	0.28	125	23	0.33	0		0.197	0.01	5.64	1.27	0.068
Cottonwood Spring	81.62	1.79	62.13	1.23	12.22	0.31	4.41	0.02	31	0.175	390	20	0.03	0		0.166	0.008	0.102	0.02	0.002
Grapevine East Spring	77.59	1.8	74.72	2.19	19.2	0.09	7.03	0.09	173	2.61	272	35	0.132	0.141	0	0.236	0.006	0.145	0.03	0.01
Grapevine Spring	62.68	0.95	36.87	0.24	6.24	0.1	1.86	0.08	12.4	0.041	256	9.17	0.091	0.093	0.002	0.09	0.003	0.369	0.083	0.002
Lonetree Spring	115.69	3.03	121.17	0.09	50.86	1.24	14.37	0.06	303.5	1.44	450	57	0.06	0		0.451	0.012	0.087	0.02	0.003
Sam Magee Spring	55.45	0.84	57.09	0.6	20.54	0.16	6.63	0.17	186	0.134	138	29.9	0.3	0.5	0.025	0.269	0.007	15.4	3.48	0.159
Burro Spring	56.95	0.56	47.11	1.23	15.84	0.04	4.29	0.002	75.9	0.087	220	20.1	0.094	0		0.157	0.006	1.79	0.404	0.012
Pipe Spring	65.52	0.64	50.48	1.25	14.59	0.11	4.69	0.08	110.5	0.018	206	19.6	0.137	0		0.126	0	1.734	0.392	0.033
Two Trees Spring	46.46	0.71	34.77	0.86	7.43	0.02	1.51	0.04	22.2	0.002	196	12.5	0.23	0		0.113	0.005	2.09	0.47	0.003
IGS	42.01	0.92	33.86	1.1	7.25	0.05	1.74	0.06	21.8	0.001	176	12.7	0.198	0.094	0.004	0.11	0.006	2.81	0.63	0.01
IGPS	37.23	0.65	17.61	0.32	1.28	0.006	0.58	0.01	3.72	0.011	150	3.31	0.032	0.1	0.005	0		0.862	0.195	0.021
Horn Spring	87.78	1.71	81.99	1.06	32.51	0.18	13.66	0.21	239.1	0.701	280	39.3	0.203	0		0.207	0.01	0.549	0.124	0.002
Salt Spring	126.99	3.16	143.8	0.38	47.73	0.21	19.16	0.24	674.3	0.695	190	38.1	0.365	0		0.16	0.006	4.38	0.989	0.058
Monument Spring	89.48	2.37	72.91	0.56	92.63	6.99	8.48	0.24	199.8	4.37	234	162.9	0.572	0		0.482	0.015	9.66	2.18	0.316
Hawaii Spring	49.30	0.003	36.3	0.53	12.29	0.34	2.54	0.003	42	0.012	190	14.9	0.129	0		0.11	0.002	2.79	0.63	0.021
Hermit Spring	49.00	0.39	31.5	1.18	6.36	0.13	1.5	0.02	13.5	0.003	194	10.9	0.14	0.099	0.001	0.087	0.003	2.9	0.655	0.064
Santa Maria Spring	27.71	0.4	41.22	0.68	12.83	0.08	3.85	0.02	23	0.06	167	26.7	0.051	0		0.228	0	6.24	1.41	0.021
Dripping Spring	30.50	0.62	27.65	0.97	4.57	0.03	1.08	0.01	8.72	0.05	134	11.8	0.189	0.154	0.003	0.13	0.001	5.7	1.29	0.024

## Results from spring water uranium analyses.

Sample Station	Date	238 (pCi/l)	1- $\sigma$	238 (ug/l)	234 (pCi/l)	AR	1- $\sigma$
Dripping Spring	3/17/95	0.47	0.05	1.3	1.65	3.5	0.946
Santa Maria Spring	3/17/95	2.21	0.03	6.2	4.3	1.9	0.083
Hawaii Spring	3/18/95	0.94	0.02	2.6	2.68	2.8	0.21
Hermit Source Spring	3/18/95	1.01	0.02	2.8	2.89	2.9	0.18
Monument Creek	3/18/95	3.24	0.04	9	6.71	2.1	0.066
Cedar Spring	3/18/95	5.57	0.05	15.6	10.59	1.9	0.052
Salt Creek	3/19/95	5.23	0.05	14.6	8.03	1.5	0.041
Horn Creek	4/30/94	8.76	0.09	24.7	8.22	0.94	0.032
	3/19/95	33.21	0.12	92.7	27.82	0.8	0.011
	6/5/95	9.9	0.08	27.6	9.48	1	0.023
Two Trees Spring	4/30/94	0.643	0.05	1.81	2.26	3.5	0.654
	6/5/95	0.59	0.02	1.6	2.16	3.7	0.31
Pipe Creek	4/29/94	0.723	0.05	2.04	2.04	2.8	0.52
	6/4/95	0.85	0.02	2.4	2.33	2.7	0.157
Burro Spring	4/29/94	0.861	0.08	2.43	2.23	2.6	0.59
Cremation Creek	6/4/95	2.72	0.06	7.6	5.35	2	0.108
Sam Magee Spring	6/3/95	1.35	0.02	3.8	2.2	1.6	0.083
Lonetree Spring	6/3/95	1.71	0.03	4.8	2.71	1.6	0.071
Boulder Creek	6/3/95	2.46	0.03	6.9	4.84	2	0.084
Grapevine Spring	5/13/95	0.42	0.01	1.2	1.54	3.6	0.286
Grapevine East Spring	5/13/95	1	0.05	2.8	1.68	1.7	0.198
Grapevine-Hell Spring	5/13/95	2.5	0.06	7	4.94	2	0.117
Cottonwood Spring	5/12/95	0.41	0.01	1.1	1.47	3.6	0.42
Cottonwood West Spring	5/13/95	1.6	0.03	4.5	3.53	2.2	0.095
Page Spring	5/12/95	1.41	0.05	3.9	2.24	1.6	0.139
	9/9/95	1.31	0.03	3.7	2.09	1.6	0.111
Indian Garden Pump Station	4/30/94	0.074	0.06	0.21	0.356	4.8	9.25
Bright Angel Creek (N. Rim)	4/30/94	0.154	0.08	0.055197	0.819	3.8	5.32

**APPENDIX III: Discharge measurements from South Rim springs for the 1994-1995 water year.**

Station	Water Year	Mean Q			Max		Min		Source
		cfs	gpm	l/m	cfs	gpm	cfs	gpm	
Blue Springs	1994-1995	220.0	98742.6	373824.0	230	103231			Huntoon, 1982
Havasu Springs	1994-1995	65.0	29174.0	110448.0	66.6	29892			Huntoon, 1982
Page Springs	1994-1995	0.00059	0.3	1					This Study
Cottonwood Spring	1994-1995	0.01200	5.4		0.029		0.002		USGS
Cottonwood West Spring	1994-1995	0.00015	0.1	0.25			0		This Study
Grapevine Hell Spring	1994-1995	0.00012	0.1	0.2			0		This Study
Grapevine East Spring	1994-1995	0.00118	0.5	2					This Study
Grapevine Spring	1994-1995	0.00029	0.1	0.5					This Study
Boulder Spring	1994-1995	0.00007	0.0	0.125			0		This Study
Lonetree Spring	1994-1995	0.00059	0.3	1					This Study
Sam Magee Spring	1994-1995	0.00029	0.1	0.5					This Study
Cremation Spring	1994-1995	0.00003	0.0	0.05			0		This Study
Burro Spring	1994-1995	0.00235	1.1	4					This Study
Pipe Spring	1994-1995	0.061	27.4	104	0.23	103.2	0.01	4.5	USGS
Two Trees Spring	1995	0.13	58.3	221	0.16	71.8	0.12	53.9	USGS
SD Tank IGS	1994-1995	1.09	489.2	1852	1.6	718.1	0	0.0	USGS
Kolb Seep	1994-1995	0.0018	0.8	3			0		This Study
Indian Garden Creek	1994-1995	1.35	605.9	2294	1.6	718.1	0.48	215.4	USGS
Horn Spring	1994-1995	0.00029	0.1	0.5					This Study
Salt Spring	1994-1995	0.00015	0.1	0.3					This Study
Cedar Spring	1994-1995	0.00006	0.0	0.1			0		This Study
Monument Spring	1994-1995	0.00294	1.3	5.0					This Study
Hawaii Spring	1994-1995	0.00177	0.8	3.0					This Study
Hermit Source Spring	1994-1995	0.00294	1.3	5.0					This Study
Hermit/Hawaii Spring	1994-1995	0.70	314.2	1189	1.9	852.8	0.49	219.9	USGS
Santa Maria Spring	1994-1995	0.00029	0.1	0.5					This Study
Dripping Spring	1994-1995	0.00059	0.3	1.0					This Study

## BIBLIOGRAPHY

- Allocco, R., Governa, M.E., Saibene, L., Scesi, L. and Zuppi, G.M., 1989. Hydrodynamic parameters of the Bossea karst system evaluated from hydrogeochemical and structural analyses. In: IAEA (Editor), Isotope techniques in the study of the hydrology of fractured and fissured rocks. International Atomic Energy Agency, Vienna, p. 139.
- Appelo, C.A.U. and Postma, D., 1993. Geochemistry, groundwater, and pollution. A.A. Balkema/Rotterdam/Brookfield, pp. 270 -300.
- Brown, B.T. and Moran S.M., 1979. An inventory of surface water resources in Grand Canyon National Park, Arizona. Final Report to Division of Resource Management, Grand Canyon National Park, 208 Water Quality Project, Part I, Water Resource Inventory.
- Beus, S., 1990. Temple Butte Formation. In: Beus, S. and Morales, M. (Editors), 1990. Grand Canyon Geology. New York Oxford: Museum of Northern Arizona, pp. 107-118.
- Blakey, R.C., 1990. Supai Group and Hermit Formation. In: Beus, S. and Morales, M. (Editors), 1990. Grand Canyon Geology. New York Oxford: Museum of Northern Arizona, pp. 147-182.
- Buttlar and Libby, 1954. Natural Distribution of Cosmic-Ray Produced Tritium. J. Inorganic and Nuclear Chemistry, v. 1, pp. 71-91.
- Cowart, J.B., Kaufman, M.I., and Osmond J.K., 1978. Uranium-Isotope variations in groundwaters of the Floridan aquifer and boulder zone of South Florida. Journal of Hydrology, v. 36, pp. 161-172.
- Energy Fuels Nuclear, Inc. 1985. Environmental Impact Statement-Canyon Uranium Mining proposal, Coconino County, AZ. Kaibab National Forest, Southwest Region, US Department of Agriculture, Appendix F.
- Fontes, J.CH., 1980. Environmental isotopes in groundwater hydrology. In: P. Fritz and J.CH. Fontes (Editors), Handbook of Environmental Isotope Geochemistry. v. 1: The Terrestrial Environment, B. Elsevier, Amsterdam, pp. 75-85.
- Foust, R.D. and Hoppe S., 1985. Seasonal trends in the chemical composition of Grand Canyon Waters. Flagstaff, AZ: Report prepared for US National Park Service, Ralph M. Bilby Research Ctr., University of Northern Arizona, pp. 30-35.
- Gaspar, E., 1987. Modern Trends in Tracer Hydrology. Vol. 1. CRC Press, Florida, p. 50.
- Goings, D.B., 1985. Spring flow in a portion of Grand Canyon National Park, Arizona, Unpublished Master's Thesis, University of Nevada, Las Vegas.

- Holloway, R.W., 1993. Tritium in surface waters of the western United States. *Radiochimica Acta.*, v. 62, pp. 217-220.
- Huntoon, P.W., 1974. The karstic groundwater basins of the Kaibab Plateau, Arizona. *Water Resour. Res.*, v. 10(3) pp. 579-590.
- , 1982. The ground-water systems that drain to the Grand Canyon of Arizona. Laramie, WY: Department of Geology and Water Resources Institute, University of Wyoming, pp. 1-25.
- Huntoon, P.W., Billingsley, G.H., Breed, W.J., Sears, J.W., Ford, T.D., Clark, N.D., Babcock, R.S. and Brown, E.H., 1980. Geologic map of the Grand Canyon National Park, Arizona: Grand Canyon Natural History Assn., and Mus. Northern Arizona, Scale 1:62500.
- Huntoon, P.W. and Sears, J.W., 1975. Bright Angel and Eminence Faults. *Geol. Soc. of Amer.*, v. 86, pp. 465-472.
- International Atomic Energy Agency, 1960-1991. World survey of isotopes concentration in precipitation. Environmental Isotope Data No. 6. International Atomic Energy Agency, Vienna.
- Ivanovich, M. and Harmon, R.S., 1992. Uranium-series disequilibrium. Oxford Science Publ., Clarendon Press. pp. 259-333.
- Kronfeld, J., Vogel, J.C., Talma, A.S., 1994. A new explanation for extreme  $^{234}\text{U}/^{238}\text{U}$  disequilibria in a dolomitic aquifer. *Earth and Plan. Sc. Lett.*, v. 123, pp. 81-93.
- Metzger, D., 1961. Geology in relation to availability of water along the south-rim, Grand Canyon National Park, Arizona. Geological Survey Water-Supply Paper 1475-C, pp. 100-130.
- Middleton, L.T. and Elliot, D.K., 1990. Tonto Group. In: Beus, S. and Morales, M. (Editors), 1990. Grand Canyon Geology. New York Oxford: Museum of Northern Arizona, pp. 83-106.
- Milanovic, P.T., 1981. Karst Hydrogeology. Water Resour. Publ., Michigan, USA, pp. 209-220.
- Montgomery and Associates, 1993. Unpublished report, Projections for decrease in spring flow resulting from proposed groundwater withdrawal near Tusayan, Arizona.
- Morse, J.W., Shanbhag, P.M., Saito, A., Choppin, G.R., 1984. Interaction of uranyl ions in carbonate media. *Chem. Geol.*, v. 42, pp. 85-99.
- Moser, H., Wolf, M., Fritz, P., Fontes, J.C.H., Florkowski, T. and Payne, B. R., 1988. Deuterium, oxygen-18, and tritium in Stripa groundwater. *Geoch. et Cosmo. Acta.*, v. 53, pp. 1757-1763.

- Murphy, C.E., 1992. Tritium transport and cycling in the environment. *Health Phys.*, v. 65, pp. 683-697.
- National Park Service, Grand Canyon Science Center, 1996. Precipitation data written communication.
- Osmond, J.K., Kaufman, M.I., Cowart, J.B., 1974. Mixing volume calculations, sources and aging trends of Floridan aquifer water by uranium isotopic methods. *Geochimica et Cosmochimica Acta*, v. 38, pp. 1083-1100.
- Osmond, J.K., Cowart, J.B., 1976. The Theory and uses of Natural Uranium Isotopic Variations in Hydrology. *Atomic Energy Review*, 14.4, pp. 621-677.
- Osmond, J.K., 1980. Uranium Disequilibrium in Hydrologic Studies. In: P. Fritz and J.CH. Fontes (Editors), *Handbook of Environmental Isotope Geochemistry*. Vol 2: The Terrestrial Environment, B. Elsevier, Amsterdam, pp. 75.
- Parkhurst, D.L., Thorstenson, D.C., Plummer, L.N., 1993. PHREEQE, A geochemical reaction model based on an ion pairing aqueous model. IGWMC - FOS 39 PC.
- Phillips, F.M., Mattick, J.L., Duval, T.A., Elmore, D. and Kuble, P.W., 1988. Chlorine-36 and tritium from nuclear weapons fallout as tracers for long-term liquid and vapor movement in desert soils. *Water Resour. Res.*, v. 24(11), pp. 1877-1892.
- Plummer, L.N., Busby, J.F., Lee, R.W., Hanshaw, B.B., 1990. Geochemical modeling of the Madison Aquifer in parts of Montana, Wyoming, and South Dakota. *Water Resour. Res.*, v. 26, pp. 1981-2014.
- Reynolds, S.J., 1988. Geologic map of Arizona, map 26. AGS and USGS, Scale 1:1000000.
- Sears, J.W., 1990. Geologic structure of the Grand Canyon Supergroup. In: Beus, S. and Morales, M. (Editors), 1990. *Grand Canyon Geology*. New York Oxford: Museum of Northern Arizona, pp. 71-82.
- United States Environmental Protection Agency, 1979. *Radiochemical Analytical Procedures for analysis of environmental samples*. US EPA, monitoring laboratory, Las Vegas.
- United States Geological Survey, Flagstaff, Arizona, Monroe, S. and Bills, D., 1996. Spring discharge and well data. Oral Communication.
- Wenrich, K., 1985. Mineralization of breccia pipes in Northern Arizona. *Econ. Geol.*, v. 80, pp. 1722-1735.
- , 1986. Geochemical exploration for mineralized breccia pipes in northern Arizona, USA Appl. *Geochem.*, v. 1, pp. 469-485.
- Zukosky, K., 1994. Stable isotope and trace element signatures of the south rim, Grand Canyon, Arizona. Unpublished Master's Thesis, University of Nevada, Las Vegas.